

# **A Functional Analysis of Enterocyte Fatty Acid-Binding Proteins**

by

**William Stacy Lagakos**

A Dissertation submitted to the  
Graduate School of New Brunswick  
Rutgers, The State University of New Jersey  
in partial fulfillment of the requirements

for the degree of

Doctor of Philosophy

Graduate Program in Nutritional Sciences

Written under the direction of

**Judith Storch**

and approved by

---

---

---

---

New Brunswick, New Jersey

[October, 2009]

# **ABSTRACT OF THE DISSERTATION**

## **A Functional Analysis of Enterocyte Fatty Acid-Binding Proteins**

by **William Stacy Lagakos**

Dissertation Director:

**Judith Storch**

Intestinal- and liver- fatty acid-binding proteins (IFABP and LFABP, respectively) are expressed at high levels in mammalian small intestinal enterocytes and bind the major products of dietary triacylglycerol (TG) digestion. The precise role of FABPs in processing these diet-derived lipids is unknown. We investigated the acute metabolism of fatty acids and monoacylglycerol in fasted WT and FABP<sup>-/-</sup> in small intestinal mucosa *in vivo*. Two minutes after intraduodenal administration of [<sup>14</sup>C]oleate or [<sup>3</sup>H]monoolein, mucosal radioactivity was recovered primarily in TG. Recovery of [<sup>14</sup>C]oleate in TG relative to phospholipids (PL) was significantly reduced in IFABP<sup>-/-</sup> mice. No changes were found in the expression of lipid synthetic genes, suggesting a non-transcriptional, trafficking defect. Recovery of [<sup>14</sup>C]oleate in lipid fractions was unaffected by LFABP ablation, although significantly less was oxidized. Oxidative capacity was unchanged in LFABP<sup>-/-</sup> intestinal mucosa homogenates, suggesting LFABP may target fatty acids toward catabolic fates. Incorporation of [<sup>3</sup>H]monoolein into TG relative to PL was markedly reduced in LFABP<sup>-/-</sup> despite no changes in the expression of lipid synthetic genes. While those results suggest a trafficking defect, reports on the binding of monoacylglycerol by LFABP are mixed. Therefore, the monoacylglycerol -binding capability of liver cytosol from wild-type and LFABP<sup>-/-</sup> mice was assessed by gel filtration chromatography. The [<sup>14</sup>C]oleate associated with ~14kDa proteins was absent in LFABP<sup>-/-</sup> liver cytosol. Interestingly,

[<sup>3</sup>H]monoolein was present in the ~14kDa fractions from WT but not LFABP<sup>-/-</sup> cytosol.

Immunoblotting confirmed the presence of LFABP in the ~14kDa fractions from WT, but not LFABP<sup>-/-</sup>. These results suggest that LFABP is a monoacylglycerol-binding protein in a physiological setting.

The systemic effects of enterocyte FABP deletion were examined by comparing body composition via dual energy X-ray absorptiometry and energy metabolism via indirect calorimetry. During food deprivation, LFABP<sup>-/-</sup> mice lost more fat mass and, accordingly, had a lower respiratory quotient than WT. LFABP<sup>-/-</sup> mice lost less fat-free mass and maintained a higher level of energy expenditure relative to WT. These findings suggest that ablation of enterocyte FABPs manifest specific cellular effects in their native tissues due to lipid trafficking defects, as well as systemic effects.

## Table of Contents

Abstract .....	ii
List of Tables .....	v
List of Figures .....	vi
List of Abbreviations .....	ix
 <b>Chapter 1: Introduction and Review of the Literature</b>	 1
Introduction	2
Intestinal lipid metabolism	4
“Compartmentation” of intestinal lipid metabolism	6
Fatty acid-binding proteins	12
Evidence for a role of LFABP in intestinal lipid metabolism	18
LFABP <sup>-/-</sup> mouse	19
Evidence for a role of IFABP in intestinal lipid metabolism	19
IFABP <sup>-/-</sup> mouse	21
Specific aims of the studies	22
 <b>Chapter 2: Differential partitioning of FA in enterocytes from IFABP<sup>-/-</sup> mice</b>	 23
Abstract	24
Introduction	25
Materials and Methods	28
Results	35
Discussion	61
 <b>Chapter 3: LFABP ablation alters the anabolic and catabolic metabolism of lipids</b>	 69
Abstract	70
Introduction	71
Materials and Methods	78
Results	87
Discussion	113
 <b>Chapter 4: LFABP is a cytosolic monoacylglycerol-binding protein</b>	 122
Abstract	123
Introduction	124
Materials and Methods	127
Results	130
Discussion	136
 <b>Chapter 5: General conclusions and future directions</b>	 138
 <b>Literature Cited</b>	 149
 <b>Curriculum Vita</b>	 162

## List of Tables

### Chapter 1

Table 1-1. Members of FABP family	13
-----------------------------------	----

### Chapter 2

Table 2-1. qPCR primer sequences	34
Table 2-3. Metabolism of FA in SI of fasted mice	41
Table 2-4. Metabolism of dietary-derived FA in the SI of fed mice	41
Table 2-5. Effect of IFABP ablation on BW and FM in fed and fasted mice	49
Table 2-6. BMD and BMC in fed and fasted WT and IFABP <sup>-/-</sup> mice	51
Table 2-7. Composition of fecal fat is unaffected by IFABP ablation	53
Table 2-8. RQ is normal in 3-4 month old male IFABP <sup>-/-</sup> mice	55
Table 2-9. Metabolic rate is normal in 3-4 month old male IFABP <sup>-/-</sup> mice	55

### Chapter 3

Table 3-1. qPCR primer sequences	86
Table 3-2. Effect of LFABP ablation on body composition	104
Table 3-3. RQ is normal in 3-4 month old male LFABP <sup>-/-</sup> mice	107
Table 3-4. Metabolic rate is normal in 3-4 month old male LFABP <sup>-/-</sup> mice	107

## List of Figures

### Chapter 1

Figure 1-1. Dietary fat digestion	3
Figure 1-2. Triacylglycerol synthesis	5
Figure 1-3. Lipid metabolism in enterocytes	7
Figure 1-4. Graphic of compartmentation of SI lipid metabolism	11
Figure 1-5. Tertiary structure of FABPs from human, cow, and rat	14
Figure 1-6. NMR solution structure of apo- and holo-IFABP	17

### Chapter 2

Figure 2-1. LFABP expression in the intestinal mucosa	36
Figure 2-2. Lipid composition of the SI mucosa in 48 hour fasted mice	37
Figure 2-3. Mass of lipid classes in the SI mucosa of 48 hour fasted mice	38
Figure 2-4. Effect of IFABP ablation on the compartmentation of FA	42
Figure 2-5. Expression of lipid metabolism genes in the SI mucosa	44
Figure 2-6. Oxidation of bloodstream-derived FA in the SI mucosa	45
Figure 2-7. Expression levels of genes involved in FA oxidation	46
Figure 2-8. Body weight of IFABP <sup>-/-</sup> and WT mice	48
Figure 2-9. DEXA scan of fed and fasted WT and IFABP <sup>-/-</sup> mice	50
Figure 2-10. 24 hour RQ in fed and fasted WT and IFABP <sup>-/-</sup> mice	56
Figure 2-11. 24 hour metabolic rate in fed and fasted WT and IFABP <sup>-/-</sup> mice	57
Figure 2-12. No effect of IFABP ablation on intestinal TG secretion	59
Figure 2-13. No effect of IFABP ablation on intestinal TG secretion	60

### Chapter 3

Figure 3-1. Verification of genotype by PCR	85
Figure 3-2. IFABP expression in the intestinal mucosa	88
Figure 3-3. Absolute mass of lipid subclasses in the SI of fasted mice	89
Figure 3-4. Metabolism of FA in the SI mucosa of fasted mice	92
Figure 3-5. Metabolism of MG in the SI mucosa of fasted mice	94
Figure 3-6. Partitioning of FA and MG in the intestinal mucosa	96
Figure 3-7. Expression of lipid metabolism genes in the SI mucosa	97
Figure 3-8. Oxidation of [ $^{14}\text{C}$ ]oleate in intestinal mucosa	99
Figure 3-9. Oxidative capacity is not affected by LFABP ablation	101
Figure 3-10. Growth of LFABP <sup>-/-</sup> and WT mice	103
Figure 3-11. Fecal fat is unaffected by LFABP ablation	106
Figure 3-12. 24 hour RQ in fed and fasted WT and LFABP <sup>-/-</sup> mice	108
Figure 3-13. Metabolic rate in fed and fasted WT and LFABP <sup>-/-</sup> mice	109
Figure 3-14. No effect of LFABP ablation on intestinal TG secretion	111
Figure 3-15. No effect of LFABP ablation on intestinal TG secretion	112

### Chapter 4

Figure 4-1. Representative chromatogram of WT liver cytosol	131
Figure 4-2. [ $^{14}\text{C}$ ]Oleate retention in WT and LFABP <sup>-/-</sup> liver cytosol	133
Figure 4-3. [ $^3\text{H}$ ]Monoolein retention by WT and LFABP <sup>-/-</sup> liver cytosol	135

## **Chapter 5**

Figure 5-1. Potential trafficking routes for FABP-bound lipids	141
Figure 5-2. One precursor pool of FA to acylate each position of TG	143
Figure 5-3. Multiple precursor pools of FA supplying TG	144



## List of Abbreviations

ACADL	Long-chain acyl-CoA dehydrogenase
ACS	Acyl-CoA synthetase
BMC	Bone mineral content
BMD	Bone mineral density
BSAL	Bile salt activated lipase
CCOX	Cytochrome c oxidase
CE	Cholesteryl ester
Chol	Cholesterol
CM	Chylomicron
DG	Diacylglycerol
DGAT	Diacylglycerol acyltransferase
FA	Fatty acid
FABP	Fatty acid-binding protein
G3P	Glycerol-3-phosphate
GI	Gastrointestinal
GPAT	Glycerol-3-phosphate acyltransferase
IFABP	Intestinal fatty acid-binding protein
LFABP	Liver fatty acid-binding protein
LPAT	Lysophosphatidate acyltransferase
MG	Monoacylglycerol
MGAT	Monoacylglycerol acyltransferase
MGL	Monoacylglycerol lipase
NADHDe	Nicotine adenine dinucleotide dehydrogenase
PAP	Phosphatidate phosphohydrolase
PL	Phospholipid
PPAR $\alpha$	Peroxisome proliferator-activated receptor- $\alpha$
SI	Small intestine
SUCCDe	Succinate dehydrogenase
TG	Triacylglycerol
WT	Wild-type

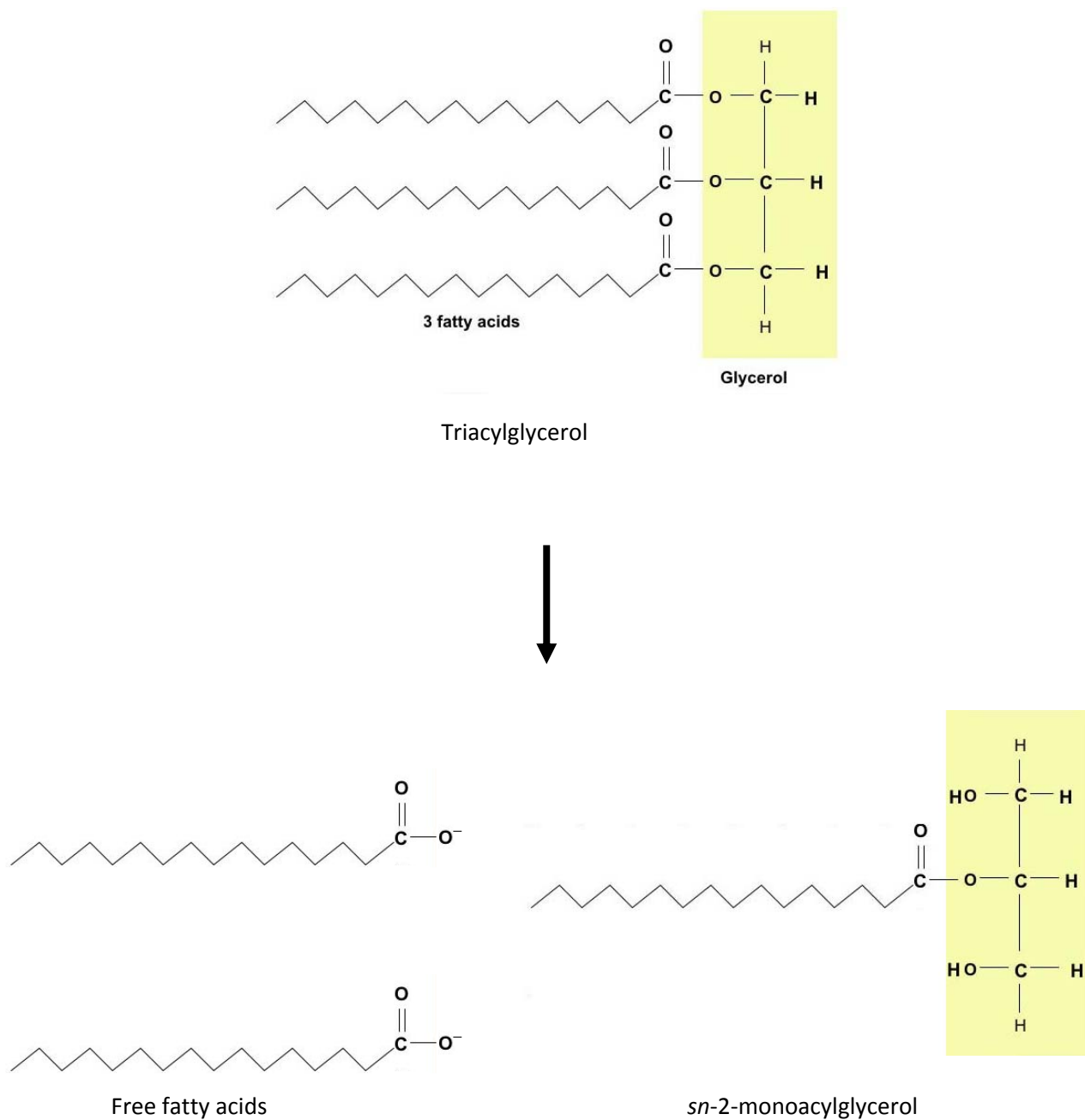
## **Chapter 1.**

### **Introduction and Review of the Literature**

## INTRODUCTION

Fat is a major source of energy in the diet and provides the essential fatty acids, linoleic acid and linolenic acid. Upon consumption, dietary fat, which is primarily in the form of triacylglycerol, is digested into its constituent fatty acids and monoacylglycerols in the gastrointestinal tract. These products are absorbed into the intestinal epithelial cells where they are re-synthesized into triacylglycerols, packaged into chylomicrons, and secreted into the lymphatic circulation for delivery to peripheral tissues. The intestine has the capacity to assimilate almost all of the dietary lipids that it receives, >95% under normal physiological conditions. In fact, certain mammals can eat up to 50g fat *per kilogram of body weight* and still absorb 97% of it, losing no more than if they were consuming only 5g/kg, which is remarkable considering the average human diet consists of much less, ~1.5g/kg (Petit et al., 2007).

Dietary fat is acted on by a series of lipases throughout the gastrointestinal tract, gastric lipase, pancreatic lipase, and bile-salt activated lipase. Gastric lipase and pancreatic lipase hydrolyze triacylglycerol's *sn*-1 and *sn*-3 fatty acids only. Even though one of the lipases, bile-salt activated lipase, has the capacity to hydrolyze *sn*-2-monoacylglycerol (Wang et al., 1983), physiological sampling has shown that the major end products of dietary fat digestion are fatty acids and *sn*-2-monoacylglycerol (Hofmann and Borgstroem, 1964) (**Figure 1**). These end products are solubilized by bile salts in the proximal small intestinal lumen and absorbed as monomers by the absorptive epithelium of the small intestine (Murota and Storch, 2005; Verkade and Tso, 2001).

**Figure 1-1**

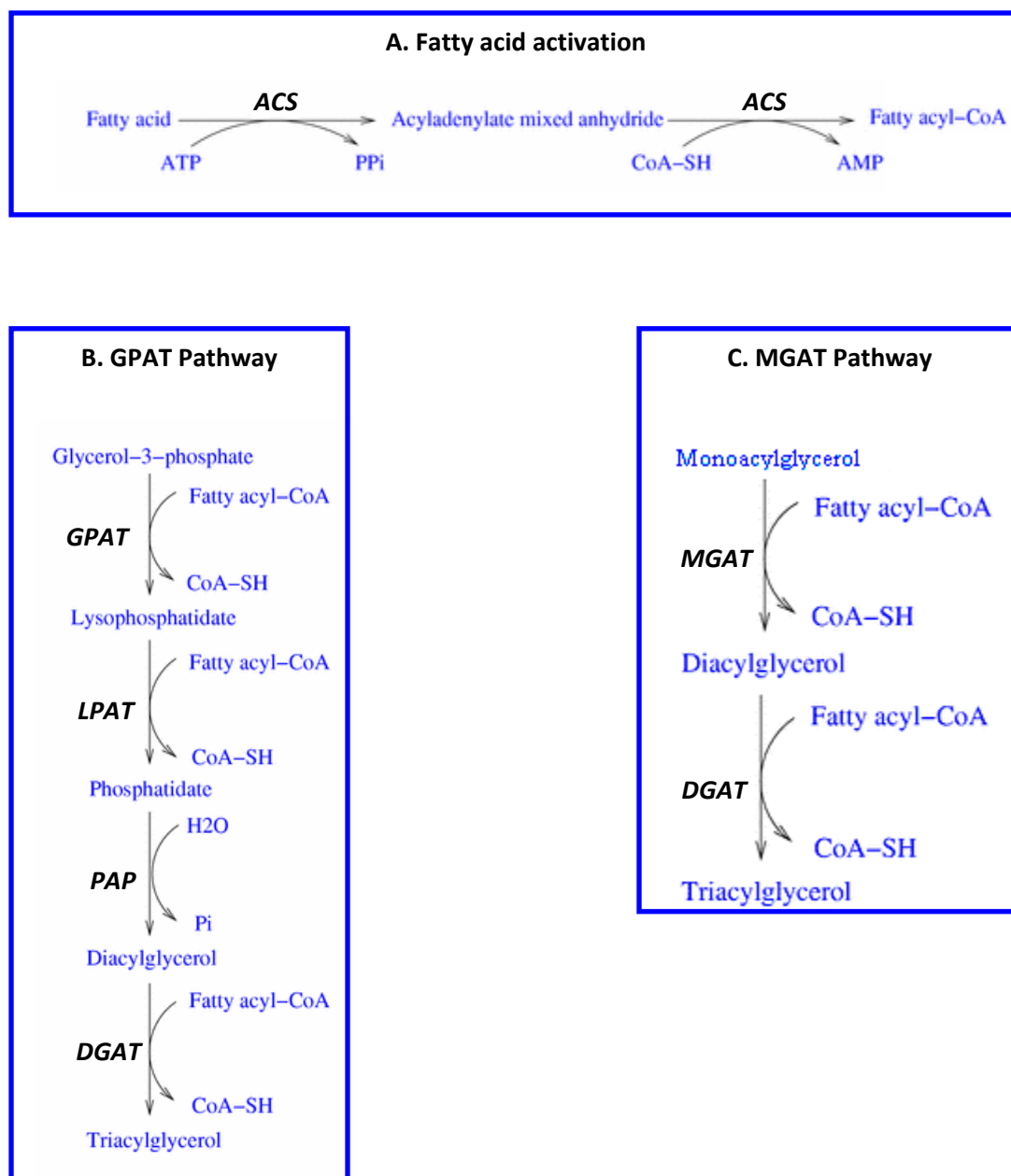
**Figure 1-1. Dietary fat digestion.** Dietary fat is largely triacylglycerol, which is comprised of three fatty acids esterified to a glycerol. During digestion in the gastrointestinal tract, triacylglycerols are hydrolyzed to fatty acids and *sn*-2-monoacylglycerol.

## *INTESTINAL LIPID METABOLISM*

The intestine is unique in its mode of triacylglycerol synthesis. Most tissues synthesize triacylglycerols via the GPAT pathway (**Figure 2**) which begins with acylation of glycerol-3-phosphate to form lysophosphatidic acid, catalyzed by glycerol-3-phosphate O-acyltransferase (GPAT, EC 2.3.1.15). The fatty acid substrates in this and the subsequent reactions are first “activated” in an ATP-dependent reaction catalyzed by acyl-CoA synthetase (ACS, EC 6.2.1.3) to form fatty acyl-CoA. Lysophosphatidic acid is then acylated to phosphatidic acid and dephosphorylated to diacylglycerol by 2-acylglycerol-3-phosphate O-acyltransferase (LPAT, EC 2.3.1.52) and phosphatidate phosphatase (PAP, EC 3.1.3.4), respectively. Finally, diacylglycerol is acylated by diacylglycerol O-acyltransferase (DGAT, EC 2.3.1.20) to form triacylglycerol, or directed toward phospholipid synthesis. Although the intestine also has the GPAT pathway, >80% of intestinal triacylglycerol synthesis occurs via the monoacylglycerol acyltransferase (MGAT) pathway (Bugaut et al., 1984). The MGAT pathway only forms triacylglycerol and consists of the sequential acylation of monoacylglycerol by 2-acylglycerol O-acyltransferase (MGAT, EC 2.3.1.22) and DGAT.

Inevitably, fatty acids and monoacylglycerol must traverse the cytosol from their point of entry at the cell’s apex (or at the basolateral surface), to the intracellular organelles where they are metabolized. As these molecules are hydrophobic and thus not highly soluble in the aqueous matrix of the cytoplasm, it is generally thought that a binding/transport protein(s) is required to enable efficient processing of these diet-derived substrates. Fatty acid-binding proteins are major candidates. The available evidence for a role of FABPs in intestinal lipid assimilation is discussed below. A major focus of my research is to understand the role of enterocyte FABPs in intestinal lipid metabolism at the cell and molecular levels.

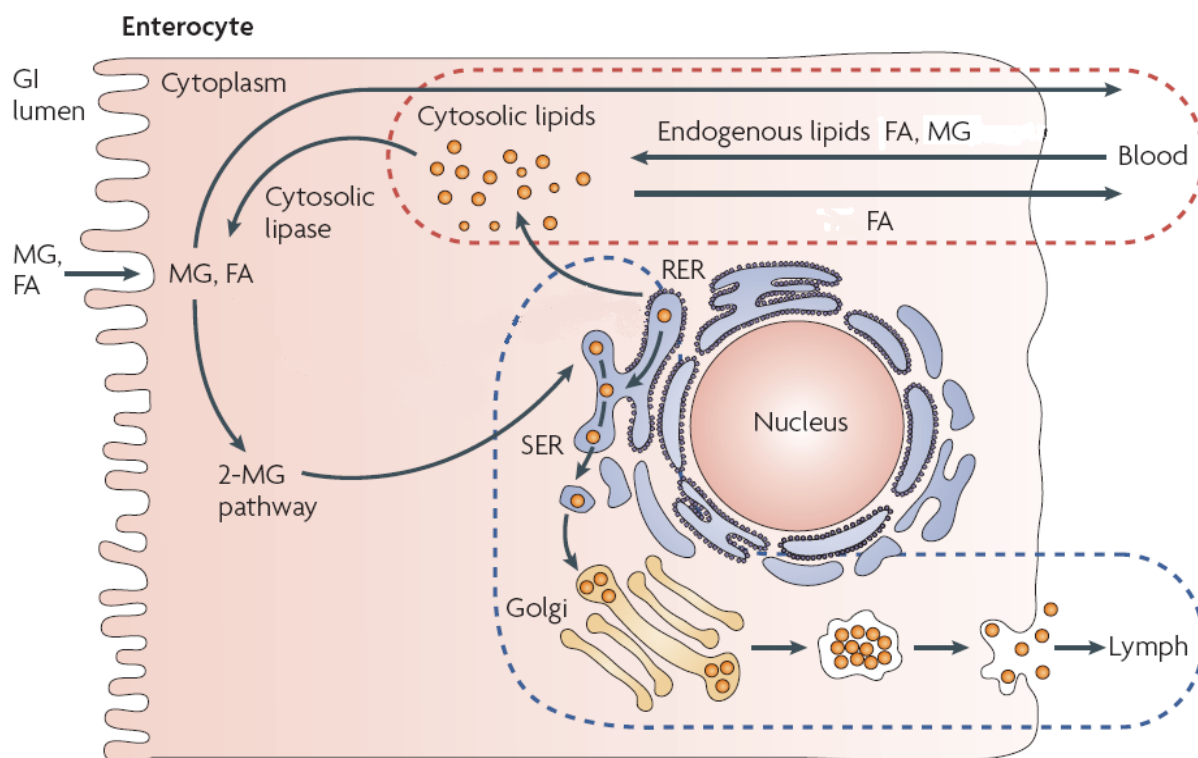
Figure 1-2



**Figure 1-2. Triacylglycerol synthesis.** A) Fatty acid activation by ACS is necessary for the subsequent acylation reactions. B) Schematic of the GPAT pathway. C) Schematic of the MGAT pathway. ACS, acyl-CoA synthetase; GPAT, glycerol-3-phosphate acyltransferase; LPAT, lysophosphatidate acyltransferase; PAP, phosphatidate phosphohydrolase; MGAT, monoacylglycerol acyltransferase; DGAT, diacylglycerol acyltransferase.

### *“COMPARTMENTATION” OF INTESTINAL LIPID METABOLISM*

The intestine obtains lipids from two distinct sources: “endogenous” from the mesenteric artery, which are presented to the basolateral surface of the enterocyte; and “dietary,” delivered directly from the small intestinal lumen to the enterocyte’s apical surface (**Figure 3**). Interestingly, evidence suggests that the manner in which lipids are presented to the enterocytes strongly dictates their fate; thus it is said the intestine exhibits “compartmental” lipid metabolism. In pioneering work by Gangl and Ockner (1975), rats were given radiolabeled fatty acids intraduodenally or intravenously and astounding compartmentation within the intestinal mucosa was observed: endogenous (intravenous) fatty acids were primarily oxidized or targeted to phospholipid synthesis while dietary (intraduodenal) fatty acids were synthesized into triacylglycerol, resulting in a considerably greater TG/PL ratio for dietary fatty acids. This was later confirmed in humans (Gangl et al., 1978). Previously, Hyun and coworkers (1967) gave rats an intragastric radiolabeled fatty acid emulsion and followed the dispersion of radioactivity in the portal vein and lymph simultaneously. They observed that dietary (intragastric) fatty acids entered the lymph as triacylglycerol, or portal vein as free fatty acids. The information from these two findings suggests that dietary free fatty acids are converted into triacylglycerols within enterocytes and are subsequently secreted into the lymph.

**Figure 1-3**

**Figure 1-3. Lipid metabolism in enterocytes.** One enterocyte is shown, with the substrates fatty acids (FA) and monoacylglycerol (MG) entering at the the apical surface (from the gastrointestinal [GI] lumen) or basolateral surface (from the bloodstream). Lumenal lipids are primarily incorporated into triacylglycerols/chylomicrons via the MGAT pathway (2-MG pathway). Bloodstream-derived lipids are primarily used for phospholipid synthesis or oxidation. Adapted from Porter et al., 2007.



Further evidence for metabolic compartmentation was obtained from cell culture studies. Using apical administration to mimic dietary fatty acids and basolateral administration to mimic endogenous fatty acids, Trotter and Storch (1991) confirmed this “compartmentation” phenomenon in cultured Caco-2 cells, a model for intestinal absorptive cells. Compared with basolateral administration, apical delivery of palmitic acid consistently favored incorporation into triacylglycerols over phospholipids, resulting in a greater TG/PL ratio. These studies were extended when Ho et al. (2002) demonstrated that in Caco-2 cells, apically administered lipids resulting in the greatest TG/PL ratio were monoolein > oleic acid > palmitic acid; and that the TG/PL ratio was lower when any of these lipids were administered to the basolateral surface. Taken together, the *in vivo* and *in vitro* studies clearly demonstrate that upon absorption, intestinal enterocytes direct fatty acids and monoacylglycerol to distinct intracellular metabolic fates depending on their sites of uptake. Recently, it has been demonstrated that compartmentation of monoacylglycerol also occurs in rat and mouse intestinal mucosa (Storch et al., 2008).

Compartmentation of intestinal lipid metabolism also extends into secreted lipoproteins. Mansbach et al., (1992) utilized an intraduodenal steady state infusion of unlabeled triolein accompanied by a [<sup>3</sup>H]oleate intravenous infusion, and analyzed mucosal and lymphatic lipids. The specific activity of chylomicron triacylglycerols was significantly lower than that of mucosal triacylglycerols, suggesting mucosal triacylglycerols derived from plasma [<sup>3</sup>H]oleate were selected against for incorporation into chylomicrons. This observation implies the presence of two functionally distinct triacylglycerol pools within the enterocyte. Nevin et al. (1995) subsequently demonstrated that the intestine directs fatty acids into two functionally and physically distinct triacylglycerol pools, one used for chylomicron synthesis and the other for storage. In these experiments, various intraduodenal lipid infusions designed to alter the

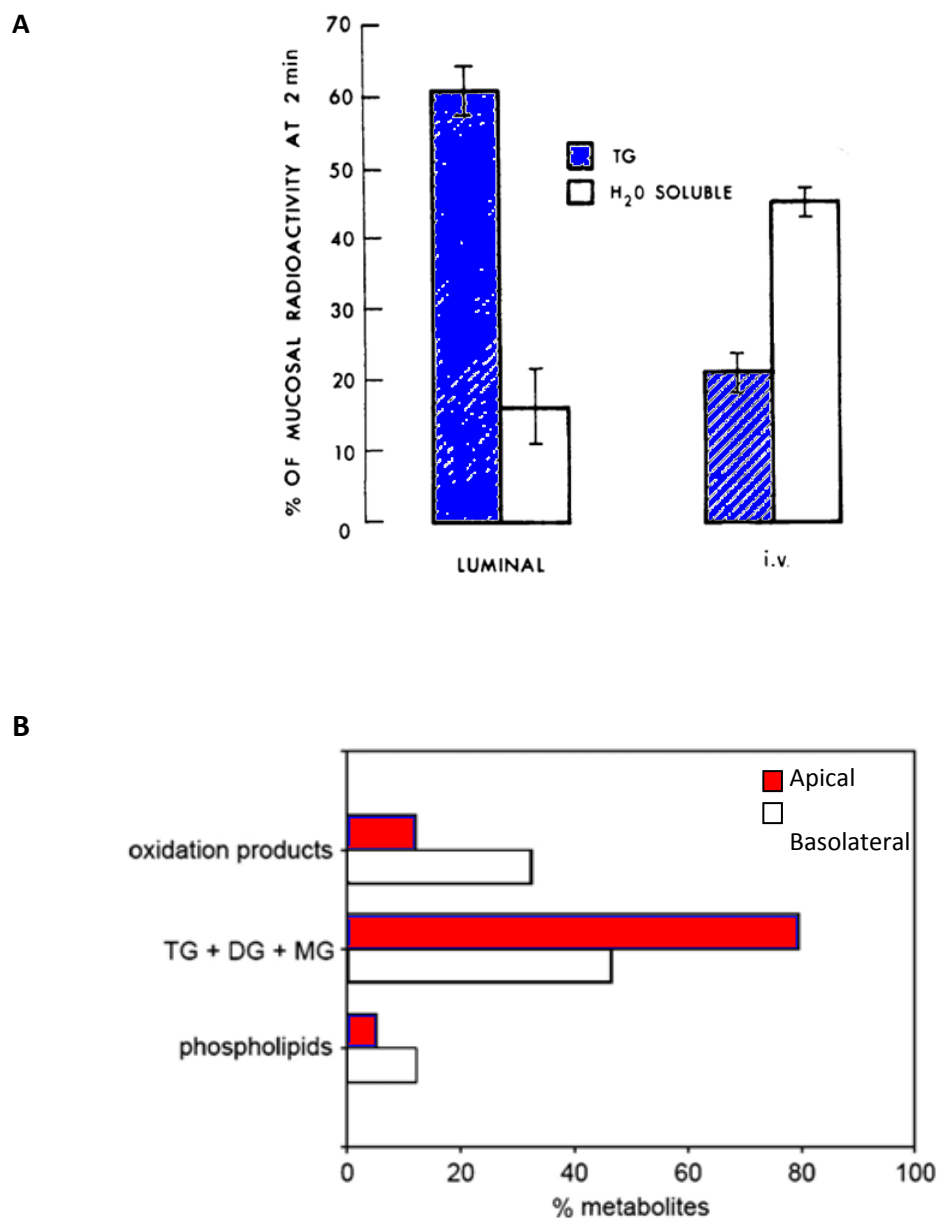
efficiency of triacylglycerol secretion into the lymph were administered to rats. Low triacylglycerol infusion rates into bile-diverted rats yielded the lowest output of lipid into the lymph and high triacylglycerol infusion rates with phosphatidylcholine yielded the greatest output of lipid into the lymph. The protocol which produced the least amount of triacylglycerol secreted into the lymph resulted in the greatest amount of administered lipids recovered in a lipase-accessible triacylglycerol storage pool, which was previously shown to be selected against as a source of chylomicron triacylglycerol. However, the condition with the greatest amount of lipid secreted into the lymph produced the exact opposite: <6% of the administered lipid was recovered in the triacylglycerol storage pool. Thus in conditions that favored triacylglycerol secretion into the lymph, absorbed lipids were directed away from the storage pool and into the pre-chylomicron triacylglycerol pool, further suggesting a functional divergence of the two intestinal triacylglycerol pools (Nevin et al., 1995).

The postprandial development of triacylglycerol storage in lipid droplets in mouse intestine was recently demonstrated, visually, by coherent anti-Stokes Raman scattering (Zhu et al., 2009). In these studies, enterocyte cytosolic lipid droplets were shown to vary in size and abundance in direct proportion to the amount of dietary fat being consumed. Interestingly, some of these lipid droplets exceeded 10 $\mu$ m in diameter, which is approximately 10-fold greater than chylomicrons; possibly suggesting that lipid from this triacylglycerol storage pool is hydrolyzed before being incorporated into chylomicrons. Earlier findings from Robertson and coworkers (2002) showed that, in humans, five hours after fat ingestion, consuming a glucose beverage stimulated intestinal triacylglycerol secretion in the form of chylomicrons (Robertson et al., 2002). Consuming plain water had no effect. Moreover, jejunal biopsies from those who consumed the glucose solution contained significantly less lipids than biopsies from the water

only group. Collectively, these results might indicate that at least a portion of chylomicron triacylglycerols are derived from an enterocyte cytosolic lipid storage pool.

In addition to the anabolic fate of fatty acids in triacylglycerol and phospholipid synthesis, the enterocyte also displays a unique fuel requirement, relying largely on glutamine for ATP production (Watford et al., 1979; Windmueller and Spaeth, 1977). This literature is relevant for two reasons: 1) As our studies have shown, LFABP is a candidate to regulate fatty acid oxidation (Chapter 3); and 2) the experimental model used by Windmueller and Spaeth confirms the results of Gangl and Ockner using a completely different methodologic approach. Utilizing an externalized intestinal segment with an intact arterial supply and complete venous drainage, Windmueller and Spaeth (1978) showed that the intestine clears approximately 1% of the total mesenteric arterial free fatty acid flux. Of this, approximately 42% is oxidized, 25% incorporated into neutral lipids and 33% incorporated into phospholipids. Endogenous fatty acids accounted for less than 3% of the total CO<sub>2</sub> released from the intestine, while the most quantitatively important contributors were ketone bodies (50%) and glutamine (35%). These results, obtained for endogenous fatty acid metabolism by the intestine, were virtually identical to those of Gangl and Ockner's (1975) experiments in an intact rat, when the intestine absorbed approximately 1% of circulating fatty acids, of which 42% were oxidized, 30% incorporated into neutral lipids and 28% in phospholipids. Taken together, the current view of intestinal lipid metabolism includes the presence of differential metabolic pathways and divergent trafficking patterns for lipid substrates.

The divergent binding of fatty acids to enterocyte FABPs depending on their site of administration (discussed below; Alpers et al., 2000) and the translocation of enterocyte FABPs upon fat feeding (Trevaksis et al., 2007) suggest that enterocyte FABPs may be involved in intestinal lipid trafficking.

**Figure 1-4**

**Figure 1-4. Graphical representation of the compartmentation observed in intestinal lipid metabolism.** A) Percent of palmitic acid incorporated into triacylglycerols (blue bars) and oxidized (open bars) in rat small intestinal mucosa two minutes after apical (luminal) or basolateral (i.v.) administration (adapted from Gangl and Ockner, 1975). B) Fate of oleic acid in mouse small intestine two minutes after apical (red bars) or basolateral (open bars) administration (adapted from Storch et al., 2008).

### *FATTY ACID BINDING PROTEINS*

Fatty acid binding proteins (FABPs) are 14-15kDa proteins that have been well-conserved throughout evolution, appearing in species as diverse as *Drosophila melanogaster*, *Caenorhabditis elegans*, dust mites, and desert locusts, but are absent in plants and fungi (Esteves et al., 2006). Although nucleotide sequence varies many-fold, FABP family members share a common protein tertiary structure: a  $\beta$ -barrel comprised of two antiparallel five-stranded  $\beta$ -pleated sheets connected by two short  $\alpha$ -helical domains (**Figure 5**). Most mammalian tissues express relatively high levels of one or more FABP. For example, liver expresses LFABP exclusively, while the intestine expresses both LFABP and IFABP (Ockner et al., 1982); IFABP expression is restricted to the intestine. FABPs are expressed at high levels particularly in tissues with high lipid flux or metabolism such as cardiac muscle, liver, intestine, and adipose. The dissociation constants of fatty acids for various FABPs are within in their physiological intracellular concentration range (Richieri et al., 1994; Knudson et al., 1999; Glatz et al., 1984), and binding to FABP highly increases their aqueous solubility. These observations have led to the suggestion that FABPs are involved in intracellular metabolism and/or translocation of fatty acids.

Nine mammalian FABPs have been identified thus far, and the characterization of mice genetically lacking one or more FABP has provided insights into their physiological functions in vivo (**Table 1**).

**Table 1-1**

FABP type	Gene	Expression	Phenotype of KO mice
LFABP	Fabp1	liver, small intestine, kidney	Defective hepatic <sup>1</sup> and intestinal fatty acid oxidation <sup>2</sup>
			Impaired intestinal monoacylglycerol metabolism <sup>2</sup>
			Blunted loss of fat-free mass when fasted <sup>2</sup>
IFABP	Fabp2	small intestine	Impaired intestinal fatty acid metabolism <sup>3</sup>
			Accelerated loss of fat mass when fasted <sup>3</sup>
HFABP	Fabp3	cardiac and skeletal muscle, brain, mammary, kidney, adrenals, ovaries, testis, placenta, lung, stomach	Defective muscle fatty acid oxidation compensated by increased glucose utilization <sup>1</sup>
AFABP	Fabp4	adipocyte, macrophages	Protected against diet-induced atherosclerosis <sup>1</sup>
			Modest decreases in plasma glucose and insulin <sup>1</sup>
			Double KO with KFABP shows strong protection against insulin resistance and hepatosteatosis <sup>1</sup>
KFABP	Fabp5	epidermis adipocyte, macrophages, mammary, tongue, testis, liver, lung, brain, heart and skeletal muscle, retina, kidney	Defective transepidermal water loss <sup>1</sup>
			No effect on AFABP expression <sup>1</sup>
			Double KO with AFABP shows strong protection against insulin resistance and hepatosteatosis <sup>1</sup>
IBABP	Fabp6	distal intestine	
BFABP	Fabp7	central nervous system	Increased anxiety and fear memory <sup>1</sup>
MFABP	Fabp8	peripheral nerve myelin	
TFABP	Fabp9	testis	

**Table 1-1. Members of the FABP family.** See text for details. Adapted from Storch and Corsico (2008). HFABP, heart FABP; AFABP, adipocyte FABP; KFABP, keratinocyte FABP; IBABP, ileal bile acid-binding protein; BFABP, brain FABP; MFABP, myelin FABP; TFABP, testis FABP. <sup>1</sup>Storch and Corsico (2008); <sup>2</sup>Chapter 3; <sup>3</sup>Chapter 2.

**Figure 1-5**

**Figure 1-5. Tertiary structure of FABPs from human, cow, and rat.** Note the similar orientation of the clamshell-like  $\beta$ -barrel (yellow) and  $\alpha$ -helical domains (red) independent of species or FABP type (Lomize et al., 2006).

### ENTEROCYTE FATTY ACID-BINDING PROTEINS

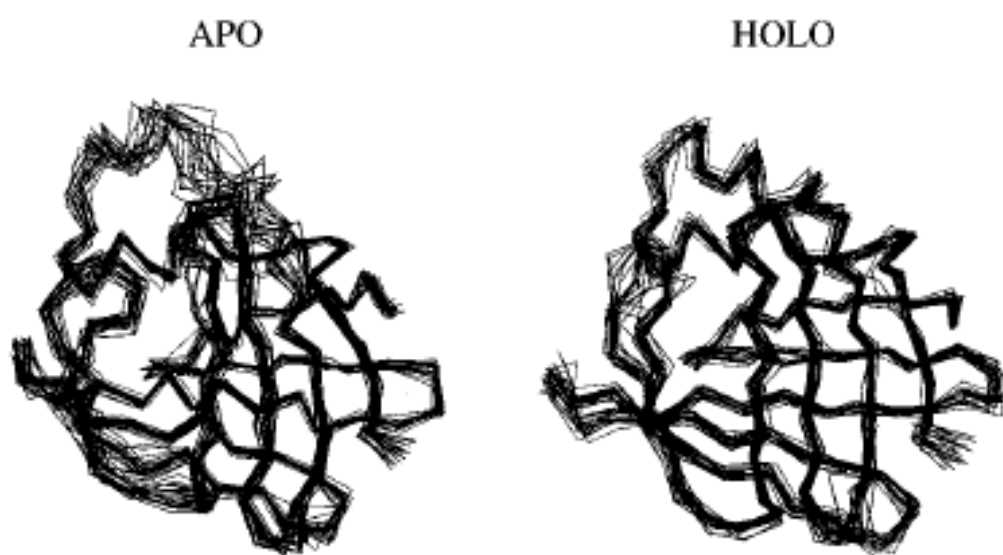
As mentioned above, the intestine expresses two FABP types: intestinal- and liver- FABP. LFABP binds long chain fatty acids, lysopholipids, monoacylglycerol, and in a molar ratio of 2FA:1FABP (1:1 for other lipids) (Storch and Thumser, 2000). IFABP binds both saturated and unsaturated fatty acids with similar affinity, and although IFABP and LFABP bind saturated fatty acids with similar affinity, LFABP binds unsaturated fatty acids with greater affinity. For example, the dissociation constants for stearic acid (18:0) and linolenic acid (18:3n3) binding to IFABP are 6nM and 380nM, respectively, while for LFABP they are 9nM and 69nM, respectively (Richieri et al., 1994).

What is the significance of a single cell type having high expression of two related proteins? Evolution rarely displays complete functional redundancies, suggesting that these two proteins have divergent roles in intestinal lipid metabolism. The lack of complete overlap in substrate specificity may provide some clues as to their roles, although additional evidence was provided by Hsu and Storch (1996). In a series of *in vitro* studies using purified FABPs and model membranes, the rate of fatty acid transfer from IFABP to acceptor vesicles was found to be much faster than from LFABP, and was not affected by ionic strength of the buffer, but was sensitive to the composition and concentration of acceptor vesicles. It was concluded that fatty acid transfer from IFABP occurs via a collisional mechanism, whereas transfer from LFABP was dependent on fatty acid solubility in the aqueous phase, in other words, it occurs by a diffusional mechanism. Moreover, fatty acids are transferred both to and from FABPs and as seen in **Figure 6**, Hodson and coworkers (1997) have demonstrated by NMR spectroscopy that IFABP exhibits marked backbone variability in the apo- relative to holo form. Therefore it is possible that since IFABP fatty acid transfer is mediated collisionally, perhaps apo-IFABP interacts differently, or with a different type of membrane than holo-IFABP, which would imply



that IFABP may be involved in fatty acid targeting to specific membranes. Moreover, IFABP's  $\alpha$ -helical domain was found to be critical for its collisional transfer mechanism, and further studies demonstrated the importance of electrostatic and hydrophobic interactions in determining the fatty acid transfer rate (Corsico et al., 1998; Corsico et al., 2005). On the other hand, LFABP's diffusional mechanism could mean that it acts primarily as a buffer for excess fatty acids, a notion that would be indirectly supported by its upregulation by dietary fat (Drozdzowski et al., 2004). Alternatively, LFABP may be involved in targeted delivery of long chain fatty acids to particular proteins. Indeed, as discussed below, evidence for a role for hepatic LFABP in fatty acid uptake, oxidation, and incorporation into TG, obtained in studies of the LFABP-null mouse (Davidson et al., 2003; Erol et al., 2003), suggests a more specific role; however it remains possible that the changes are caused by alterations in the cytosolic free fatty acid concentrations brought about by the absence of LFABP.

Luxon and Milliano (1999) provided direct support for a role of FABP in intestinal lipid transport in a physiological setting. By using fluorescence recovery after photobleaching, they observed that intracellular diffusion of a non-metabolizable fluorescent fatty acid analog (NBD-stearate) was higher in the jejunum than in the duodenum and ileum, and directly proportional to the local FABP concentration. This relationship seems to be very specific for FABP because it remains true in various unrelated conditions where FABP concentration is known to be altered, such as in female versus male hepatocytes, and clofibrate-treated versus control hepatocytes (Luxon et al., 1996). Furthermore, when hepatocytes were incubated with bromopalmitate, an inhibitor of fatty acid-binding to FABP, NBD-stearate diffusion decreased while the amount recovered in membrane fractions increased proportionately. These studies in liver and intestinal cells strongly suggest that IFABP and/or LFABP is involved in the transport of fatty acids after their entry into the cell.

**Figure 1-6**

**Figure 1-6. NMR solution structure of apo- and holo-IFABP.** 20 superimposed backbone structures of apo-IFABP and oleate-bound holo-IFABP. Note the increased backbone variability in apo-IFABP (Hodson et al., 1997).

*EVIDENCE FOR A ROLE OF LFABP IN INTESTINAL LIPID METABOLISM*

There are correlations between LFABP and intestinal lipid metabolism that collectively point toward a physiological relationship. LFABP mRNA levels are the highest in the part of the intestine that is exposed to and absorbs the most dietary fat (Agellon et al., 2002). Upon initiation of a high fat diet, intestinal LFABP is rapidly upregulated greater than 2.5-fold, and remains elevated commensurate with the dietary fat content (Petit et al., 2007). Interestingly, in the study by Petit and coworkers (2007), high fat diet-fed mice exhibited normal intestinal triacylglycerol secretion, relative to chow-fed mice, after an oral lipid bolus. Thus, it is possible that during a high fat diet, elevated intestinal LFABP expression helps to maintain normal lipemia despite increased fat intake.

As mentioned above, LFABP binds fatty acids with high affinity. The digestive products present in the post-prandial intestinal lumen should contain approximately half as much monoacylglycerol as fatty acids; monoacylglycerol is a major end product of dietary triacylglycerol digestion. There is controversy, however, about the ability of LFABP to bind monoacylglycerol in a physiologically relevant manner. A study by Thumser and coworkers showed that monoacylglycerol was unable to displace a fluorescent short chain fatty acid analog from LFABP, and they concluded that LFABP had no appreciable binding affinity for monoacylglycerol (Thumer et al., 1996). However, Storch and coworkers, using a different experimental approach, showed that LFABP did bind monoacylglycerol, albeit with 10-fold less affinity than fatty acids (Storch et al., 1993; unpublished findings). Importantly, the steady-state solution structure for an LFABP-monoacylglycerol complex has been recently solved via NMR spectroscopy (unpublished findings), further supporting the idea that LFABP does indeed bind monoacylglycerol. It is thus not unreasonable to suppose from these studies, collectively, that LFABP is involved in intestinal monoacylglycerol, as well as fatty acid, metabolism. A portion of

my dissertation research was to determine the monoacylglycerol-binding capability of LFABP in a physiological setting, namely liver cytosol.

#### *LFABP<sup>-/-</sup> MOUSE*

Research on LFABP-null mice has primarily focused on the liver-specific effects of LFABP deletion. More specifically, it was shown that LFABP<sup>-/-</sup> hepatocytes exhibit impaired fatty acid uptake, oxidation, and incorporation into triacylglycerols (Davidson et al., 2003; Newberry et al., 2003; Erol et al., 2003). A portion of my studies were to determine the intestinal and systemic effects of LFABP gene deletion in mice.

#### *EVIDENCE FOR A ROLE OF IFABP IN INTESTINAL LIPID METABOLISM*

IFABP expression first appears at parturition and is increased by a high fat diet (Gordon et al., 1985; Ockner and Manning, 1974). As mentioned above, IFABP expression is restricted to the intestine, where it is co-expressed with liver fatty acid-binding protein (LFABP). Alpers et al. (2000) utilized an intestinal explant and FABP type-specific antibodies to determine the amount of added radioactive fatty acids that would be bound by IFABP and LFABP after apical versus basolateral administration. Although more fatty acids bound to LFABP regardless of administration site, slightly more fatty acids bound to IFABP during apical administration than with basolateral administration, suggesting a relative “apical” localization of IFABP. This is in accord with our observation (Chapter 2) that IFABP ablation affected apical but not basolaterally-derived fatty acid metabolism. High fat feeding increases both IFABP and LFABP content in rat intestine (Drozdowski et al., 2004) and significantly increased FA-binding to IFABP but not LFABP (Alpers et al., 2000). If the intestine contains a pre-chylomicron triacylglycerol pool and separate storage/pre-VLDL triacylglycerol pool, as suggested by Nevin et al. (1995) and

Tso et al. (1984), these findings might imply that IFABP sequesters fatty acids for the secretory pre-chylomicron TG pool. Moreover, we found that IFABP ablation reduces the incorporation of diet-derived fatty acids into triacylglycerol relative to phospholipids. Taken together, these findings support a role for IFABP in intestinal lipid metabolism, however the precise mechanisms of its involvement are not yet clear.

#### *IFABP POLYMORPHISM AT CODON 54*

There is a polymorphism in the gene coding for IFABP which results in a substitution of threonine for alanine at codon 54. Estimates for the frequency of the threonine-coding allele, I(A54T), vary somewhat with different populations, and have been reported as 0.28-0.34 (Gomez et al., 2007; Yamada et al., 1997). I(A54T) has been associated with postprandial and fasting lipemia in human populations, suggesting both direct (postprandial) and indirect (fasting) effects on plasma triacylglycerol levels (Agren et al., 1998; Georgopoulos et al., 2000; Dworatzek et al., 2004). The IFABP mutant I(A54T) has a two-fold greater affinity for long-chain fatty acids than the wild-type form (Baier et al., 1995; Storch et al., 2002) and increased triacylglycerol secretion was observed when I(A54T) was overexpressed in Caco-2 cells, relative to an I(T54A) overexpressing line (Baier et al., 1996). Similar results were found in human fetal intestinal explants: possession of at least one threonine-encoding allele was associated with increased secretion of nascent triacylglycerol, increased apolipoprotein B synthesis, and increased chylomicron but not VLDL secretion (Levy et al., 2001). Interestingly, the IFABP polymorphism A54T was found to be associated with resistance to alcoholic cirrhosis (Salguero et al., 2005), suggesting an indirect role for IFABP in mediating specific hepatic effects.

### *IFABP<sup>-/-</sup> MOUSE*

Mice lacking IFABP were generated by Vassileva et al. (2000). Male IFABP<sup>-/-</sup> were heavier than WT on a chow diet, and this difference was slightly attenuated by a high fat diet. Female IFABP<sup>-/-</sup>, on the other hand, were no heavier on chow and gained less weight on a high fat diet. Agellon and coworkers later demonstrated that after a high fat diet enriched with beef tallow or safflower, male but not female IFABP<sup>-/-</sup> weighed more than WT and developed fatty livers (Agellon et al. 2007), further suggesting a gender-specific role of IFABP in energy partitioning. Moreover, and in direct contrast to LFABP<sup>-/-</sup>, IFABP<sup>-/-</sup> are hyperinsulinemic and hypertriglyceridemic (Vassileva et al., 2000). Interestingly, IFABP<sup>-/-</sup> and I(A54T) seem to have opposite effects on the liver. And although their effects on plasma lipids appear similar, as will be shown below, IFABP-ablation does not change the lipemic response to a large oral lipid load.

Most of the research on the function of IFABP has centered on its *in vitro* binding characteristics and regulation of expression by dietary fat. Therefore, parts of my studies were focused on determining the lipid metabolic and systemic effects of IFABP gene deletion in mice.

### *SPECIFIC AIMS*

#### **SPECIFIC AIM 1: To examine the role of IFABP in intestinal lipid metabolism and energy**

**homeostasis.** Intestinal lipid composition, lipid metabolism, and secretion were analyzed in WT and IFABP<sup>-/-</sup> mice, and the cause of the differences in acute fatty acid metabolism was further explored to determine if IFABP functioned as a fatty acid trafficking protein *in vivo*. The systemic effects of IFABP ablation were assessed by measuring energy expenditure, respiratory quotient, and body composition in fed and fasted WT and IFABP<sup>-/-</sup> mice.

#### **SPECIFIC AIM 2: To examine the role of LFABP in intestinal lipid metabolism and energy**

**homeostasis.** Intestinal lipid composition, lipid metabolism, and secretion were analyzed in WT and LFABP<sup>-/-</sup> mice, and causes of the differences in fatty acid oxidation and monoacylglycerol metabolism were further explored to determine their mechanism. The systemic effects of LFABP ablation were assessed by measuring energy expenditure, respiratory quotient, and body composition in fed and fasted WT and LFABP<sup>-/-</sup> mice.

#### **SPECIFIC AIM 3: To determine whether LFABP is a monoacylglycerol-binding protein in liver.**

Monoacylglycerol metabolism was altered in LFABP<sup>-/-</sup> intestinal mucosa and enzyme levels were unchanged. Reports on the ability of LFABP to bind monoacylglycerol have been mixed, therefore, this issue was addressed using cytosol preparations and gel filtration chromatography.

## **Chapter 2.**

**Differential partitioning of fatty acids in enterocytes from  
intestinal fatty acid-binding protein-null (IFABP<sup>-/-</sup>) mice**



**ABSTRACT**

Intestinal fatty acid-binding protein (IFABP) is expressed at high levels in the mammalian small intestine and binds the major product of dietary triacylglycerol digestion, fatty acids. The precise role of IFABP in processing these diet-derived lipids is unknown. IFABP-null mice appear to grow normally and absorb dietary fat similar to their wild-type (WT) counterparts. We investigated the acute metabolism of fatty acids in fasted WT and IFABP<sup>-/-</sup> small intestinal mucosa *in vivo*. Two minutes after intraduodenal administration of [<sup>14</sup>C]oleate, mucosal [<sup>14</sup>C] was recovered primarily in triacylglycerols, with no difference between WT and IFABP<sup>-/-</sup>. However, recovery of [<sup>14</sup>C]oleate in the phospholipid fraction was significantly greater in IFABP<sup>-/-</sup> mice ( $p < 0.01$ ), resulting in a reduced TG/PL ratio. No changes were found in the expression of IFABP or lipid synthetic genes, suggesting the results may be due to a non-transcriptional, trafficking function of IFABP. Appearance of triacylglycerols and [<sup>14</sup>C] in plasma after an oral gavage of [<sup>14</sup>C]oleate in olive oil was unaffected by IFABP ablation, supporting the hypothesis that newly synthesized phospholipids are not a major source of chylomicron phospholipids. Food deprivation increased [<sup>14</sup>C]oleate oxidation in WT and IFABP<sup>-/-</sup> mucosa similarly. The expression of genes involved in intestinal fatty acid oxidation were also unchanged by IFABP ablation. Overall, given the absence of transcriptional changes, the effects of IFABP ablation on metabolism suggest it may be involved in fatty acid trafficking into complex lipids, perhaps directing fatty acids toward triacylglycerol rather than phospholipid synthesis.

## INTRODUCTION

### *INTESTINAL FATTY ACID-BINDING PROTEIN*

IFABP is a member of the 14-15kDa intracellular fatty acid binding protein family and is expressed at high levels in the absorptive epithelium of the intestine. IFABP expression first appears at parturition and is increased by a high fat diet (Gordon et al., 1984; Ockner and Manning, 1974). Utilizing a series of fluorescence resonance energy transfer assays, Storch and coworkers demonstrated that IFABP obtains and transfers long chain fatty acids by directly interacting with phospholipid membranes (Thumser and Storch, 2000; Hsu and Storch, 1996). Moreover, IFABP's  $\alpha$ -helical domain was found to be critical for its collisional transfer mechanism, and further studies demonstrated the importance of electrostatic and hydrophobic interactions in determining the fatty acid transfer rate (Corsico et al., 1998; Corsico et al., 2005).

As mentioned above, IFABP expression is restricted to the intestine, where it is co-expressed with liver fatty acid-binding protein (LFABP). IFABP binds both saturated and unsaturated fatty acids with similar affinity, and although IFABP and LFABP bind saturated fatty acids with similar affinity, LFABP binds unsaturated fatty acids with greater affinity. For example, the dissociation constants for stearic acid (18:0) and linolenic acid (18:3n3) binding to IFABP are 6nM and 380nM, respectively, while for LFABP they are 9nM and 69nM, respectively (Richieri et al., 1994). Due to this highly specific interaction, it is likely that long chain fatty acids are the major physiological ligand for IFABP.

Alpers et al. (2000) utilized an intestinal explant and FABP type-specific antibodies to determine the amount of added radioactive fatty acids that would be bound by IFABP and LFABP after apical versus basolateral administration. Although more fatty acids bound to LFABP regardless of administration site, slightly more fatty acids bound to IFABP during apical administration than with basolateral administration suggesting a relative "apical" localization of

IFABP. High fat feeding increases both IFABP and LFABP content in rat intestine (Drozdowski et al., 2004) and significantly increased FA-binding to IFABP but not LFABP (Alpers et al., 2000). If the intestine contains a pre-chylomicron triacylglycerol pool and separate storage/pre-VLDL triacylglycerol pool, as suggested by Nevin et al. (1995) and Tso et al. (1984), these findings might imply that IFABP sequesters fatty acids for the secretory pre-chylomicron TG pool. Moreover, as will be shown below, IFABP ablation reduces the incorporation of fatty acids into triacylglycerol relative to phospholipids (Lagakos et al., unpublished observations). Also, when wild-type IFABP was overexpressed in Caco-2 cells, a dose-dependent decrease in incorporation of palmitic acid into complex lipids was observed (Darimont et al., 2000). Taken together, these findings provide support for a role for IFABP in intestinal lipid metabolism, however the precise mechanisms of its involvement are not yet clear.

#### *IFABP POLYMORPHISM AT CODON 54*

There is a polymorphism in the gene coding for IFABP which results in a substitution of threonine for alanine at codon 54. Estimates for the frequency of the threonine-coding allele, I(A54T), varies slightly among different populations, in the range of 0.28-0.34 (Gomez et al., 2007; Yamada et al., 1997). I(A54T) has been associated with postprandial and fasting lipemia in human populations, implying both direct (postprandial) and indirect (fasting) effects on plasma triacylglycerol levels (Agren et al., 1998; Georgopoulos et al., 2000; Dworatzek et al., 2004). The IFABP mutant I(A54T) has a two-fold greater affinity for long-chain fatty acids than the wild-type form (Baier et al., 1995; Storch et al., 2002) and increased triacylglycerol secretion was observed when I(A54T) was overexpressed in Caco-2 cells relative to an I(T54A) overexpressing line (Baier et al., 1996). Similar results were found in a human fetal intestinal explant: I(A54T) was associated with increased secretion of nascent triacylglycerol, increased apolipoprotein B

synthesis, and increased chylomicron but not VLDL secretion (Levy et al., 2001). Interestingly, the IFABP polymorphism A54T was found to be associated with resistance to alcoholic cirrhosis (Salguero et al., 2005), suggesting an indirect role for IFABP in mediating specific hepatic effects.

#### *IFABP<sup>-/-</sup> MOUSE*

Mice lacking IFABP were generated by Vassileva et al. (2000). Male IFABP<sup>-/-</sup> were heavier than WT on a chow diet, and this difference was slightly attenuated by a high fat diet. Female IFABP<sup>-/-</sup>, on the other hand, were no heavier on chow and gained less weight on a high fat diet. Agellon and coworkers later demonstrated that after a high fat diet enriched with beef tallow or safflower, male but not female IFABP<sup>-/-</sup> weighed more than WT and developed fatty livers (Agellon et al., 2007), further suggesting a gender-specific role of IFABP in energy partitioning. Moreover, and in contrast to LFABP<sup>-/-</sup>, IFABP<sup>-/-</sup> were found to be mildly hyperinsulinemic and hypertriglyceridemic (Vassileva et al., 2000). Interestingly, IFABP<sup>-/-</sup> and I(A54T) seem to have opposite effects on the liver. And although their effects on plasma lipids appear similar, IFABP-ablation does not change the lipemic response to a large oral lipid load (**Figure 2-11**).

Most of the research on IFABP's function has centered on the in vitro binding characteristics, regulation of expression by dietary fat, and hepatic effects of gene ablation. Therefore, the focus of this portion of my research is to explore the role of IFABP in intestinal lipid metabolism and energy homeostasis by comparing IFABP-null and wild-type mice.

## MATERIALS AND METHODS

### *a. Materials*

Oleic acid and *sn*-2-monoolein were obtained from NuChek Prep, Inc. (Elysian, MN). [<sup>3</sup>H]oleic acid ([9,10-<sup>3</sup>H]oleic acid, 26.3 Ci/mmol) and [<sup>14</sup>C]oleic acid ([1-<sup>14</sup>C]oleic acid, 54 mCi/mmol) were obtained from Perkin Elmer-New England Nuclear (Stelton, CT). [<sup>3</sup>H]monoolein (*sn*-2-[9,10-<sup>3</sup>H]monoolein, 40–60 Ci/mmol) was from American Radiochemical (St. Louis, MO). Authentic neutral lipid and PL standards were purchased from Doosan Serdary Research Laboratories (Toronto, Canada) and Avanti Polar Lipids (Alabaster, AL), respectively. Sodium taurocholate (TC) was purchased from Calbiochem (La Jolla, CA), and FA-free BSA was obtained from Sigma Aldrich (St. Louis, MO). TLC plates (Silica Gel G, 250 μm, 150Å) were obtained from Whatman (South Plainfield, NJ). Rabbit antibodies to purified rat LFABP and IFABP were generated by Affinity Bioreagents (Golden, CO). All other materials were reagent grade or better.

### *b. Animals*

IFABP<sup>-/-</sup> mice on a C57BL/6J background were created by Vassileva and coworkers (Vassileva et al., 2000). They were back-crossed with C57BL/6J mice 6 times and were therefore considered to be >98% congenic. The IFABP<sup>-/-</sup> mice were provided to us by L.B. Agellon. Wild-type mice from Jackson Laboratories (Bar Harbor, ME) were used as controls. Mice were used at 3-4 months of age and 25-30g body weight. Experiments were performed in the fasted state, typically between 8 AM and 11 AM when food was removed 48 hours earlier. Animals were maintained on a 12 hour light and dark cycle and fed Purina standard rodent chow (60% carbohydrate, 12% fat, 28% protein by kcal).

### *c. Preparation of lipids for bloodstream administration*

Stock solutions were prepared by drying (per mouse) 7.5 $\mu$ Ci [ $^{14}$ C]oleate (140nmol) under a nitrogen stream, then adding 0.5% (final volume) ethanol, and 150 $\mu$ L of a solution containing 0.1M NaCl and mouse serum (1:1).

*d. Preparation of lipids for intraduodenal administration*

Stock solutions were prepared by drying (per mouse) 1.5 $\mu$ Ci [ $^{14}$ C]oleate (28nmol) under a nitrogen stream, then adding 150 $\mu$ L of 10mM sodium taurocholate in 0.1M NaCl.

*a. Surgical procedures*

The mice were weighed and anesthetized with ketamine/xylazine/ace promazine (80/100/150mg/kg, intraperitoneal, respectively). For intravenous administration, the jugular vein was exposed and cannulated, and a 28-gauge needle with the injection solution was secured in place by surgical string. For intraduodenal administration, a small section of the intestine was exposed and a small incision was made with microsurgical scissors within 1cm of the pylorus. A blunt-tip 18-gauge needle was passed into the intestine via the incision and secured in place by surgical string. Next, for both methods of delivery, two minutes after the injection, the intestine was removed and measured lengthwise, rinsed with 60mL ice-cold 0.1M NaCl, opened longitudinally and mucosa scraped with glass microscope slides into tubes in dry ice.

*b. Immunoblotting*

Mucosa was harvested as described above and homogenized in 20 volumes of PBS pH 7.4 with 0.5% (v/v) protease inhibitors (Sigma 8340) on ice with a Potter-Elvehjem homogenizer. Protein concentration was determined by the Bradford assay (Bradford, 1976). 50 $\mu$ g of total cell protein was loaded onto 12% polyacrylamide gels and separated by SDS-PAGE. The proteins were transferred onto polyvinylidene difluoride membranes using a semi-dry transfer system (BioRad) for 1 h at 20V. The membranes were incubated in a 5% nonfat dry milk or 2% gelatin blocking solution overnight at 4°C and then probed with primary antibody for 1h. After thorough

washing, blots were then incubated with anti-rabbit, -chicken, or -mouse IgG-horseradish peroxidase conjugate, as necessary, for 1h and then developed by chemiluminescence (ECL reagent, GE Healthcare, Piscataway, NJ). Protein expression was quantified densitometrically with ImageJ software (NIH).

*c. Lipid extraction and metabolite analysis*

The mucosal samples were diluted with 20 volumes of PBS pH 7.4 per gram (wet weight) with 0.5% (v/v) protease inhibitors (Sigma 8340), homogenized by 20 strokes with a Potter-Elvehjem homogenizer on ice, and stored at -80°C for lipid extraction within two days. The homogenate was diluted to a protein concentration of 1mg/mL and 1mL was used for lipid extraction. Lipids were extracted using chloroform-methanol (2:1; v/v) by the method of Folch, Lees, and Sloane-Stanley (1957). The organic lipid layer was dried under a nitrogen stream, re-suspended in chloroform/methanol (2:1) and spotted onto Silica gel-G TLC plates along with standards of known mass. The TLC plate was developed in a nonpolar solvent system consisting of hexanes, diethyl ether, and acetic acid (70:30:1 v/v). For experiments where  $^{14}\text{C}$  was used, radioactivity was visualized by exposure to phosphorimager plates and analyzed by the Storm 840 Phosphorimager. When  $^3\text{H}$  was used, the lipid spots were visualized by exposure to iodine vapors, and scraped into scintillation vials containing 5mL scintillation fluid. The scintillation vials were vortexed and allowed to settle overnight before analysis in a scintillation counter.

*d. Mucosal lipid composition*

To determine mucosal lipid composition, the intestinal mucosa was harvested as described above, however the intestine was divided equally into two segments (proximal and distal) prior to scraping the mucosa. Thin-layer chromatography of extracted lipids and known amounts of standards was performed as described above and the iodine-stained TLC plates

were scanned by a Hewlett-Packard Scanner. Absolute values for the masses of individual lipid subclasses were obtained by a densitometric analysis using ImageJ software.

*e. Fatty acid oxidation*

Fatty acid oxidation was measured by the method of Ontko and Jackson (1964) with minor modifications. In brief, 1mL of 1mg/mL sample homogenate was incubated in a 15mL test tube with a smaller 0.5mL Eppendorf tube containing tissue paper soaked in 1M benzethonium hydroxide to capture released  $^{14}\text{CO}_2$ . 1mL of 7% PCA was added to the homogenate to release  $^{14}\text{CO}_2$  and selectively solubilize [ $^{14}\text{C}$ ]acid-soluble metabolites by reducing the solubility of remaining [ $^{14}\text{C}$ ]oleate. The tube was capped quickly and incubated overnight at 37°C with shaking. The radioactivity of the tissue paper and a sample from the 3000 x g supernatant of the acidified homogenate was analyzed by scintillation counting. The sum of the radioactivity contained in the supernatant and in the tissue paper was divided by the total amount of radioactivity contained in 1mg of the sample homogenate to determine the percent of fatty acids oxidized.

*f. Quantitative RT-PCR for mRNA expression analysis*

The protocol for mRNA acquisition and analysis was adapted from Chon et al. (2008). Briefly, tissues were homogenized in 4M guanidinium thiocyanate, 25mM sodium citrate, 0.1M  $\beta$ -mercaptoethanol using several strokes of a Polytron. Total RNA was further purified by phenol extraction and the RNeasy clean up kit (Qiagen, Valencia, CA) along with DNase treatment to minimize genomic DNA contamination. Reverse transcription was performed using 1 $\mu$ g of RNA, random primers, an RNase inhibitor, and reverse transcriptase (Promega Madison, WI) in a total volume of 25  $\mu$ L. Primer sequences were retrieved from Primer Bank (Harvard Medical School QPCR primer data base, **table 2-1**). The efficiency of PCR amplification was analyzed for all primers to confirm similar amplification efficiency. Real time PCR reactions were performed in



triplicate using an Applied Biosystems 7300 instrument. Each reaction contained 80ng cDNA, 250nM of each primer, and 12.5 $\mu$ l of SYBR Green Master Mix (Applied Biosystems, Foster City, CA) in a total volume of 25  $\mu$ l. Relative quantification of mRNA expression was calculated using the comparative Ct method normalized to  $\beta$ -actin.

*g. Body weight*

Mice were as described in *Animals*. Body weight was measured weekly on a continuous basis over the course of 4-6 months after birth.

*h. Food intake*

For the measurement of food intake, mice were individually housed in wire-mesh bottomed metabolic cages and a known amount of food was given to each mouse. The 'crumbs' were collected regularly and the remaining food was weighed weekly. The crumb weight was subtracted from the gross food intake, and the difference divided by 7 to give the average daily food consumption. This was performed for 1-2 weeks per mouse and weekly results were averaged. Week-to-week measurements were consistent.

*i. Fecal composition*

Two days worth of feces were collected at various time points during the feeding study for analysis of fecal weight and lipid composition. The feces were dried and weighed, then 1mg (dry weight) was dissolved in 10mL water overnight and 1mL was used for lipid extraction as described above.

*j. Body Composition*

Body composition was analyzed by dual energy x-ray absorptiometry (DEXA, PIXImus; GE-Lunar Corp., Madison, WI) in fed mice and after 48h food deprivation. Total fat, lean, and bone mineral mass were evaluated excluding the head and tail. Mice were anesthetized with

ketamine/xylazine/ace promazine (80/ 100/150mg/kg, intraperitoneal, respectively) for the procedure.

*k. Energy expenditure*

Energy expenditure was assessed by the University of Cincinnati's Mouse Metabolic Phenotyping Center. Mice were placed in an indirect calorimetry chamber 3 hours prior to the dark phase (3pm) and oxygen consumption and carbon dioxide production were measured for 24 hours. The data obtained from 6am to 3pm the following day were averaged and represent "fed" values. At 3pm on day 2, food was removed and measurements continued for 18 hours. The data obtained from 6am to 9am the following day (15-18 hours after food was removed) were averaged and represent "fasted" values. Metabolic rate data are expressed as kcal/hr and kcal/hr/kg body weight, and gas exchange data are expressed as mL/kg/min.

*l. Oral fat tolerance test*

An oral fat tolerance test was performed as described in Newberry et al. (2006). Briefly, 10 $\mu$ Ci of [ $^{14}$ C]oleate and [ $^3$ H]monoolein were dried under a nitrogen stream. 500 $\mu$ L of olive oil was added and the solution was vortexed vigorously. The olive oil bolus was administered via oro-gastric gavage to conscious, overnight fasted mice. 30 minutes prior to the gavage, Tyloxapol was injected (500mg/kg i.p.) to block peripheral lipoprotein clearance. 50 $\mu$ L of blood was taken from the saphenous veins immediately prior to, and at 1, 2, and 4hrs post-gavage.

*m. Statistical methods*

Statistical comparisons were performed using independent two-sided t-tests, or ANOVA. Differences were considered significant if the p-value was less than 0.05.

**Table 2-1****qPCR primer sequences**

$\beta$ -ACTIN	forward reverse	5'-GGC TGT ATT CCC CTC CAT CG-3' 5'-CCA GTT GGT AAC AAT GCC ATG T-3'
MGAT2	forward reverse	5'-TGG GAG CGC AGG TTA CAG A-3' 5'-CAG GTG GCA TAC AGG ACA GA-3'
ER GPAT (GPAT3)	forward reverse	5'-TAT CCA AAG AGA TGA GTC ACC CA-3' 5'-CAC AAT GGC TTC CAA CCC CTT-3'
MT GPAT (GPAT1)	forward reverse	5'- CTG CTT GCC TAC CTG AAG ACC-3' 5'- GAT ACG GCG GTA TAG GTG CTT-3'
DGAT1	forward reverse	5'-TGT TCA CGT CAG ACA GTG GTT-3' 5'-CCA CCA GGA TGC CAT ACT TGA T-3'
DGAT2	forward reverse	5'-TTC CTG GCA TAA GGC CCT ATT-3' 5'-AGT CTA TGG TGT CTC GGT TGA C-3'
MGL	forward reverse	5'-CAG AGA GGC CCA CCT ACT TTT-3' 5'-ATG CGC CCC AAG GTC ATA TTT-3'
PPAR $\alpha$	forward reverse	5'-TCG GCG AAC TAT TCG GCT G-3' 5'-GCA CTT GTG AAA ACG GCA GT-3'
CB1	forward reverse	5'-GGG CAC CTT CAC GGT TCT G-3' 5'-GTG GAA GTC AAC AAA GCT GTA GA-3'
ACADL	forward reverse	5'-TCC AGA GGT CAG TCA ACA TGA-3' 5'-CCT GGT CAA TTT TTC GAG AGT CC-3'
ACOX1	forward reverse	5'-GCA CCC CGA CAT AGA GAG C-3' 5'-TAA ACT CCG GGT AAC TGT GGA-3'
CCOX	forward reverse	5'-TCA ACG TGT TCC TCA AGT CGC-3' 5'-AGG GTA TGG TTA CCG TCT CCC-3'
NADH De	forward reverse	5'-GGT ACT TTG CTT GCT TGA TGA GA-3' 5'-TGG GAA GAT ATA CGG CTG AGG-3'
SUCCDE	forward reverse	5'-AAT TTG CCA TTT ACC GAT GGG A-3' 5'-CTC CTG GGA CTC ATC CTT CTT-3'

**Table 2-1. qPCR primer sequences.** MGAT (monoacylglycerol acyltransferase-2), ER GPAT (endoplasmic reticulum glycerol-3-phosphate-3), MT GPAT (mitochondrial GPAT-1), DGAT (diacylglycerol acyltransferase), MGL (monoacylglycerol lipase), PPAR $\alpha$  (peroxisome proliferator activated receptor- $\alpha$ ), CB1 (cannabinoid receptor-1), ACADL (long chain acyl-CoA dehydrogenase), ACOX1 (acyl-CoA oxidase-1), CCOX (cytochrome C oxidase), NADH De (nicotine adenine dinucleotide dehydrogenase), SUCCDE (succinate dehydrogenase).

## RESULTS

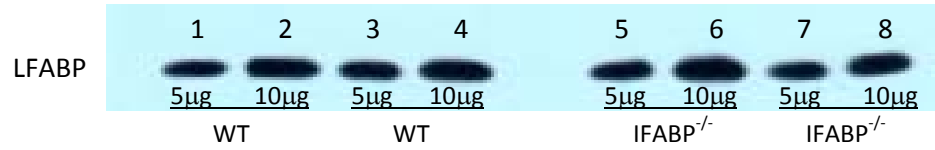
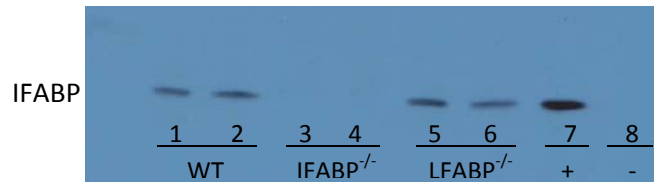
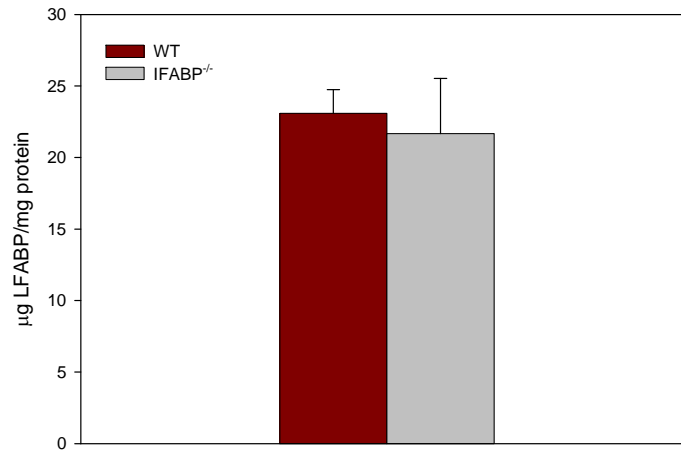
### *LFABP EXPRESSION IS NOT UPREGULATED IN IFABP<sup>-/-</sup> SMALL INTESTINAL MUCOSA*

Due to the overlapping ligand specificity and similar intracellular localization, it was possible that ablation of one of the enterocyte FABPs would result in compensatory upregulation of the other one. However, as shown in **Figure 1**, LFABP protein levels were unchanged IFABP-null mice relative to WT ( $23.1 \pm 1.6$  vs.  $21.7 \pm 3.9$   $\mu\text{g}/\text{mg}$ , in WT and IFABP<sup>-/-</sup>, respectively, NS).

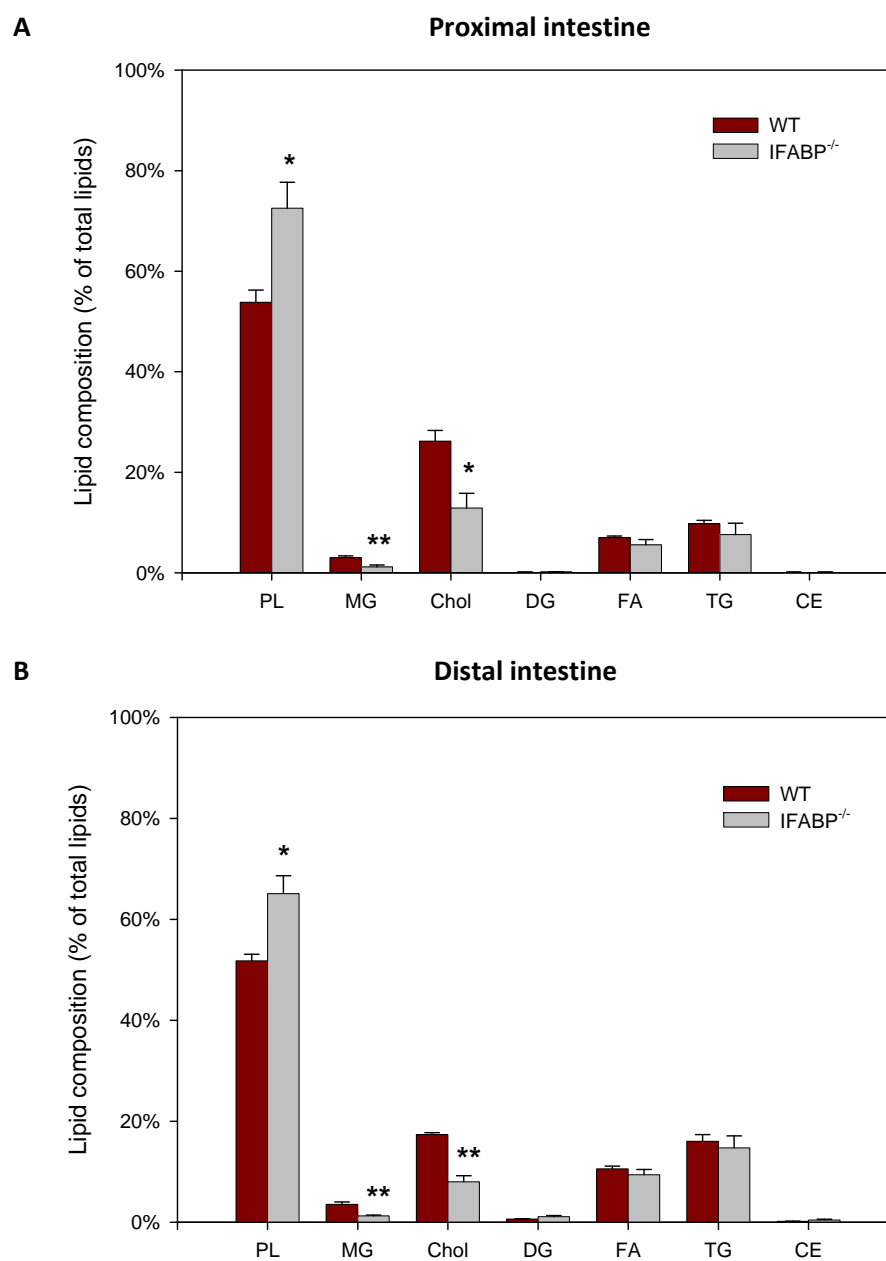
### *INTESTINAL LIPID COMPOSITION*

Lipid composition of the proximal and distal intestinal mucosa in the fasted mouse intestine was analyzed by lipid extraction and separation by TLC, and the lipid spots were visualized and quantified with iodine staining as described in Materials and Methods. There were no gross alterations in the total lipid mass of the proximal ( $655.0 \pm 95.5$   $\mu\text{g}/\text{mg}$  vs.  $460.7 \pm 102.5$   $\mu\text{g}/\text{mg}$  in WT and IFABP<sup>-/-</sup>, respectively, NS) or distal ( $714.6 \pm 55.2$   $\mu\text{g}/\text{mg}$  vs.  $720.2 \pm 63.7$   $\mu\text{g}/\text{mg}$  in WT and IFABP<sup>-/-</sup>, respectively, NS) intestinal mucosa per mg protein. However, some changes were found in individual lipid subclasses. As seen in **Figure 2-2a**, proximal intestinal mucosa from IFABP-null mice contains less cholesterol relative to WT ( $12.9\% \pm 2.9\%$  vs.  $26.2\% \pm 2.1\%$  of total lipids,  $p < 0.05$ ), and more phospholipids ( $72.5\% \pm 5.1\%$  vs.  $53.8\% \pm 2.4\%$  of total lipids,  $p < 0.05$ ). A similar pattern is observed in the distal mucosa (cholesterol:  $17\% \pm 0.4\%$  vs.  $8\% \pm 1.2\%$  in WT and IFABP<sup>-/-</sup>, respectively,  $p < 0.01$ ; phospholipids:  $65\% \pm 3.5\%$  vs.  $52\% \pm 1.3\%$  in WT and IFABP<sup>-/-</sup>, respectively, NS) (**Figure 2-2b**).

When the lipid composition data are expressed as mass per mg mucosa protein the decreases in monoacylglycerol and cholesterol were also seen, however the phospholipid mass was not significantly different (**Figure 2-3**).

**Figure 2-1****A****B****C**

**Figure 2-1. LFABP expression in the intestinal mucosa.** (A) Representative immunoblot of tissue homogenates of samples from 2 WT animals and 2 IFABP<sup>-/-</sup> animals. Lanes 1-8: 5µg and 10µg of tissue homogenate protein from each mucosal sample. Lanes 1-4: Wild-type. Lanes 5-8: IFABP<sup>-/-</sup>. (B) Immunoblot of intestinal mucosa for IFABP. Lanes 1-2: Wild-type. Lanes 3-4: IFABP<sup>-/-</sup>. Lanes 5-6: LFABP<sup>-/-</sup>. Lane 7: purified IFABP. Lane 8: purified LFABP. (C) LFABP expression in intestinal mucosa homogenates. Results are means ± standard deviation, n=4 per group.

**Figure 2-2**

**Figure 2-2. Lipid composition of the intestinal mucosa in 48 hour fasted male mice.** Mucosa was harvested, lipids extracted, and quantified as described in Materials and Methods. Data are expressed as a percent of the total lipid mass. **(A)** Lipid composition of the proximal intestine mucosa. **(B)** Lipid composition of the distal intestine mucosa. Results are means  $\pm$  SE,  $n=4-6$  per group, \* $p<0.05$  vs. WT.

Figure 2-3

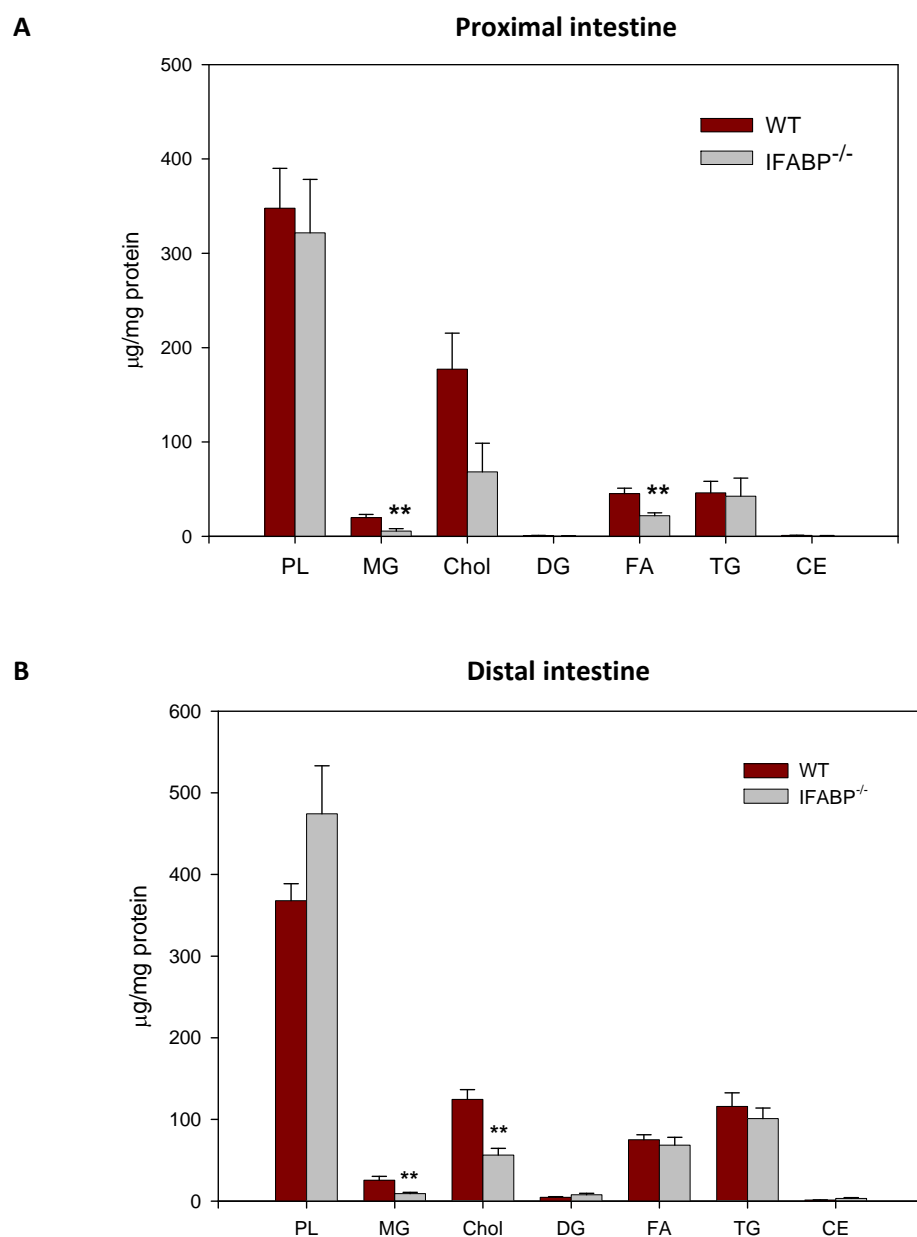


**Figure 2-3. Absolute mass of individual lipid classes in the intestinal mucosa of 48 hour fasted male mice.** Lipids were extracted as described in Materials and Methods, separated by TLC along with standards of known mass, and then iodine stained and scanned for densitometric analysis. **(A)** Lipids of the proximal intestine mucosa. **(B)** Lipids of the distal intestine mucosa. Results are means  $\pm$  SE,  $n=4-6$  per group, \*\* $p<0.01$  vs. WT.

### *IN VIVO FATTY ACID METABOLISM*

The acute trafficking of fatty acid was monitored by analyzing the fate of [ $^{14}\text{C}$ ] in the intestinal mucosa harvested 2 minutes after bolus administration of [ $^{14}\text{C}$ ]oleate. The differential metabolism of dietary vs. endogenous-derived lipids was assessed by administering the bolus either intraduodenally, to mimic dietary presentation of the lipids to the apical surface of enterocytes, or by jugular vein cannula, to mimic bloodstream-delivery to the basolateral surface of enterocytes. These experiments were performed in 3-4 month old, 48hr starved male mice.

As previously shown in fed mice and rats, after intraduodenal administration of [ $^{14}\text{C}$ ]oleate to fasted WT mice, mucosal [ $^{14}\text{C}$ ] recovery was predominantly in triacylglycerols ( $55.6\% \pm 2.6\%$ ) or free fatty acids ( $20.9\% \pm 1.7\%$ ) (**Table 2-3**). Recovery of [ $^{14}\text{C}$ ]oleate in phospholipids was  $7.5\% \pm 1.1\%$ . The TG/PL ratio, which represents the two major anabolic end points for fatty acids in the intestinal mucosa, was  $8.9 \pm 1.3$  (**Figure 2-4**).

The anabolic fates of bloodstream-derived fatty acids in intestinal enterocytes show a markedly different pattern of assimilation compared to dietary-derived fatty acids. For example, recovery of [ $^{14}\text{C}$ ]oleate in triacylglycerols was reduced by 58% ( $p < 0.01$ ). Correspondingly, incorporation into phospholipids was doubled ( $p < 0.01$ ) (**Table 2-3**). The resultant TG/PL ratio was reduced approximately 80% for bloodstream compared to dietary derived lipid substrates ( $8.9 \pm 1.3$  vs.  $1.8 \pm 0.2$ ,  $p < 0.01$ ) (**Figure 2-4**). Moreover, [ $^{14}\text{C}$ ]oleate recovery was increased in cholesteryl ester ( $p < 0.05$ ), diacylglycerols, & monoacylglycerols ( $p < 0.01$ ) for bloodstream-delivery relative to dietary, in accord with previous findings for WT mice (Storch et al., 2008).



*REDUCED INCORPORATION OF DIETARY-DERIVED FATTY ACIDS INTO TRIACYLGLYCEROL  
RELATIVE TO PHOSPHOLIPIDS IN THE SMALL INTESTINAL MUCOSA OF IFABP-NULL MICE*

Two minutes after the intraduodenal administration of [ $^{14}$ C]oleate, [ $^{14}$ C] recovery in free fatty acids, monoacylglycerols, diacylglycerols, and cholesteryl esters was unaffected by IFABP ablation. There was a moderately reduced [ $^{14}$ C] recovery in triacylglycerols ( $55.6\% \pm 2.6\%$  vs.  $48.0\% \pm 2.3\%$  in WT and IFABP $^{-/-}$ , respectively, NS) and a significantly increased recovery in the phospholipid fraction ( $7.5\% \pm 1.1\%$  vs.  $14.1\% \pm 2.5\%$  in WT and IFABP $^{-/-}$ , respectively,  $p < 0.05$ ) (**Table 2-3**), resulting in a 54% reduction in the TG/PL ratio in the IFABP $^{-/-}$  mice ( $p < 0.05$ , **Figure 2-4**).

To further probe these findings and determine if they are regulated by feeding status, this experiment was repeated directly comparing fed and 48 hour fasted WT and IFABP $^{-/-}$  mice. In agreement with previous results for WT mice (Storch et al., 2008), being in the fed state induced a ~32% decrease in the TG/PL ratio in both groups, driven primarily by increased incorporation of [ $^{14}$ C]oleate into phospholipids (**Table 2-4**). Thus the significantly reduced TG/PL in IFABP-null mice was maintained in the fed state, however, IFABP genotype had no effect on the response to fasting vs. feeding.

*NO EFFECT OF IFABP ABLATION ON THE INCORPORATION OF BLOODSTREAM-DERIVED FATTY ACIDS INTO FAT-SOLUBLE METABOLITES IN THE SMALL INTESTINAL MUCOSA*

Incorporation of bloodstream-derived [ $^{14}$ C]oleate into complex lipids was largely unaffected by IFABP-ablation (**Table 2-3**) and the TG/PL ratio was unchanged (**Figure 2-4**). Thus, IFABP ablation appears to affect the metabolic fate of diet-derived but not bloodstream-derived fatty acid.

**Table 2-3**

Bloodstream-derived [1- <sup>14</sup> C]oleic acid			Dietary-derived [1- <sup>14</sup> C]oleic acid		
	WT	IFABP <sup>-/-</sup>		WT	IFABP <sup>-/-</sup>
PL	14.0% ± 1.4%	19.5% ± 4.3%	PL	7.5% ± 1.1%‡	14.1% ± 2.5%*
MG	6.7% ± 0.9%	6.9% ± 1.5%	MG	2.7% ± 0.7%‡	2.6% ± 0.2%‡
DG	11.3% ± 0.9%	9.3% ± 0.5%	DG	7.4% ± 0.5%‡	8.6% ± 0.4%
FA	30.0% ± 4.2%	26.6% ± 4.8%	FA	20.9% ± 1.7%†	21.4% ± 2.1%
TG	26.4% ± 3.9%	31.7% ± 2.3%	TG	55.6% ± 2.6%‡	48.0% ± 2.3%‡
CE	11.7% ± 2.3%	5.9% ± 2.0%	CE	5.4% ± 0.9%†	5.4% ± 1.5%

**Table 2-3. Metabolism of bloodstream-derived and dietary-derived [<sup>14</sup>C]oleate in the small intestinal mucosa of 48h fasted mice.** Incorporation of [<sup>14</sup>C]oleate into fat-soluble metabolites in the small intestinal mucosa 2 minutes after administration as described in Materials and Methods. Results are means ± SE, n=4-7 for bloodstream delivery and 7-10 for dietary delivery, ‡p<0.01, †p<0.05 vs. bloodstream-derived FA, \*p<0.05 vs. WT.

**Table 2-4**

Dietary-derived [1- <sup>14</sup> C]oleic acid		
	WT	IFABP <sup>-/-</sup>
PL	10.9% ± 1.6%	17.9% ± 3.3%
MG	4.4% ± 1.3%	3.0% ± 0.0%
DG	8.2% ± 1.2%	8.5% ± 0.5%
FA	19.0% ± 3.2%	19.1% ± 3.2%
TG	50.1% ± 4.2%	43.5% ± 1.1%
CE	6.7% ± 2.1%	8.1% ± 1.3%
TG/PL	4.9 ± 0.8	2.7 ± 0.4*

**Table 2-4. Metabolism of dietary-derived [<sup>14</sup>C]oleate in the small intestinal mucosa of fed mice.** Incorporation of [<sup>14</sup>C]oleate into fat-soluble metabolites in the small intestinal mucosa 2 minutes after intraduodenal administration as described in Materials and Methods. Results are means ± standard deviation, n=4 per group, \*p<0.05 vs. WT.

Figure 2-4

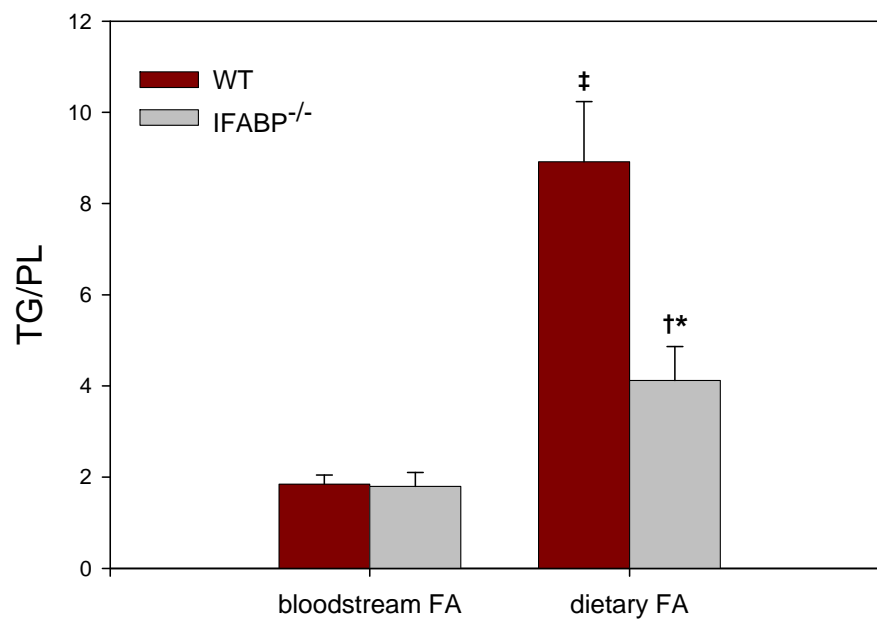


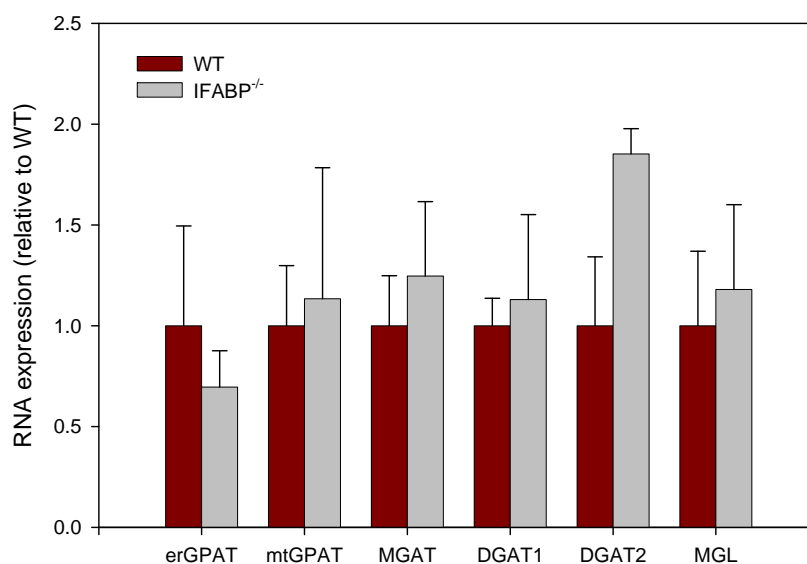
**Figure 2-4. Effect of IFABP ablation on the metabolic compartmentation of [<sup>14</sup>C]oleate in mouse small intestine.** Incorporation of [<sup>14</sup>C]oleate into triacylglycerol relative to phospholipid (TG/PL) 2 minutes after delivery to either the basolateral (bloodstream-derived) or apical (dietary-derived) surface of the intestine in 48 hour fasted mice as described in Materials and Methods. Results are means  $\pm$  SE, n=4-7 for bloodstream delivery and 7-10 for dietary delivery, ‡*p*<0.01, †*p*<0.05 vs. bloodstream-derived FA, \**p*<0.05 vs. WT.

*NO EFFECT OF IFABP-ABLATION ON THE EXPRESSION OF LIPID METABOLISM GENES IN THE SMALL INTESTINAL MUCOSA*

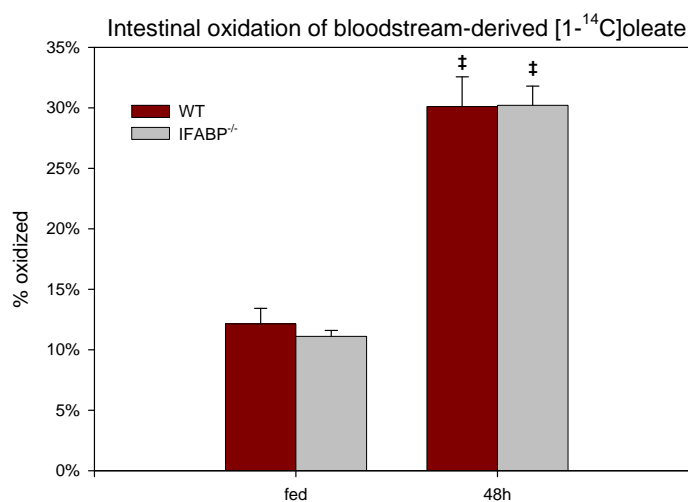
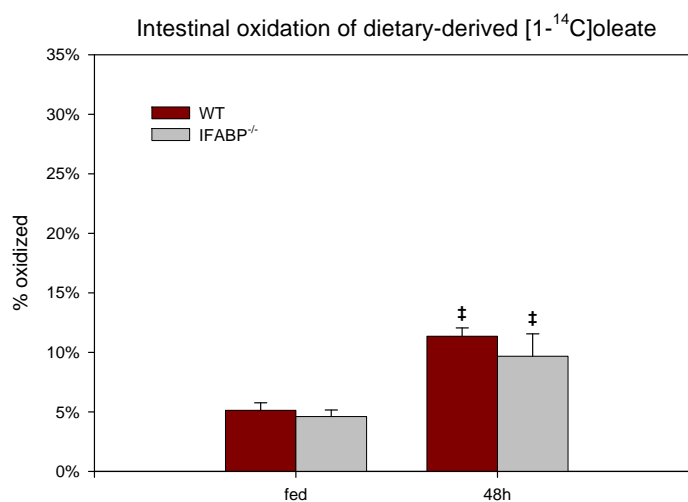
To determine if any of the observed changes could have been caused by altered gene expression, or conversely, to ensure that a potential defect in fatty acid trafficking was not being masked by secondary alterations in gene expression, the mRNA levels of enzymes involved in fatty acid metabolism were analyzed by qPCR. As seen in **Figure 2-5**, no changes were observed in any of the genes tested.

*NO EFFECT OF IFABP ABLATION ON SMALL INTESTINAL FATTY ACID OXIDATION*

Fasting more than doubled intestinal fatty acid oxidation regardless of whether the substrate, [<sup>14</sup>C]oleate, was delivered to the apical or basolateral surface of the enterocyte ( $p < 0.01$ , **Figure 2-6**). As expected (Gangl and Ockner, 1975), significantly more bloodstream-derived fatty acids were oxidized relative to dietary fatty acids ( $p < 0.01$ ). Intestinal fatty acid oxidation was completely intact in IFABP<sup>-/-</sup> mice (**Figure 2-6**). Similarly, expression levels of the genes involved in fatty acid oxidation were unaffected by IFABP ablation (**Figure 2-7**).

**Figure 2-5**

**Figure 2-5. Expression of lipid metabolism genes in the small intestinal mucosa.** Relative gene expression was determined by qPCR. Reaction conditions and primers are described in Materials and Methods and **Table 2-1**. Results are means  $\pm$  SEM,  $n=3-4$  per group. Glycerol-3-phosphate acyltransferase-3 (erGPAT), mitochondrial glycerol-3-phosphate acyltransferase (mtGPAT), monoacylglycerol acyltransferase-2 (MGAT), diacylglycerol acyltransferase-1 (DGAT1), diacylglycerol acyltransferase-2 (DGAT2), monoacylglycerol lipase (MGL).

**Figure 2-6****A****B**

**Figure 2-6. Oxidation of bloodstream-derived and dietary-derived [<sup>14</sup>C]oleate in the small intestinal mucosa.** Recovery of [<sup>14</sup>C] from [<sup>14</sup>C]oleate in [<sup>14</sup>C]acid-soluble metabolites and <sup>14</sup>CO<sub>2</sub> in the small intestinal mucosa 2 minutes after administration as described in Materials and Methods. (A) Oxidation of bloodstream-derived fatty acid. (B) Oxidation of dietary –derived fatty acid. Results are means ± SE. Fasted animals: n=4-7 for bloodstream delivery and 7-10 for dietary delivery; fed animals: n=4 per group. ‡*p*<0.01 vs. fed.

Figure 2-7

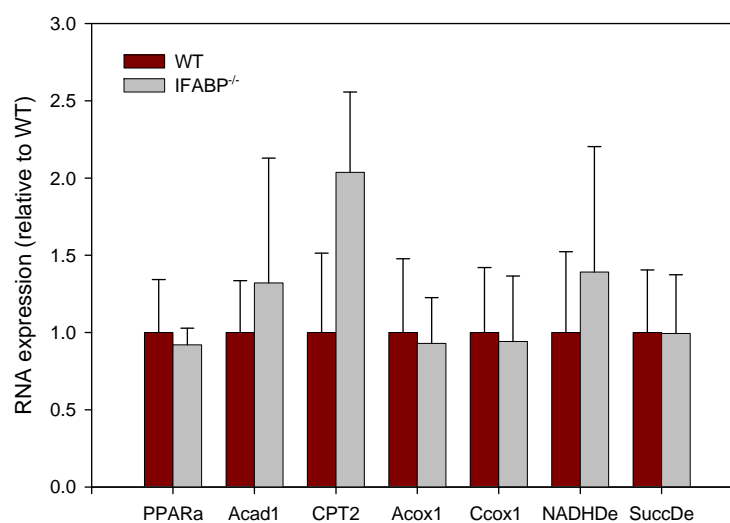


**Figure 2-7. Expression levels of genes involved in mitochondrial  $\beta$ -oxidation, peroxisomal fatty acid oxidation, and electron transport in the small intestinal mucosa.** Relative gene expression was determined by qPCR. Reaction conditions and primer sequences are described in Materials and Methods and **Table 2-1**. Results are means  $\pm$  SEM, n=3-4 per group. Peroxisome proliferator receptor- $\alpha$  (PPAR $\alpha$ ), long-chain acyl-CoA dehydrogenase-1 (Acad1), carnitine palmitoyltransferase-2 (CPT2), acyl-CoA oxidase-1 (Acox2), cytochrome C oxidase-1 (Ccox1), NADH dehydrogenase (NADHDe), succinate dehydrogenase (SuccDe).

### *BODY WEIGHT*

As shown in **Figure 2-8**, the body weight of male IFABP<sup>-/-</sup> mice did not differ from WT at any age from birth until five months.

### *BODY COMPOSITION*

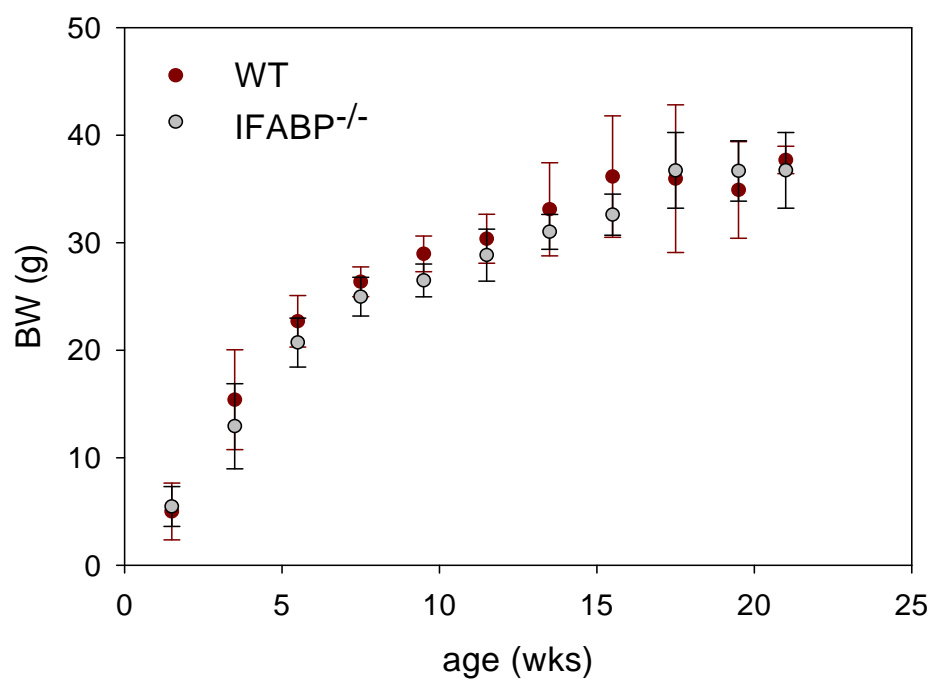
IFABP mice weighing  $29.1 \pm 0.7$ g had a similar body composition as WT mice in the fed state (**Table 2-5**). Moreover, as visualized by DEXA body scans and shown in **Figure 2-9**, IFABP<sup>-/-</sup> mice appear similar to WT regardless of feeding status. Absolute fat mass was unaffected by IFABP ablation in the fed state ( $6.9 \pm 0.7$ g vs.  $5.5 \pm 0.7$ g,  $p=0.208$ ). After 48h food deprivation, both groups of mice lost approximately 5g of total mass, or 17-18% of their initial body weight. However, although the absolute amount of fat mass lost by IFABP mice was approximately similar to WT ( $1.5 \pm 0.4$ g vs.  $1.8 \pm 0.1$ g in WT and IFABP<sup>-/-</sup> mice, respectively, NS), IFABP-null mice lost significantly more fat mass (WT:  $6.9$ g  $\rightarrow$   $5.3$ g = -22%; IFABP<sup>-/-</sup>:  $5.5$ g  $\rightarrow$   $3.7$ g = -35%,  $p<0.05$ ).

As seen in **Table 2-6**, bone mineral density in WT mice was  $0.0522 \pm 0.001$ g/cm<sup>2</sup> and this was not affected by genotype or feeding status. Similarly, total bone mineral content in WT mice was  $0.417 \pm 0.009$ g and  $0.4261 \pm 0.0122$  in IFABP<sup>-/-</sup>, NS.

### *INTESTINE LENGTH*

In WT mice, the total length of the intestine, from the pyloric sphincter to the cecum, was  $39.9 \pm 0.7$ cm ( $1.6 \pm 0.1$ cm/g BW). This was unaffected by IFABP ablation ( $38.8 \pm 0.07$ cm,  $1.8 \pm 0.1$ cm/g BW).



**Figure 2-8**

**Figure 2-8. Body weight of IFABP<sup>-/-</sup> and WT mice.** Before weaning, the mean body weight includes both male and female pups. After weaning, only values for males are shown. Upon weaning, mice were housed 3-4 per cage and weighed weekly. Results are means  $\pm$  SE, n=12-15 per group.

**Table 2-5**

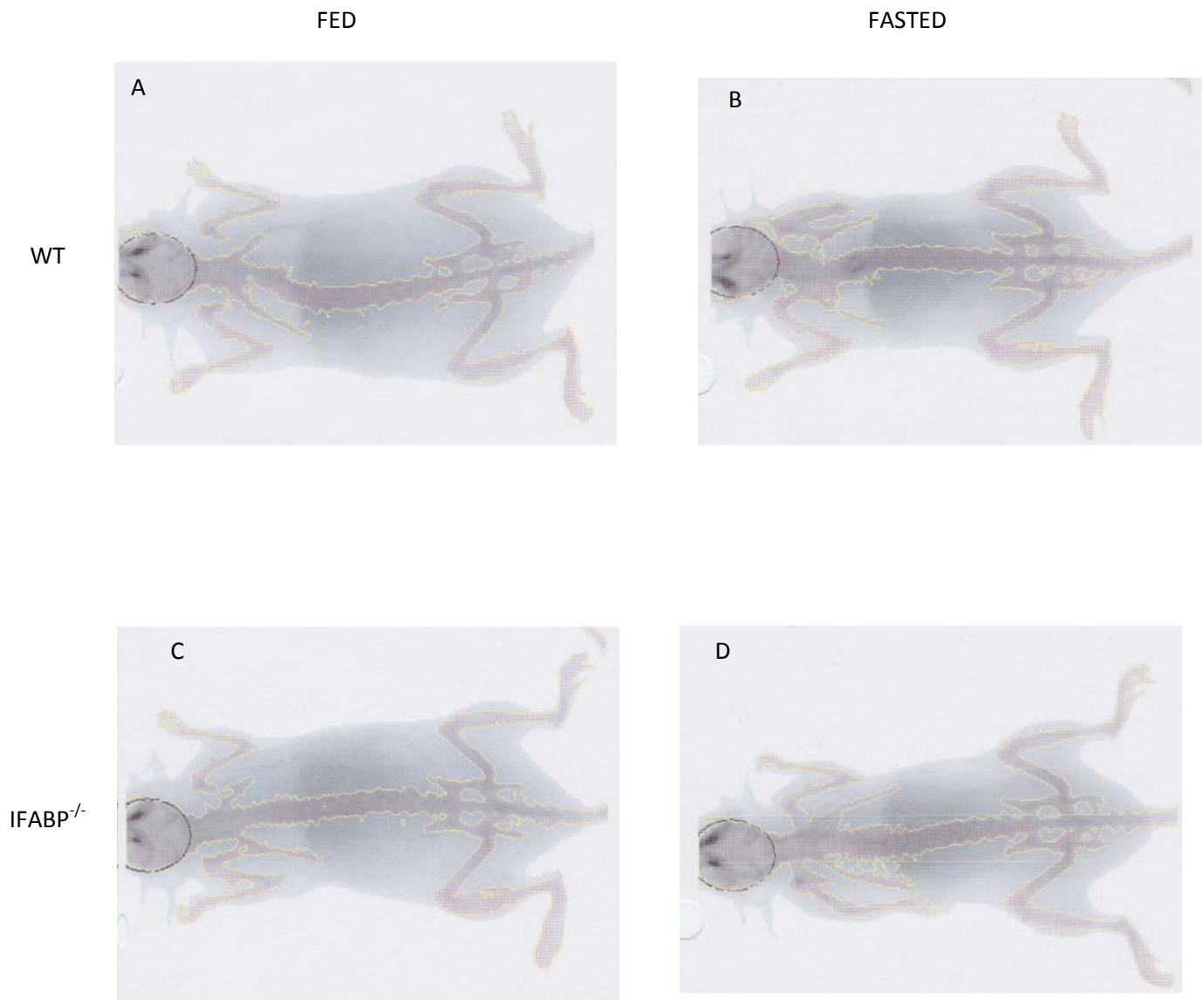
	WT	IFABP <sup>-/-</sup>
Fed BW (g)	31.1 ± 0.9	29.1 ± 0.7
Fasted BW (g)	25.3 ± 1.0	22.6 ± 0.9
Δ (%)	-18.8% ± 1.9%	-22.7% ± 2.0%

	WT	IFABP <sup>-/-</sup>
Fed fat mass (g)	6.9 ± 0.7	5.5 ± 0.7
Fasted fat mass (g)	5.3 ± 0.7	3.7 ± 0.7
Δ (%)	-21.9% ± 5.6%	-35.2% ± 3.0%*

**Table 2-5. Effect of IFABP ablation on body weight (a) and fat (b) in the fed and fasted state.**

Measurements were assessed by DEXA (Lunar PIXIMUS) in the fed state and 48h after food deprivation, as described in Materials and Methods. Results are means ± SE, n=11-17 per group,

\**p*<0.05 vs. WT.

**Figure 2-9**

**Figure 2-9. DEXA scan of WT and IFABP<sup>-/-</sup> before (fed) and after (fasted) 48 hours of food deprivation.** Mice were anesthetized and subject to DEXA scanning with the GE Lunar PIXIMUS as described in Materials and Methods. Representative DEXA scans of WT and IFABP<sup>-/-</sup> animals in the fed and fasted states. **(A)** WT scanned just after feeding. **(B)** Same mouse pictured in (A) after 48 hours of food deprivation. **(C)** IFABP<sup>-/-</sup> scanned just after feeding. **(D)** Same mouse pictured in (C) after 48 hours of food deprivation. N=11-17 per group.

**Table 2-6**

	<b>FED</b>		<b>FASTED</b>	
	WT	IFABP <sup>-/-</sup>	WT	IFABP <sup>-/-</sup>
BMD (g/cm <sup>2</sup> )	0.0523 ± 0.0008	0.0538 ± 0.0008	0.0535 ± 0.0007	0.0538 ± 0.0008
BMC (g)	0.4174 ± 0.0087	0.4261 ± 0.0122	0.4383 ± 0.0092	0.4423 ± 0.0105

**Table 2-6. Bone mineral density (BMD) and bone mineral content (BMC) in fed and fasted WT and IFABP<sup>-/-</sup> mice.** Assessed by dual energy X-ray absorptiometry as described in Materials and Methods.

### FOOD INTAKE

To more thoroughly assess energy metabolism, 10-15 mice of each genotype were caged individually to measure food intake. WT mice on a standard chow diet consumed  $2.3 \pm 0.1$  grams, or  $11.4 \pm 0.4$  kcal per day. IFABP<sup>-/-</sup> mice under identical conditions consumed  $2.2 \pm 0.1$  grams, or  $10.9 \pm 0.7$  kcal per day (NS).

### FECAL COMPOSITION

Feces were collected to analyze gross fat absorption. Feces were collected every other day for 4-8 days, were dried and weighed, and the dry weight was divided by 4-8 to determine daily fecal output. The excrement amounted to  $0.77 \pm 0.06$  grams in WT mice and  $0.62 \pm 0.06$  grams in IFABP<sup>-/-</sup> mice (NS). As seen in **Table 2-7**, the total lipid mass was  $8.7 \pm 1.6$   $\mu\text{g}/\text{mg}$  feces in WT mice, and the lipid composition was mainly phospholipids ( $2.9 \pm 0.8$   $\mu\text{g}/\text{mg}$  feces, or  $31.2\% \pm 2.7\%$  of the total lipids), cholesterol ( $1.6 \pm 0.3$   $\mu\text{g}/\text{mg}$  feces, or  $18.3\% \pm 1.0\%$ ), fatty acids ( $1.7 \pm 0.2$   $\mu\text{g}/\text{mg}$  feces, or  $20.0\% \pm 2.1\%$ ), and cholesteryl esters ( $1.7 \pm 0.4$   $\mu\text{g}/\text{mg}$  feces, or  $18.3\% \pm 2.5\%$ ). Ablation of IFABP did not significantly alter any of these parameters.

**Table 2-7**

<b>Fecal lipid (<math>\mu\text{g}/\text{mg}</math>)</b>		
	<b>WT</b>	<b>IFABP<sup>-/-</sup></b>
PL	2.9 $\pm$ 0.8	2.9 $\pm$ 0.6
MG	0.2 $\pm$ 0.1	0.2 $\pm$ 0.1
Chol	1.6 $\pm$ 0.3	1.7 $\pm$ 0.2
DG	0.2 $\pm$ 0.0	0.3 $\pm$ 0.1
FA	1.7 $\pm$ 0.2	1.8 $\pm$ 0.3
TG	0.5 $\pm$ 0.0	0.5 $\pm$ 0.1
CE	1.7 $\pm$ 0.4	1.5 $\pm$ 0.2
Total lipid	8.7 $\pm$ 1.6	7.8 $\pm$ 1.5

**Table 2-7. Amount and composition of fecal fat is unaffected by IFABP ablation.** Feces were collected every other day for 4-8 days, dried, weighed, and the dry weight was divided by 4-8 to determine daily fecal output. Lipids were extracted by the method of Folch and lipid subclasses were separated by TLC with standards of known mass, and stained with iodine for densitometric quantification, as described in Materials and Methods. Data are expressed as  $\mu\text{g}$  lipid/mg feces (dry weight). Results are means  $\pm$  SE, n=7-8 per group.

### RESPIRATORY QUOTIENT

In WT mice, the average  $V_{O_2}$  was  $76.1 \pm 1.6 \text{ mL/kg/min}$  in the fed state and significantly lower in the fasted state ( $51.0 \pm 1.4 \text{ mL/kg/min}$ ,  $p < 0.05$ , **Table 2-8**).  $V_{CO_2}$  was  $68.4 \pm 1.4 \text{ mL/kg/min}$  in the fed state and significantly lower in the fasted state ( $38.9 \pm 1.5 \text{ mL/kg/min}$ ,  $p < 0.01$ ). The absolute values for  $V_{O_2}$  and  $V_{CO_2}$  in fed and fasted IFABP<sup>-/-</sup> mice were not significantly different from WT. As seen in **Figure 2-10a**, the RQ increased during the dark period, reflecting the consumption of the standard high-carbohydrate rodent chow. As expected, the average respiratory quotient was significantly reduced upon food deprivation ( $p < 0.01$  for WT and IFABP<sup>-/-</sup>), reflecting a greater reliance on fat oxidation to meet energy requirements (**Figure 2-10b**). This reduction was slightly greater in IFABP<sup>-/-</sup> ( $-0.14 \pm 0.01$  vs.  $-0.19 \pm 0.03$  in WT and IFABP<sup>-/-</sup>, respectively, NS).

### METABOLIC RATE

In WT mice, the average metabolic rate was  $22.5 \pm 0.5 \text{ kcal/hr/kg}$  ( $0.66 \pm 0.02 \text{ kcal/hr}$ ) in the fed state and significantly lower when fasting ( $14.8 \pm 0.4 \text{ kcal/hr/kg}$  [ $0.42 \pm 0.01 \text{ kcal/hr}$ ],  $p < 0.01$ ) (**Table 2-9**). Energy expenditure was elevated when the mice were feeding (**Figure 2-10a**, dark period) as compared to when they were fasting (**Figure 2-10a**, light period, and **Figure 2-10b**). None of these variables were altered by IFABP ablation.

**Table 2-8**

Respiratory Quotient			
		WT	IFABP <sup>-/-</sup>
Fed	V <sub>O2</sub> (mL/kg/min)	76.1 ± 1.6	72.0 ± 2.3
	V <sub>CO2</sub> (mL/kg/min)	68.4 ± 1.4	68.2 ± 3.8
	RQ	0.90 ± 0.02	0.94 ± 0.03
Fasted	V <sub>O2</sub> (mL/kg/min)	51.0 ± 1.4†	47.3 ± 2.1‡
	V <sub>CO2</sub> (mL/kg/min)	38.9 ± 1.5‡	35.5 ± 1.0‡
	RQ	0.76 ± 0.01‡	0.75 ± 0.02‡
Δ	V <sub>O2</sub> (mL/kg/min)	25.1 ± 1.8	24.7 ± 3.3
	V <sub>CO2</sub> (mL/kg/min)	29.6 ± 0.8	32.8 ± 4.0
	RQ	0.14 ± 0.01	0.19 ± 0.03

**Table 2-8. Respiratory quotient is normal in 3-4 month old male IFABP<sup>-/-</sup> mice.** Mice were placed in an indirect calorimeter and gas exchange was measured to calculate the respiratory quotient as described in Materials and Methods. Results are means ± SE, n=5-6 per group, ‡p<0.01, †p<0.05 vs. fed.

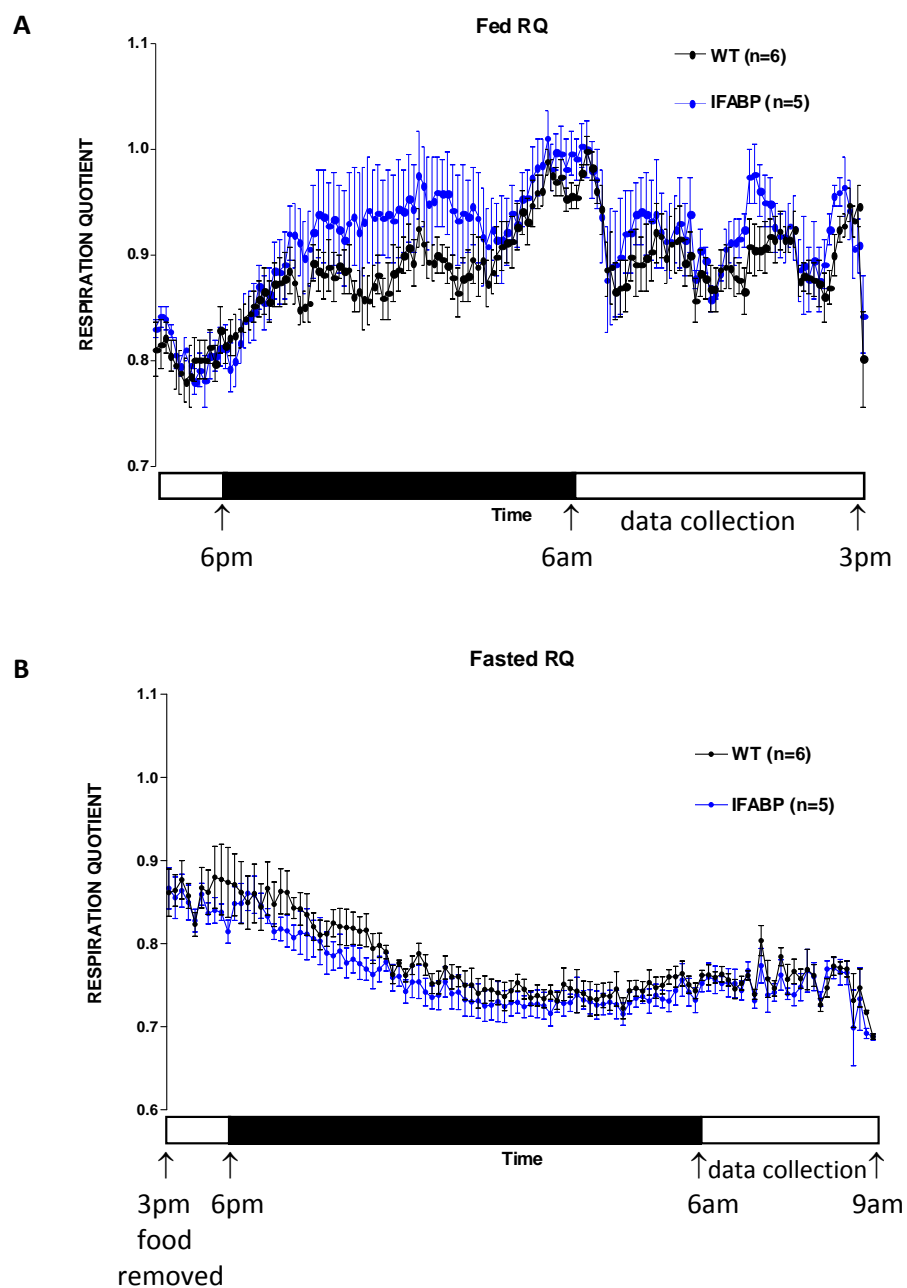
**Table 2-9**

Metabolic Rate			
		WT	IFABP <sup>-/-</sup>
Fed	kcal/hr/kg	22.5 ± 0.5	21.4 ± 0.7
	kcal/hr	0.66 ± 0.02	0.67 ± 0.03
Fasted	kcal/hr/kg	14.8 ± 0.4‡	13.7 ± 0.6‡
	kcal/hr	0.42 ± 0.01‡	0.42 ± 0.02‡
Δ	kcal/hr/kg	7.7 ± 0.5	7.7 ± 1.0
	kcal/hr	0.24 ± 0.02	0.25 ± 0.03

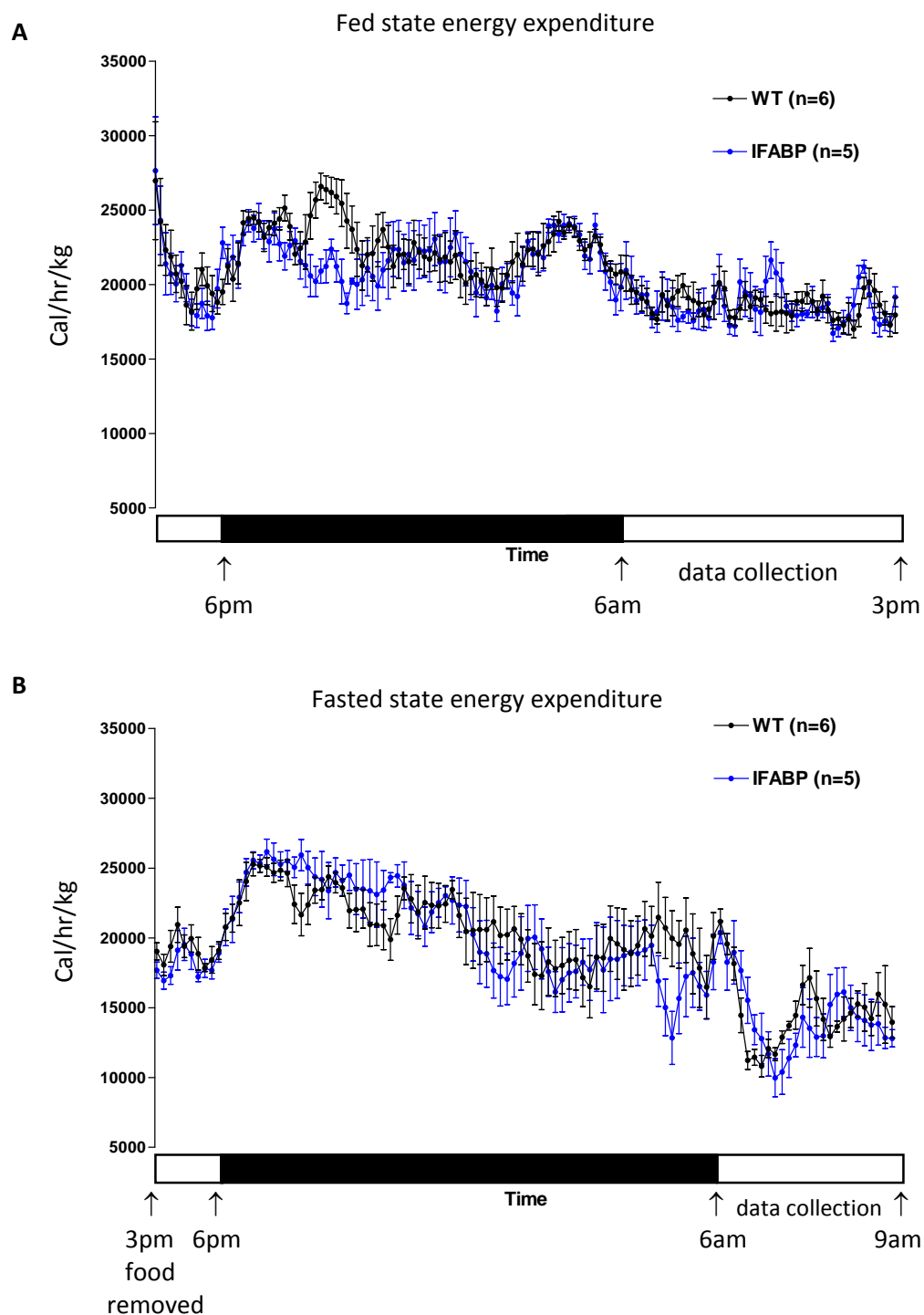
**Table 2-9. Metabolic rate is normal in 3-4 month old male IFABP<sup>-/-</sup> mice.** Mice were placed in an indirect calorimeter and gas exchange was measured to calculate the metabolic rate as described in Materials and Methods. Results are means ± SE, n=5-6 per group, ‡p<0.01 vs. fed.



Figure 2-10



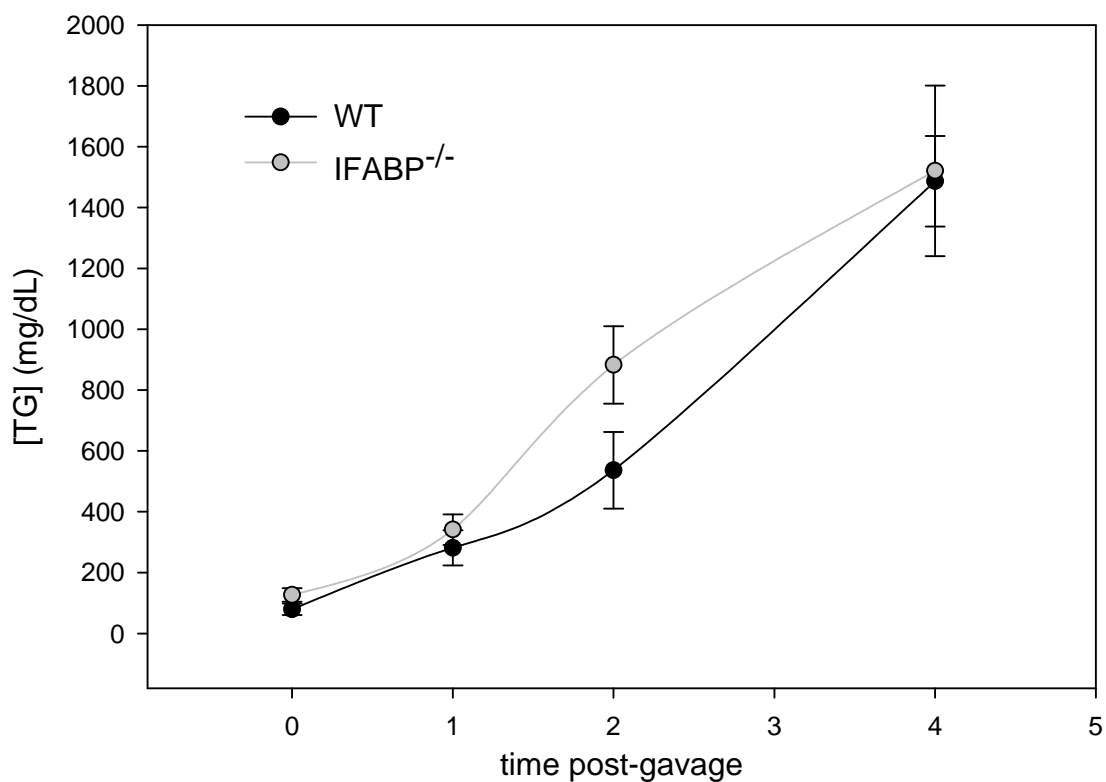
**Figure 2-10. 24 hour Respiratory quotient.** RQ was measured as described in Materials and Methods. N=5-6 per group.

**Figure 2-11**

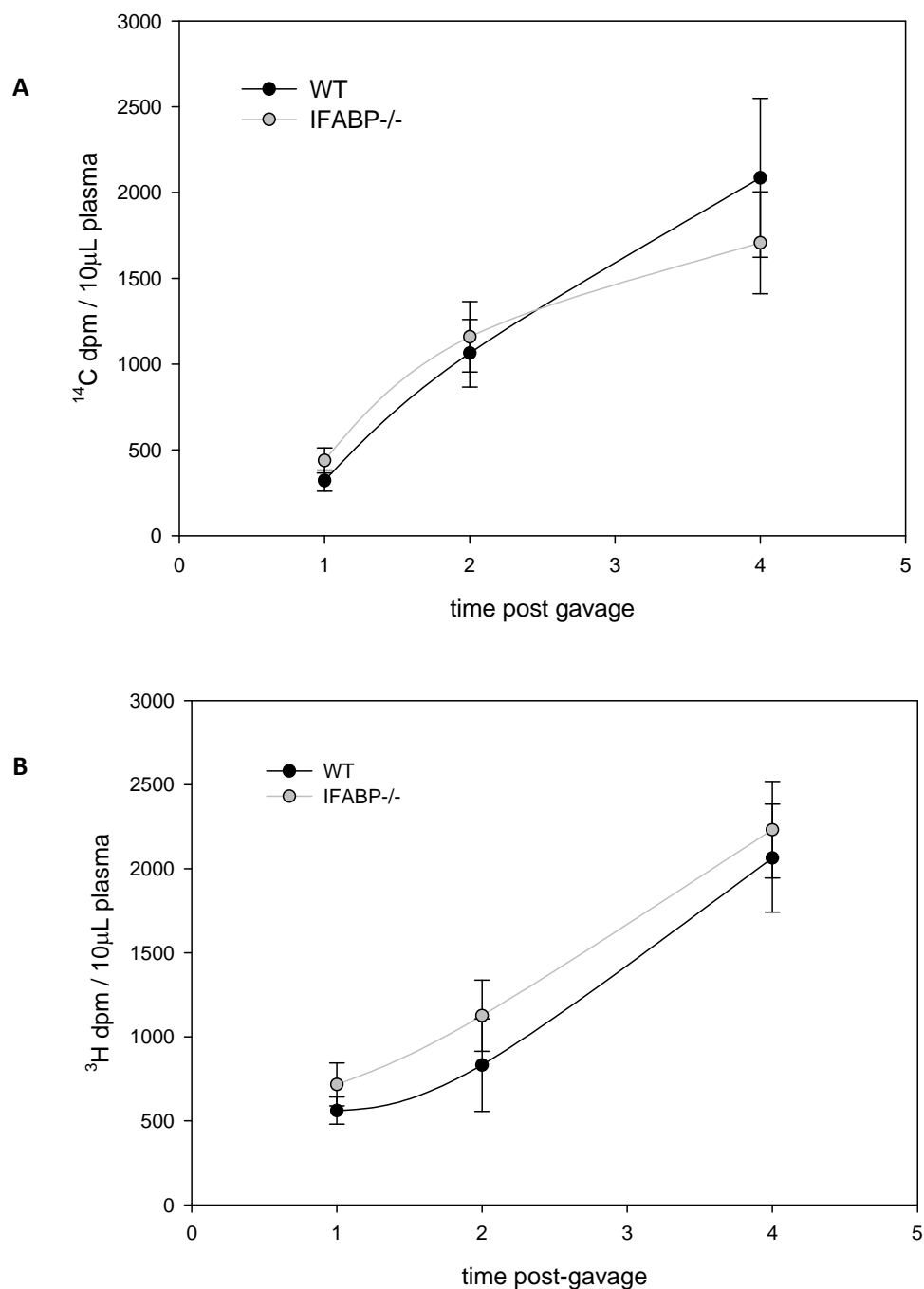
**Figure 2-11. 24 hour Metabolic rate.** Metabolic rate was measured as described in Materials and Methods. **(A)** 24 hour metabolic rate in mice with ad libitum access to Purina Rodent Chow. **(B)** 24 hour metabolic rate in fasting mice. N=5-6 per group.

#### *ORAL FAT-TOLERANCE TEST*

To assess the intestinal processing of a large lipid load, an oral fat tolerance test (OFTT) was performed. An intraperitoneal injection of tyloxapol was employed to block peripheral lipoprotein clearance, thus the increase in plasma triacylglycerols after the gavage reflects specifically intestinal triacylglycerol secretion. After an orogastric gavage of 500 $\mu$ L olive oil containing [ $^{14}$ C]oleic acid and [ $^3$ H]monoolein, plasma triacylglycerols rose steadily both groups (**Figure 2-12**). This observation confirms the finding that the acute synthesis of triacylglycerols is normal in IFABP-null intestine. Moreover, plasma [ $^{14}$ C] and [ $^3$ H] from [ $^{14}$ C]oleate and [ $^3$ H]monoolein, respectively, also increased similarly in both groups during the time range studied (**Figure 2-13**).

**Figure 2-12**

**Figure 2-12. No effect of IFABP ablation on intestinal triacylglycerol secretion.** Fasting, conscious mice were administered an intraperitoneal injection of tyloxapol and then given 500 $\mu$ L olive oil, [ $^{14}$ C]oleate, and [ $^3$ H]monoolein by oro-gastric gavage as described in Materials and Methods. Blood was drawn prior to the gavage and at various time points thereafter. Results are means  $\pm$  SEM, n=4-5 per group.

**Figure 2-13**

**Figure 2-13. No effect of IFABP ablation on intestinal triacylglycerol secretion.** Plasma radioactivity during the oral fat-tolerance test described in Figure 2-11. **(A)** Plasma [ $^{14}\text{C}$ ] from the [ $^{14}\text{C}$ ]oleate present in the oral lipid bolus. **(B)** Plasma [ $^3\text{H}$ ] from the [ $^3\text{H}$ ]monoolein present in the oral lipid bolus. Results are means  $\pm$  SEM,  $n=4-5$  per group.

## DISCUSSION

### *FABP EXPRESSION*

Due to their partial overlap in tissue expression patterns and ligand specificities, upregulation of LFABP in the intestine of IFABP-null mice would not have been unexpected. However, in accord with Vassileva et al. (FASEB 2000), this was not the case. The same group (Agellon et al., 2006) later showed a 50% increase in LFABP abundance in the IFABP<sup>-/-</sup> intestine, however these studies were performed with 7-9 month old mice, as opposed to 5-6 by Vassileva, or 3-4 in the current study. Although the mere presence of LFABP could still metabolically compensate for the loss of IFABP, the observation that it was not upregulated supports the existence of a functional distinction between the two enterocyte FABPs.

### *MUCOSAL LIPID COMPOSITION*

Lipid composition of the intestinal mucosa was analyzed to determine the chronic effects of IFABP ablation on the intestinal mucosa. Overall, there were no major changes in the lipid composition of the intestinal mucosa in the IFABP-null animals. IFABP ablation reduced the monoacylglycerol content in the entire intestine. It should be noted that the contribution of monoacylglycerols to intestinal lipids is quantitatively very small (2-3%). Monoacylglycerol is not a physiological ligand for IFABP, and LFABP levels are unchanged in IFABP<sup>-/-</sup> enterocytes, so this probably does not represent a reduction in intestinal monoacylglycerol-binding capacity. Furthermore, the most quantitatively important source for intestinal monoacylglycerols is dietary fat and these mucosal samples came from fasted mice. Monoacylglycerol lipase and monoacylglycerol acyltransferase mRNA levels were unchanged. Thus, the direct cause of the decrease in monoacylglycerol content is unknown.

Cholesterol mass was reduced in the intestinal mucosa of IFABP-null mice. IFABP-overexpressing HIEC-6 cells exhibited reduced cholesterol uptake, which paralleled and was likely secondary to decreased expression of cholesterol transporters NPC1L1 and CD36, and increased SR-B1 (Montoudis et al., 2008). These findings are in contrast to those presented here, although the two models differ in at least one important aspect. HIEC-6 cells normally express very low levels of IFABP, so even with a 90-fold increase the levels are still 50-fold less than that in WT mice. Moreover, Montoudis et al. did not quantify cholesterol mass, so it is possible that despite the effects on cholesterol uptake and gene expression, the amount of cellular cholesterol may have been increased bringing the effects of IFABP-overexpression into agreement with those of IFABP ablation.

#### *INTESTINAL FATTY ACID METABOLISM IN VIVO*

IFABP ablation did not alter the incorporation of bloodstream-derived [ $^{14}\text{C}$ ]oleate into complex lipids. However when presented with [ $^{14}\text{C}$ ]oleate intraduodenally, to mimic dietary delivery to the apical surface of the enterocyte, there was a marked reduction in its incorporation in triacylglycerols relative to phospholipids. This was due to a modest reduction in incorporation in triacylglycerols and a significant increase in phospholipids. Notably, expression of the genes involved in complex lipid synthesis was unchanged. Thus, it is possible that IFABP directs fatty acids away from incorporation in phospholipids by trafficking them toward triacylglycerol synthesis. This would only apply to newly arrived dietary fatty acids as the absolute phospholipid mass (per mg protein) was not significantly increased, triacylglycerol mass was unchanged, and bloodstream-derived fatty metabolism was normal in IFABP-null mice. This is in accord with the findings of Alpers (2000), who showed that IFABP bound to more apically-administered fatty acids than basolaterally-administered fatty acids. Darimont et

al. (2000) compared acute fatty acid metabolism in control Caco-2 cells (an enterocyte-like cell model) and those engineered to overexpress IFABP, which, due to the low endogenous IFABP expression in control cells, is analogous to IFABP<sup>-/-</sup> and WT. They found no major effect on the acute (15min) incorporation of [<sup>14</sup>C]palmitate into triacylglycerols or phospholipids. The discord between those findings and the results presented here (incorporation of palmitate into phospholipids was not lower in the IFABP-overexpressing cell line) may have been due to: many known differences between Caco-2 cells and enterocytes (e.g., Caco-2 cells lack the MGAT pathway [Trotter and Storch, 1993]); the longer incubation time (15min vs. 2min); the substrate used (palmitate vs. oleate); or that LFABP was increased ~50% in IFABP-overexpressing cells. Moreover, studies on IFABP-overexpressing cell lines frequently give mixed results. For example: IFABP-expressing fibroblasts exhibited increased oleate incorporation into triacylglycerols and elevated cellular triacylglycerol mass (Prows et al., 1996); however, an IFABP-expressing clone of hBRIE 380 cells (rat intestinal cells) assimilated oleate similar to control cells (Holehouse et al., 1998). Therefore, in the mouse knockout model, and in accord with the relatively apical localization of IFABP (Alpers et al., 2000), IFABP ablation appears to have a very specific effect on the trafficking of newly arrived fatty acids that are presented to the apical surface of enterocytes. More importantly, this phenotype is not observed in LFABP-null mice and thus represents a functional distinction between the two enterocyte FABPs.

#### *INTESTINAL FATTY ACID OXIDATION*

IFABP-ablation had no effect on the oxidation of dietary or bloodstream-derived fatty acids. Similarly, the peroxisomal, mitochondrial, and electron transport genes involved in fatty acid oxidation were unchanged. Fatty acid oxidation is markedly impaired in LFABP-null mice



yet completely intact in IFABP<sup>-/-</sup>, which represents another functional difference between the two enterocyte fatty acid binding proteins.

### *ENERGY METABOLISM*

Reports on the effect of IFABP ablation on growth, body weight, and the response to dietary fat have been inconsistent. In the current studies, male IFABP-null mice weighed the same as WT mice from birth to at least 5 months of age when fed a chow diet upon weaning. In 2000, Vassileva et al. (2000 FASEB) reported that: 1) male IFABP-null mice are heavier than WT; 2) this phenotype appears at least as early as 6 weeks of age; and 3) the difference in body weight is modestly attenuated by 10 weeks of feeding a high saturated fat, high cholesterol diet. These effects were restricted to males, and females actually gained less weight after the dietary treatment. Later the same group (Agellon et al., 2007) fed an older cohort (30-40wks vs. 15-25wks) high fat diets enriched with either saturated or polyunsaturated fats for 2 weeks. The PUFA diet increased bodyweight in IFABP-null mice relative to WT. All mice fed the SFA diet gained less weight than those on the PUFA. IFABP ablation enhanced weight gain on either diet although somewhat less so on the SFA diet. Given that the results from the earlier report show that the IFABP-null mice would have already been significantly heavier by the time they started the dietary treatment (at 30-40 weeks of age), these results are difficult to interpret. Moreover, the cause for discord between these findings and those in the current report is unknown, however it should be noted that relative to other genetic mouse models of obesity, the initial difference in body weight reported by Vassileva is minute (~2g). Thus, taken together, the results suggest that IFABP ablation has a minimal, if any, effect on body weight.

## FOOD INTAKE

Consistent with the bodyweight phenotype, food intake was unaffected by IFABP ablation and to date there are no other reports of food intake in IFABP-null mice. Similarly, IFABP-null mice accumulate as much fat and fat-free mass as their WT counterparts. Interestingly, however, after 48 hours of food deprivation IFABP-null mice lost significantly more fat mass (~22% vs. ~35% of initial fat mass in WT and IFABP-null mice, respectively). Although the proximal cause for this is yet to be identified, it is assumed to be indirect because IFABP is not expressed in adipose tissue. Since fat mass is not a major component of bodyweight in mice, and variability is high, total body weight was not significantly reduced in IFABP-null mice after 48 hours of food deprivation relative to WT mice. This finding points to a subtle yet potentially vital role of IFABP in systemic energy metabolism. Exhaustion of fat mass during starvation is incompatible with life.

Indirect calorimetry provides a detailed measure of total energy expenditure and relative fuel utilization (respiratory quotient [RQ]; 0.7 reflects reliance on fat oxidation; 1.0 reflects carbohydrate oxidation). Consistent with the absence of a body weight phenotype, IFABP-ablation did not affect total energy expenditure in the fed state or after overnight fasting. The proportion of fats and carbohydrates oxidized was also not statistically significantly affected by IFABP-ablation in either metabolic state (fed and fasted). A lower RQ in overnight fasted IFABP-null mice would not have been surprising because by 48 hours of food deprivation, they have lost more fat mass than WT mice. The fasting-induced decrease in RQ was slightly greater in IFABP<sup>-/-</sup> mice, although the difference was not statistically significant. It is possible that overnight fasted IFABP-null mice rely on fat only slightly more than WT, in accord with the RQ results, but IFABP-null mice lose more fat mass than WT during a more prolonged period of food deprivation (i.e., when fat oxidation is greater), in accord with the DEXA results. In other words,

the genotype effect on respiratory quotient may have been undetectable after overnight fasting, but would become apparent by 48 hours of food deprivation. Assessing the kinetics of the reduction in fat mass during food deprivation by serial DEXA measurements would help to clarify this. Another possibility, and probably the most likely, is that the difference between WT and IFABP-null mice in the absolute amount of fat mass lost is not quantitatively large enough to affect RQ. In other words, although indirect calorimetry clearly detected the expected large reduction in RQ induced by overnight fasting (0.9 to 0.8 in the fed and fasting states, respectively) it may lack the sensitivity to detect smaller differences, like those expected between WT and IFABP-null mice. In either case, as with the potential relationship between the IFABP polymorphism A54T and energy balance, this area deserves further exploration.

#### *PLASMA TRIACYLGLYCEROLS AND ORAL FAT-TOLERANCE TEST*

IFABP-ablation had no effect on fasting plasma triacylglycerols. Previous reports on this have been mixed. Vassileva et al. (FASEB 2000) reported elevated triacylglycerols in fasted IFABP-null mice, and then later reported no difference (Agellon et al., BBA 2007). Fasting plasma triacylglycerols are increased in certain populations of IFABP (A54T) homozygotes (healthy people, Salguero et al., 2005; Type II diabetics, Georgopoulos et al., 2000), but not others (healthy subjects, Agren et al., 1998) suggesting a potential role for IFABP in mediating lipemia. If one exists, it is likely indirect as fasting plasma triacylglycerols are mainly non-intestinal and IFABP expression is restricted to the intestine.

The oral fat-tolerance test provides a global estimate of fat absorptive capacity and, unlike fasting plasma triacylglycerols, reflects specifically intestinal triacylglycerol secretion. A large lipid bolus (spiked with [ $^{14}\text{C}$ ]oleate and [ $^3\text{H}$ ]monoolein) is administered by oro-gastric gavage to fasted, conscious animals, and blood is drawn at various time points to determine the

plasma triacylglycerol response. Tyloxapol is injected intraperitoneally to inhibit peripheral lipoprotein clearance; therefore the plasma triacylglycerol response reflects intestinal secretion. Theoretically, a defect in the G3P-TG synthesis pathway would selectively reduce the appearance of [ $^{14}\text{C}$ ] relative to [ $^3\text{H}$ ], whereas a defective MGAT pathway would reduce both [ $^{14}\text{C}$ ] and [ $^3\text{H}$ ]. IFABP-ablation had no effect on the appearance of triacylglycerols, [ $^{14}\text{C}$ ] (from [ $^{14}\text{C}$ ]oleate), and [ $^3\text{H}$ ] (from [ $^3\text{H}$ ]monoolein) in plasma after an oral lipid load. This was not completely unexpected because the reduced incorporation of [ $^{14}\text{C}$ ]oleate in triacylglycerols relative to phospholipids in IFABP-null mice was caused primarily by increased incorporation into newly synthesized phospholipids, which are selected against for incorporation into chylomicrons and intestinal secretion after a fat load (Scow et al., 1967; Mansbach, 1977).

Dworatzek and coworkers (2004) reported no influence of the IFABP A54T polymorphism on plasma triacylglycerols after an oral fat load. However, as mentioned above, reports on these patients have been inconsistent; e.g. Agren (1998) found increased plasma triacylglycerols after an oral fat load in A54T homozygotes. These comparisons are important because the A54T mutation increases ligand (FA) binding affinity and enhances triacylglycerol secretion in Caco-2 cells, and hypertriglyceridemia is an established risk factor for mortality. Moreover, these findings collectively point to a specific relationship between intestinal lipid metabolism and IFABP (WT, A54T, IFABPko, etc) although the precise mechanism *in vivo* remains unknown.

## CONCLUSIONS

If the major function of enterocyte FABP's involves their shared fatty acid-binding capacity, then the presence of high levels of LFABP would explain why intestinal lipid steady state composition and acute synthesis are relatively intact in IFABP<sup>-/-</sup> enterocytes. Both proteins

likely share certain functions *in vivo* (similar to many other aspects of fat digestion and metabolism), which would account for the lack of quantitatively important defects in intestinal lipid metabolism (e.g., reduced absorption). In the present study, we have identified a function for IFABP that is divergent from that of LFABP. The TG/PL from dietary [ $^{14}\text{C}$ ]oleate is significantly reduced in IFABP $^{-/-}$  (but not LFABP $^{-/-}$ ). In particular, IFABP ablation substantially reduces the incorporation of diet-derived fatty acids into triacylglycerol relative to phospholipids in the small intestine, and this is primarily driven by an increased incorporation into phospholipids. No changes were found in the expression of lipid metabolism enzymes in IFABP $^{-/-}$  intestinal mucosa. Collectively, these findings suggest that IFABP functions by physically transporting fatty acids from the apical portion of the enterocyte away from phospholipid synthesis and possibly toward triacylglycerol synthesis. Although this supports the hypothesis that IFABP functions as an intracellular fatty acid-trafficking protein, precisely which lipid substrates are acylated by IFABP-bound fatty acid (e.g., glycerol-3-phosphate, lysophosphatidic acid, phosphatidic acid-derived diacylglycerol, monoacylglycerol-derived diacylglycerol, etc.), and their end product (e.g., triacylglycerol for storage, chylomicron triacylglycerol, etc.) are still unclear.

### **Chapter 3.**

**Liver fatty acid-binding protein (LFABP) ablation alters  
the anabolic and catabolic metabolism of lipids in the  
small intestine**

**Abstract**

The goal of this research is to examine the role of liver fatty acid-binding protein (LFABP) in intestinal lipid metabolism. The intestinal epithelia express two distinct FABPs, intestinal- and liver-FABP, with partially overlapping substrate specificity and cellular localization. We found that LFABP ablation in the mouse does not markedly affect mucosal lipid composition, nor does IFABP expression increase secondary to LFABP knockout. LFABP binds both long-chain fatty acids and monoacylglycerol *in vitro*. Interestingly, while intestinal fatty acid metabolism was unchanged in LFABP<sup>-/-</sup>, incorporation of monoolein into triacylglycerol relative to phospholipids was markedly reduced compared to WT. Intestinal fatty acid oxidation in LFABP<sup>-/-</sup> was indistinguishable from WT in the fed state but the fasting-induced increase in fatty acid oxidation was significantly impaired in LFABP-null mice, by ~33%. Thus, these studies indicate that LFABP plays a key role in determining both the anabolic and catabolic fates of dietary and bloodstream-derived lipids in the intestinal enterocyte.

## INTRODUCTION

### *LIVER FATTY ACID-BINDING PROTEIN*

Liver fatty acid-binding protein (LFABP) is a small (14.2kDa) cytoplasmic lipid binding protein with high affinity for fatty acids, lysophospholipids, bile salts, and various other hydrophobic compounds (Wilkinson and Wilton, 1987; Storch et al., 1989; Storch and Thumser, 2000). LFABP is expressed at high levels in intestinal enterocytes, where it is co-expressed with IFABP, and in hepatocytes. LFABP expression begins at birth and is increased after weaning (Gordon et al., 1984). LFABP binds both saturated and unsaturated fatty acids in the nM- $\mu$ M range (Richieri et al., 1994; Richieri et al., 2000). Utilizing a fluorescence resonance energy transfer assay, Storch and coworkers demonstrated that LFABP facilitates the transfer of long chain fatty acids to membranes by a diffusional mechanism (Thumser and Storch, 2000; Hsu and Storch, 1996).

As early as 1976, LFABP was proposed to play a role in intestinal lipid metabolism. Using everted intestinal sacs, Ockner and Manning (1976) demonstrated that oleate oxidation and incorporation into triacylglycerol was markedly diminished when an inhibitor of fatty acid binding to FABP ( $\alpha$ -bromopalmitate or flavaspidic acid) was included in the assay. Interestingly, neither oleate uptake, nor microsomal MGAT and DGAT activities were diminished suggesting that the only deficient step in the process was transfer of the fatty acid from its site of absorption to the endoplasmic reticulum where TG synthesis occurs. In our present results with the LFABP<sup>-/-</sup> mice, [<sup>14</sup>C]oleate incorporation into TG in enterocytes was not affected. In the livers of these mice, on the other hand, oleate incorporation into TG and total TG mass was found to be decreased (Newberry et al., 2003). It is possible that the inhibitors used by Ockner and Manning prevent FA binding to IFABP also, such that total FABP activity was similar to that in the livers of LFABP<sup>-/-</sup> mice.



Mansbach and coworkers have established an in vitro method to isolate endoplasmic reticulum-to-Golgi trafficking in enterocytes (Kumar and Mansbach, 1996). This technique facilitated isolation and characterization of a “pre-chylomicron transport vesicle” (PCTV) which unidirectionally transports nascent “prechylomicrons” from the endoplasmic reticulum to the Golgi. The PCTV has many proteins associated with it, including vesicular proteins of the trans-Golgi and endoplasmic reticulum-Golgi intermediate compartment, as well as LFABP. Importantly, using this system it was demonstrated that lack of LFABP, either by immunoprecipitation or by using intestinal cytosol isolated from LFABP knockout mice, suppresses the incorporation of nascent triacylglycerol from the endoplasmic reticulum into PCTVs, suggesting the importance of LFABP in PCTV synthesis (Neeli et al., 2007).

#### *LFABP<sup>-/-</sup> LIVER PHENOTYPE*

In the fed state, LFABPKO mice are virtually indistinguishable from WT with the exception of slightly lower plasma insulin levels (Newberry et al., 2003 JBC). Davidson et al. (2003) observed a 75% decrease in hepatic TG accumulation and 80% reduced ketosis in 48h fasted LFABP-null mice compared to WT. Erol and coworkers (2004) showed that these fasting-induced phenotypes begin to appear as early as 18 hours after food removal. More recent studies in LFABP<sup>-/-</sup> mice have demonstrated subtle defects in hepatic branched-chain fatty acid (Atshaves et al., 2005), cholesterol (Martin et al., 2003), and bile acid metabolism (Martin et al., 2005). The most *quantitatively* important findings from LFABP-null mice thus far are suppression in liver fatty acid uptake, oxidation, and incorporation into triacylglycerol.

### *LFABP AND PPAR $\alpha$*

Peroxisome proliferator-activated receptor - $\alpha$  (PPAR $\alpha$ ) is a nuclear transcription factor with a ligand specificity and tissue expression overlapping with LFABP (Braissant et al., 1996). More specifically, both proteins are expressed in the liver and intestine, and both bind long chain fatty acids with high affinity. Thus it is possible that LFABP is involved in the actions of PPAR $\alpha$ . Early studies with immunofluorescence demonstrated that LFABP colocalizes with PPAR $\alpha$  in the nucleus and enhances the nuclear distribution of long chain fatty acids (Wolfrum et al., 2001; Huang et al., 2004). Moreover, LFABP and PPAR $\alpha$  bind with relatively high affinity and co-immunoprecipitate from liver homogenates (Hostetler et al., 2009). In hepatocytes isolated from LFABP-null mice, it was recently reported that a reduced expression of PPAR $\alpha$  target genes was found (Mcintosh et al., 2009). However, these latter results are in striking contrast to earlier findings. Erol et al. (2004) directly compared the expression of PPAR $\alpha$  target genes in livers from LFABP<sup>-/-</sup> mice and PPAR $\alpha$ <sup>-/-</sup> mice and convincingly demonstrated that in both the fed and fasted states, PPAR $\alpha$ -target genes are not dysregulated in LFABP<sup>-/-</sup> livers. A similar conclusion was obtained by Newberry et al. (2006). Moreover, we found no alterations in the expression of PPAR $\alpha$  target genes in the small intestinal mucosa of fasted LFABP<sup>-/-</sup> mice. The reasons for these apparently discrepant findings are not known.

### *CONTROVERSIAL BODY WEIGHT PHENOTYPE OF LFABP<sup>-/-</sup> MICE*

Erol and coworkers (2004) demonstrated that the body weight of LFABP-null mice was unaffected on chow and after 4 weeks of a high saturated fat (55% kcal from fat) diet (0.006% w/w cholesterol), and neither of these regimens altered plasma glucose, triacylglycerols, or free fatty acids relative to wild-type. In contrast to these results, Newberry et al. (2006) showed that when feeding a 0.15% w/w cholesterol, high saturated fat (42% kcal from fat) diet, 3 month old

female LFABP-null mice gain less weight than wild-type mice. This was later repeated by the same group (Newberry et al., 2008), who found that female LFABP-null mice gain significantly less body weight on a high fat diet (41% kcal) enriched in saturated fats, but no difference in bodyweight was found with unsaturated fats.

Martin et al. (2009) showed that, while consuming a low-fat chow diet (14% kcal from fat), older LFABP-null mice weigh more than WT. In this study, LFABP-null mice gained an additional ~4g specifically during months 6-9 which remained until the end of the study (at 18 months). Food intake was unchanged. Thus, it appears that LFABP genotype does not influence bodyweight on a standard low-fat diet in animals younger than 6 months old (Martin et al., 2009; this report, **Figure 3-10**), but appears to affect older animals or younger animals on a high fat diet. These variable findings await clarification.

It is possible that some of the inconsistencies in body weight data for the LFABP-ablated mice is due to different responsiveness to dietary fat type, however these results, too, are inconclusive. Newberry et al. have consistently demonstrated markedly reduced body weight gain in female LFABP<sup>-/-</sup> mice fed a high saturated fat diet (2006; 2008); however this contrasts with the findings of Erol et al. (2004) who showed no effect in either males or females under similar conditions. This may be due to the higher fat content used in the study by Erol (55% vs 41%), but that is counterintuitive. While Newberry's feeding regimen was much longer (20 weeks vs. 5 weeks), body weight was already significantly reduced by 5wks, when Erol reported no change. The diet used by Erol contained hydrogenated vegetable oil whereas Newberry's used beef tallow. Thus differences in the molecular composition of the dietary fats used, e.g., the presence of trans-fats in the former, may have contributed to the disagreement between the findings of Erol and Newberry.

Martin et al. (2005) demonstrated that feeding 1.25% w/w cholesterol on a purified low-fat (12% kcal from fat) diet does not alter body weight in 2-3 month old male LFABP<sup>-/-</sup> mice relative to WT (5 week dietary treatment, started when mice were 8 weeks old). Moreover, food intake was unchanged relative to wild type, and body composition was not altered by genotype or diet. In contrast to these findings, Newberry (2008) employed diets consisting of 1.25% and 2.0% w/w cholesterol, and showed that body weight gain was modestly reduced in LFABP<sup>-/-</sup> relative to WT, although this may have been confounded by lower starting body weights of the LFABP<sup>-/-</sup> mice in Newberry's study, or that female mice were used. However, the recent findings of Newberry et al. (2008; 2009) do stand in contrast with those of a later study by Martin et al. (2006), who reported significantly *increased* weight gain in cholesterol-fed female LFABP<sup>-/-</sup> mice relative to WT. Age and length of treatment was similar in the two studies, as was the 1.25% w/w cholesterol diet. The findings of Newberry's 1.25% w/w cholesterol diet study were not statistically significant at the 5-week mark (corresponding to the conclusion of Martin's dietary treatment, with no genotype-dependent effect observed for body weight gain) or at the end of the feeding study (12 weeks).

Newberry included a 2.0% w/w cholesterol dietary treatment in both studies (2008; 2009), and although this magnified the genotype effect on body weight in the 2009 study, the background diet was different (purified diet + 1.25% w/w cholesterol vs. standard chow + 2.0% w/w cholesterol) and this group of LFABP<sup>-/-</sup> mice started out with lower body weights than the WT; therefore it is improper to use these two diets to assess cholesterol dose-responsiveness. Moreover, the genotype effect on body weight gain actually appeared to be slightly greater on the 1.25% w/w cholesterol diet in the 2008 study, further complicating the interpretations of the results.

In conclusion, although there might be an interaction between LFABP genotype and dietary fat, there are many inconsistent results in the literature; more thorough studies including strict nutritional controls are necessary before a definitive conclusion can be drawn.

#### *BILE ACID METABOLISM IN LFABP<sup>-/-</sup> MICE*

LFABP binds bile salts *in vitro* (Takikawa and Kaplowitz, 1986; Thumser and Wilton, 1996) and two papers have been published examining the effect of a lithogenic diet on LFABP-null mice. Both groups used similar diets and male mice of a similar age, but as with the studies on dietary fat composition, these papers present equally equivocal results. For example, Xie et al. (2009) showed reduced body weight, lower hepatic triacylglycerols, and elevated serum bile acids in LFABP-null mice on the lithogenic diet, whereas Martin (2005) found no change in body weight (and body composition), hepatic triacylglycerols, and significantly reduced serum bile acids. There were subtle differences in the experimental methodology which may account for some of these contradictory findings. Treatment lasted 5 weeks in Martin's study and slightly less in Xie's (2-4 weeks). Prior to harvesting the livers for lipid analysis, Xie's mice were fasted for 4 hours whereas Martin's were fasted for 12 hours. This may be of particular importance because feeding status is known to have marked effects on hepatic triacylglycerols in LFABP-null mice (Newberry et al., 2003), although the more prolonged starvation (12 hours vs. 4 hours) would have been predicted to result in a greater reduction in hepatic triacylglycerols of LFABP-null relative to wild-type mice, the opposite of what is presented by these two papers. Both papers do agree, however, on the mild increase in serum total cholesterol in lithogenic diet-fed LFABP-null mice (an effect not seen in chow-fed or 48 hour starved LFABP-null animals [Newberry et al., 2003]).

LFABP-null mice demonstrated mildly reduced rates of VLDL cholesterol secretion from the liver after 2 weeks of a lithogenic diet (Xie et al., 2009). Because a similar reduction in VLDL triacylglycerol secretion was observed in 48h starved LFABP-null mice (Newberry et al., 2003), this may be a genotype effect, not a genotype-diet interaction.

Xie et al. (2009) also showed that chow-fed LFABP-null mice have reduced cholesterol absorption & increased fecal bile acid excretion (relative to WT), whereas a lithogenic diet nullifies the effect on cholesterol absorption and actually decreases fecal bile acid excretion. This confirms findings from the same group (Newberry et al., 2008) where they demonstrated a defect in cholesterol absorption that was corrected by cholesterol feeding in LFABP-null mice.

In sum, the most consistent and quantitatively important effects of LFABP-ablation on liver physiology are: reduced fatty acid oxidation/ketogenesis, and impaired triacylglycerol synthesis and accumulation. Conflicting results from the diet studies mentioned above preclude drawing any meaningful conclusions about genotype-nutrient interactions.

The majority of research on LFABP's function *in vivo* has focused on its role in hepatic lipid metabolism. Therefore, the focus of this portion of my research is on the function of LFABP in intestinal lipid metabolism. For all the studies, 3-4 month old male chow-fed LFABP<sup>-/-</sup> mice were compared to wild-type C57BL6 mice.

## MATERIALS AND METHODS

### *a. Materials*

Oleic acid and *sn*-2-monoolein were obtained from NuChek Prep, Inc. (Elysian, MN). [<sup>3</sup>H]oleic acid ([9,10-<sup>3</sup>H]oleic acid, 26.3 Ci/mmol) and [<sup>14</sup>C]oleic acid ([1-<sup>14</sup>C]oleic acid, 54 mCi/mmol) were obtained from Perkin Elmer-New England Nuclear (Stelton, CT). [<sup>3</sup>H]monoolein (*sn*-2-[9,10-<sup>3</sup>H]monoolein, 40–60 Ci/mmol) was from American Radiochemical (St. Louis, MO). Authentic neutral lipid and phospholipid standards were purchased from Doosan Serdary Research Laboratories (Toronto, Canada) and Avanti Polar Lipids (Alabaster, AL), respectively. Sodium taurocholate was purchased from Calbiochem (La Jolla, CA), and FA-free BSA was obtained from Sigma Aldrich (St. Louis, MO). TLC plates (Silica Gel G, 250 μm, 150 Å) were obtained from Whatman (South Plainfield, NJ). Rabbit antibodies to purified rat LFABP and IFABP were generated by Affinity Bioreagents (Golden, CO). All other materials were reagent grade or better.

### *b. Animals*

LFABP<sup>-/-</sup> mice on a C57BL/6J background were generated by Martin and coworkers (Martin et al., 2003), and heterozygous males were generously provided to us by B. Binas. The mice were back-crossed with C57BL/6J mice from Jackson Laboratories (Bar Harbor, ME) for six generations to create LFABP<sup>-/-</sup> mice and WT littermates to serve as controls. Some experiments included mice that had been back-crossed a seventh time; results from these experiments were consistent with the previous ones. Mice were used at 3-4 months of age and 25-30g body weight. Experiments were performed in the fasted state, typically between 8 AM and 11 AM when food had been removed 48 hours earlier. Animals were housed 3-4 per cage, maintained on a 12 hour light/dark cycle, and allowed *ad libitum* access to standard Purina rodent chow.

*c. PCR genotyping*

Genotyping was performed as described by Martin et al. (2003). In brief, a 0.5cm tail biopsy was incubated overnight at 37°C in lysis buffer (0.3M sodium acetate, 10mM Tris-HCl pH7.9, 1mM EDTA, 1% SDS, 0.2mg/mL proteinase K). The following morning, the crude tail lysate was cooled on ice and the precipitate was pelleted by centrifugation in a pre-cooled microfuge at maximum speed. 100µL of the clear supernatant was heated for 15 minutes at 95°C to obtain a heat-inactivated cleared tail lysate. PCR was performed with primers to amplify 123 base pairs of exon 2 of the WT allele (5'-caagggggtgtcagaaatcgtgc and 5'-ccagtcatggtctccagttcgca), primers to amplify 227 base pairs of a sequence specific to the knockout (neomycin resistance marker: 5'-aagagcttggcggcgaatgg and 5'-tggccatttggctgtgctc), 10X PCR buffer (SIGMA-buffer for REDTaq), dNTPs, REDTaq-polymerase (SIGMA), and the heat-inactivated cleared tail lysate in a final volume of 25µL. 10µL of the PCR reaction product was loaded directly onto a 2% agarose gel and separate electrophoretically (**Figure 3-1**).

*d. Preparation of lipids for bloodstream administration*

Stock solutions were prepared by drying (per mouse) 7.5µCi of either [<sup>14</sup>C]oleate (140nmol) or [<sup>3</sup>H]monoolein (125nmol) under a nitrogen stream, then adding 0.5% (final volume) ethanol, and 150uL of a solution containing 0.1M NaCl and mouse serum (1:1).

*e. Preparation of lipids for intraduodenal administration*

Stock solutions were prepared by drying (per mouse) 1.5µCi of either [<sup>14</sup>C]oleate (28nmol) or [<sup>3</sup>H]monoolein (25nmol) under a nitrogen stream, then adding 150uL of 10mM sodium taurocholate in 0.1M NaCl.

*f. Animals and surgical procedures*

For the experiments which required fasting, each mouse was individually housed at the time of food removal. On the day of the experiment, the mice were weighed and anesthetized



with ketamine/xylazine/ace promazine (80/ 100/150mg/kg, intraperitoneal, respectively). For intravenous administration of lipids, the jugular vein was exposed and cannulated, and a 28-gauge needle with the injection solution was secured in place by surgical string. For intraduodenal administration, a small section of the intestine was exposed and a small incision was made with microsurgical scissors within 1cm of the pylorus. A blunt-tip 18-gauge needle was passed into the intestine via the incision and secured in place by surgical string. Next, for both methods of delivery, two minutes after the injection, the intestine was removed and measured lengthwise, rinsed with 60mL ice-cold 0.1M NaCl, opened longitudinally and mucosa scraped with glass microscope slides into tubes in dry ice.

*g. Immunoblotting*

Mucosa was harvested as described above and homogenized in 20 volumes of PBS pH 7.4 with 0.5% (v/v) protease inhibitors (Sigma 8340) on ice with a Potter-Elvehjem homogenizer. Where indicated, a total membrane fraction was obtained by ultracentrifugation (100,000 x *g*, 1 hour at 4°C). Protein concentration was determined by the Bradford assay (Bradford, 1976 *Annals of Biochem*). 50µg of total cell protein or 10µg of membrane protein were loaded onto 12% polyacrylamide gels and separated by SDS-PAGE. The proteins were transferred onto polyvinylidene difluoride membranes using a semi-dry transfer system (BioRad) for 1 hour at 20V. The membranes were incubated in a 5% nonfat dry milk or 2% gelatin blocking solution overnight at 4 °C and then probed with primary antibody for 1 hour. After thorough washing, blots were then incubated with anti-rabbit, -chicken, or -mouse IgG-horseradish peroxidase conjugate, as necessary, for 1 hour and then developed by chemiluminescence (ECL reagent, GE Healthcare, Piscataway, NJ). Protein expression was quantified by densitometric analysis with ImageJ software (NIH).

The mucosal samples were diluted with 20mL of PBS pH 7.4 per gram (wet weight) and homogenized by 20 strokes with a Potter-Elvehjem homogenizer on ice and stored at -80°C lipid extraction (by the method of Folch et al., 1957) within two days. The homogenate was diluted to a protein concentration of 1mg/mL and 1mL was used for lipid extraction. Lipids were extracted twice with 10mL chloroform/methanol (2:1) and the aqueous phase discarded. The organic lipid layer was dried under a nitrogen stream, re-suspended in chloroform/methanol (2:1) and spotted onto Silica gel-G TLC plates along with standards of known mass. The TLC plate was developed in a nonpolar solvent system consisting of hexanes, diethyl ether, and acetic acid (70:30:1). For experiments where  $^{14}\text{C}$  was used, radioactivity was visualized by exposure to phosphorimager plates and analyzed by the Storm 840 Phosphorimager. When  $^3\text{H}$  was used, the lipid spots were visualized by exposure to iodine vapors, and scraped into scintillation vials containing 5mL scintillation fluid. The scintillation vials were vortexed and allowed to settle overnight before analysis in a scintillation counter.

#### *h. Mucosal lipid composition*

To determine mucosal lipid composition, the intestinal mucosa was harvested as described above, however the intestine was divided equally into two segments (proximal and distal) prior to scraping the mucosa. Thin-layer chromatography was performed as described above and the iodine-stained TLC plates were scanned by a Hewlett-Packard Scanner. Absolute values for the masses of individual lipid subclasses were obtained by densitometric analysis using ImageJ software.

#### *i. Fatty acid oxidation*

Fatty acid oxidation was measured by the method of Ontko and Jackson (1964) with minor modifications. In brief, 1mL of 1mg/mL sample homogenate was incubated in a 15mL test tube with a smaller 0.5mL Eppendorf tube containing tissue paper soaked in 1M benzethonium

hydroxide to capture released  $^{14}\text{CO}_2$ . 1mL of 7% PCA was added to the homogenate to release [ $^{14}\text{C}$ ]acid-soluble metabolites and to insolubilize any remaining [ $^{14}\text{C}$ ]fatty acid. The tube was capped quickly and incubated overnight at 37°C with shaking. The radioactivity of the tissue paper and a sample from the 3000 x g supernatant of the acidified homogenate was analyzed by scintillation counting. The sum of the radioactivity contained in the supernatant and in the tissue paper was divided by the total amount of radioactivity contained in 1mg of the sample homogenate to determine the percent of fatty acids oxidized.

*j. Quantitative RT-PCR for mRNA expression analysis*

The protocol for mRNA acquisition and analysis was adapted from Chon et al. (2008). Briefly, tissues were homogenized in 4M guanidinium thiocyanate, 25mM sodium citrate, 0.1M  $\beta$ -mercaptoethanol using several strokes of a Polytron. Total RNA was further purified by phenol extraction and the RNeasy clean up kit (Qiagen, Valencia, CA) along with DNase treatment to minimize genomic DNA contamination. Reverse transcription was performed using 1 $\mu$ g of RNA, random primers, an RNase inhibitor, and reverse transcriptase (Promega Madison, WI) in a total volume of 25 $\mu$ l. Primer sequences were retrieved from Primer Bank (Harvard Medical School QPCR primer data base) and are shown in **Table 3-1**. The efficiency of PCR amplification was analyzed for all primers to confirm similar amplification efficiency. Real time PCR reactions were performed in triplicate using an Applied Biosystems 7300 instrument. Each reaction contained 80ng cDNA, 250nM of each primer, and 12.5 $\mu$ l of SYBR Green Master Mix (Applied Biosystems, Foster City, CA) in a total volume of 25 $\mu$ l. Relative quantification of mRNA expression was calculated using the comparative Ct method normalized to  $\beta$ -actin.

*k. Body weight*

Mice were housed 3-4 per cage, maintained on a 12h light-dark cycle, and fed *ad libitum* standard rodent chow. Body weight was measured weekly on a continuous basis over the course of 4-6 months after birth.

*l. Food intake*

For the measurement of food intake, mice were individually housed in wire-mesh bottomed metabolic cages and a known amount of food was given to each mouse. The 'crumbs' were collected regularly and the remaining food was weighed weekly. The crumb weight was subtracted from the gross food intake, and the difference divided by 7 to obtain the average daily food consumption. This was repeated for 1-2 weeks per mouse and weekly results were averaged. Week-to-week measurements were consistent.

*m. Fecal composition*

Two days worth of feces were collected at various time points while the mice were individually housed for analysis of fecal weight and lipid composition. The feces were dried and weighed, then 1mg (dry weight) was dissolved in water overnight and lipid extracted and analyzed as described above.

*n. Body Composition*

Body composition was analyzed by dual energy x-ray absorptiometry (DEXA, PIXImus; GE-Lunar Corp., Madison, WI) in fed mice and after 48h food deprivation. Total fat, fat-free, and bone mineral mass were evaluated excluding the head and tail. The instrument was regularly calibrated. Mice were anesthetized with ketamine/xylazine/ace promazine (80/ 100/150mg/kg, intraperitoneal, respectively) for the procedure.

*o. Energy expenditure / RQ*

Energy expenditure was assessed by the University of Cincinnati's Mouse Metabolic Phenotyping Center. Mice were placed in an indirect calorimetry chamber 3 hours prior to the

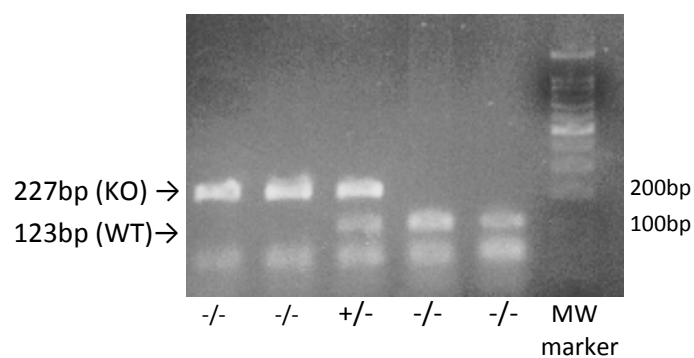
dark phase (3pm) and oxygen consumption and carbon dioxide production were measured for 24 hours. The data obtained from 6am to 3pm the following day were averaged and represent “fed” values. At 3pm on day 2, food was removed and measurements continued for 18 hours. The data obtained from 6am to 9am the following day (15-18 hours after food was removed) were averaged and represent “fasted” values. Metabolic rate data are expressed as kcal/hr and kcal/hr/kg body weight, and gas exchange data are expressed as mL/kg/min.

*p. Oral fat tolerance test*

An oral fat tolerance test was performed as described in Newberry et al. (2006). Briefly, 10 $\mu$ Ci of [ $^{14}$ C]oleate and [ $^3$ H]monoolein were dried under a nitrogen stream. 500 $\mu$ L of olive oil was added and the solution was vortexed vigorously. The olive oil bolus was administered via oro-gastric gavage to conscious, overnight fasted mice. 30 minutes prior to the gavage, Tyloxapol was injected (500mg/kg intraperitoneal) to block peripheral lipoprotein clearance. 50 $\mu$ L of blood was taken from the saphenous veins immediately prior to, and at 1, 2, and 4 hours post-gavage.

*q. Statistical methods*

Statistical comparisons were performed using independent two-sided t-tests, or ANOVA. Differences were considered significant if the p-value was less than 0.05.

**Figure 3-1**

**Figure 3-1. Verification of genotype by PCR.** PCR was performed as described in *Experimental Procedures*. Shown are three representative images of the PCR products of heterozygous (+/-), homozygous (-/-), and wild-type (+/+) mice.

**Table 3-1****qPCR primer sequences**

$\beta$ -ACTIN	forward	5'-GGC TGT ATT CCC CTC CAT CG-3'
	reverse	5'-CCA GTT GGT AAC AAT GCC ATG T-3'
MGAT2	forward	5'-TGG GAG CGC AGG TTA CAG A-3'
	reverse	5'-CAG GTG GCA TAC AGG ACA GA-3'
ER GPAT (GPAT3)	forward	5'-TAT CCA AAG AGA TGA GTC ACC CA-3'
	reverse	5'-CAC AAT GGC TTC CAA CCC CTT-3'
MT GPAT (GPAT1)	forward	5'- CTG CTT GCC TAC CTG AAG ACC-3'
	reverse	5'- GAT ACG GCG GTA TAG GTG CTT-3'
DGAT1	forward	5'-TGT TCA CGT CAG ACA GTG GTT-3'
	reverse	5'-CCA CCA GGA TGC CAT ACT TGA T-3'
DGAT2	forward	5'-TTC CTG GCA TAA GGC CCT ATT-3'
	reverse	5'-AGT CTA TGG TGT CTC GGT TGA C-3'
MGL	forward	5'-CAG AGA GGC CCA CCT ACT TTT-3'
	reverse	5'-ATG CGC CCC AAG GTC ATA TTT-3'
PPAR $\alpha$	forward	5'-TCG GCG AAC TAT TCG GCT G-3'
	reverse	5'-GCA CTT GTG AAA ACG GCA GT-3'
CB1	forward	5'-GGG CAC CTT CAC GGT TCT G-3'
	reverse	5'-GTG GAA GTC AAC AAA GCT GTA GA-3'
ACADL	forward	5'-TCC AGA GGT CAG TCA ACA TGA-3'
	reverse	5'-CCT GGT CAA TTT TTC GAG AGT CC-3'
ACOX1	forward	5'-GCA CCC CGA CAT AGA GAG C-3'
	reverse	5'-TAA ACT CCG GGT AAC TGT GGA-3'
CCOX	forward	5'-TCA ACG TGT TCC TCA AGT CGC-3'
	reverse	5'-AGG GTA TGG TTA CCG TCT CCC-3'
NADH De	forward	5'-GGT ACT TTG CTT GCT TGA TGA GA-3'
	reverse	5'-TGG GAA GAT ATA CGG CTG AGG-3'
SUCCDE	forward	5'-AAT TTG CCA TTT ACC GAT GGG A-3'
	reverse	5'-CTC CTG GGA CTC ATC CTT CTT-3'

**Table 3-1. qPCR primer sequences.** MGAT (monoacylglycerol acyltransferase-2), ER GPAT (endoplasmic reticulum glycerol-3-phosphate-3), MT GPAT (mitochondrial GPAT-1), DGAT (diacylglycerol acyltransferase), MGL (monoacylglycerol lipase), PPAR $\alpha$  (peroxisome proliferator activated receptor- $\alpha$ ), CB1 (cannabinoid receptor-1), ACADL (long chain acyl-CoA dehydrogenase), ACOX1 (acyl-CoA oxidase-1), CCOX (cytochrome C oxidase), NADH De (nicotine adenine dinucleotide dehydrogenase), SUCCDE (succinate dehydrogenase).

## RESULTS

### *IFABP PROTEIN EXPRESSION*

Due to the overlapping ligand specificity and similar intracellular localization, it was possible that ablation of one enterocyte FABP would result in compensatory upregulation of the other. However, the results showed that IFABP expression is unchanged in 3-4 month old fasted LFABP-null mice (**Figure 3-2**).

### *INTESTINAL LIPID COMPOSITION*

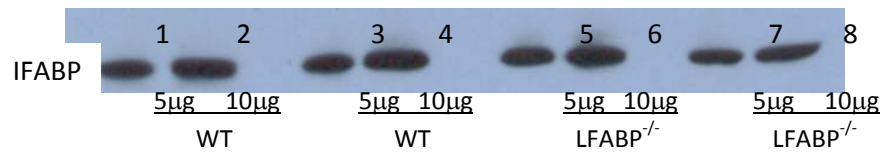
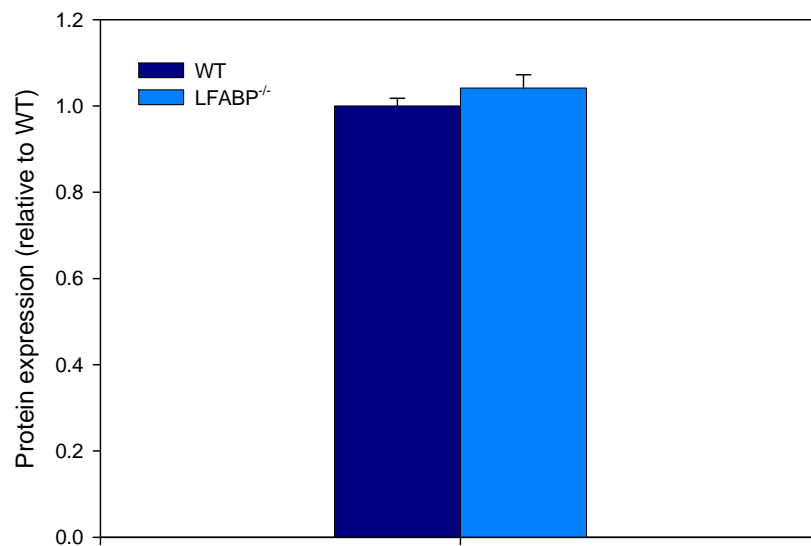
Lipid composition of the proximal and distal intestinal mucosa in the fasted mouse intestine was analyzed by lipid extraction and separation by TLC, and the lipid spots were visualized and quantified with iodine staining and densitometry. As seen in **Figure 3-3a**, the major lipid components of the proximal mucosa were phospholipids, cholesterol, and triacylglycerols representing ~54%, 26%, and 10% of the total lipids, respectively. A similar pattern was observed in the distal mucosa (**Figure 3-3b**).

LFABP-ablation caused a significant reduction in cholesterol ( $177.2 \pm 38.2$  vs.  $94.9 \pm 13.8 \mu\text{g}/\text{mg}$ ,  $p < 0.05$ ), free fatty acids ( $45.2 \pm 5.8$  vs.  $22.9 \pm 2.3 \mu\text{g}/\text{mg}$ ,  $p < 0.01$ ), and monoacylglycerols ( $19.8 \pm 3.4$  vs.  $5.8 \pm 0.6 \mu\text{g}/\text{mg}$ ,  $p < 0.01$ ) in the proximal but not distal mucosa.

### *INTESTINE LENGTH*

In WT mice, the total length of the intestine, from the pyloric sphincter to the cecum, was  $39.9 \pm 0.7 \text{ cm}$  ( $1.6 \pm 0.1 \text{ cm}/\text{g BW}$ ). This was unaffected by LFABP ablation ( $40.1 \pm 1.0 \text{ cm}$ ,  $1.5 \pm 0.1 \text{ cm}/\text{g BW}$ ).



**Figure 3-2****A****B**

**Figure 3-2. IFABP expression in the intestinal mucosa.** (A) Representative immunoblot of tissue homogenates of samples from 2 WT animals and 2 LFABP<sup>-/-</sup> animals. Lanes 1-8: 5µg and 10µg of tissue homogenate protein from each mucosal sample. Lanes 1-4: Wild-type. Lanes 5-8: LFABP<sup>-/-</sup>. (B) IFABP expression in intestinal mucosa homogenates. Results are means ± standard deviation, n=4 per group.

Figure 3-3

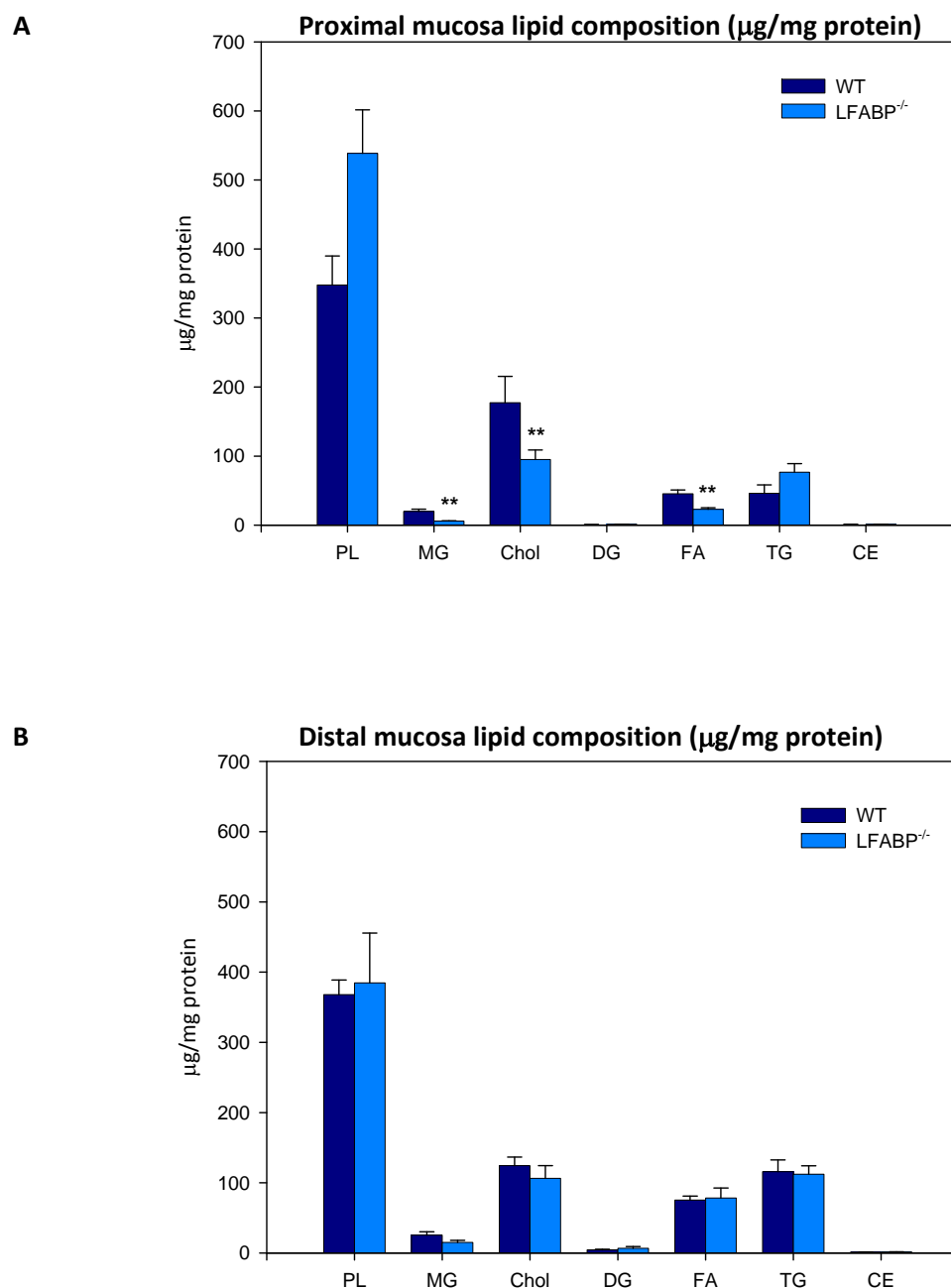


**Figure 3-3. Absolute mass of individual lipid classes in the intestinal mucosa of 48h fasted male mice.** Lipids were extracted as described in Materials and Methods, separated by TLC along with standards of known mass, and then iodine stained and scanned for densitometric analysis. **(A)** Lipids of the proximal intestine mucosa. **(B)** Lipids of the distal intestine mucosa. Total lipid mass was  $655.0 \pm 95.5 \mu\text{g}/\text{mg}$  for WT, and  $740 \pm 90.0 \mu\text{g}/\text{mg}$  for LFABP<sup>-/-</sup> in the proximal mucosa, and  $714.6 \pm 55.2 \mu\text{g}/\text{mg}$  for WT and  $704.9 \pm 111.7 \mu\text{g}/\text{mg}$  for LFABP<sup>-/-</sup> in the distal mucosa. Results are means  $\pm$  SE,  $n=4-6$  per group,  $**p<0.01$  vs. WT.

### *IN VIVO FA/MG METABOLISM*

The acute metabolism of fatty acid and monoacylglycerol was monitored by analyzing the recovery of [ $^{14}\text{C}$ ] or [ $^3\text{H}$ ] in intestinal mucosa harvested 2 minutes after bolus administration of [ $^{14}\text{C}$ ]oleate or [ $^3\text{H}$ ]monoolein, respectively. We monitored the metabolism of dietary vs. endogenous-derived lipids by administering the bolus intraduodenally, to mimic dietary presentation of the lipids to the apical surface of enterocytes, or by jugular vein cannula, to mimic bloodstream-delivery to the basolateral enterocyte surface. Since the presence of a meal in the gut could impact the uptake and metabolism of lipids by intestinal enterocytes, all experiments were performed in fasted mice.

#### *METABOLISM OF DIET-DERIVED FA AND MG IN THE INTESTINAL MUCOSA OF WT MICE*

After intraduodenal administration of [ $^{14}\text{C}$ ]oleate, mucosal [ $^{14}\text{C}$ ] recovery was predominantly in triacylglycerols ( $55.6\% \pm 2.6\%$ ) or free fatty acids ( $20.9\% \pm 1.7\%$ ) (**Figure 3-4b**). Similarly, after administration of [ $^3\text{H}$ ]monoolein, mucosal [ $^3\text{H}$ ] was recovered mainly in TG ( $65.7\% \pm 4.2\%$ ) and free fatty acids ( $16.0\% \pm 2.9\%$ ) (**Figure 3-5b**). Recovery in phospholipids was significantly lower for [ $^3\text{H}$ ]monoolein than for [ $^{14}\text{C}$ ]oleate ( $2.6\% \pm 0.2\%$  vs.  $7.5\% \pm 1.1\%$ ,  $p < 0.01$ ). The TG/PL ratio, which represents the two major anabolic end points for fatty acids and monoacylglycerols, was 3-fold greater for monoolein than for oleate ( $26.4 \pm 2.3$  vs.  $8.9 \pm 1.3$ ,  $p < 0.01$ ).

#### *METABOLISM OF BLOODSTREAM-DERIVED FA AND MG IN THE INTESTINE OF WT MICE*

Compared to gastrointestinal tract administration, the anabolic fates of bloodstream-derived [ $^{14}\text{C}$ ]-oleate and [ $^3\text{H}$ ]-monoolein in intestinal enterocytes show a markedly different pattern of assimilation. Recovery in triacylglycerols was reduced by 58% for [ $^{14}\text{C}$ ]oleate ( $p < 0.01$ )

and by 33% for [ $^3\text{H}$ ]monoolein compared with dietary delivery (**Figures 3-4a** and **3-5a**).

Correspondingly, incorporation into phospholipids doubled for bloodstream-derived [ $^{14}\text{C}$ ]oleate and increased five-fold for [ $^3\text{H}$ ]monoolein, relative to diet-derived lipids. The resultant TG/PL ratio was thus reduced approximately 90% for bloodstream compared to dietary derived lipid substrates ( $8.9 \pm 1.3$  vs.  $1.8 \pm 0.2$  and  $26.4 \pm 2.3$  vs.  $3.1 \pm 0.4$  for [ $^{14}\text{C}$ ]oleate and [ $^3\text{H}$ ]monoolein, respectively;  $p < 0.01$  for all comparisons) (**Figure 3-6**). Moreover, [ $^{14}\text{C}$ ]oleate recovery was increased in cholesteryl ester, diacylglycerols, & monoacylglycerols for bloodstream-delivery relative to dietary, whereas none of these were significantly changed for [ $^3\text{H}$ ]monoolein recovery (**Figures 3-4** and **3-5**).

Figure 3-4

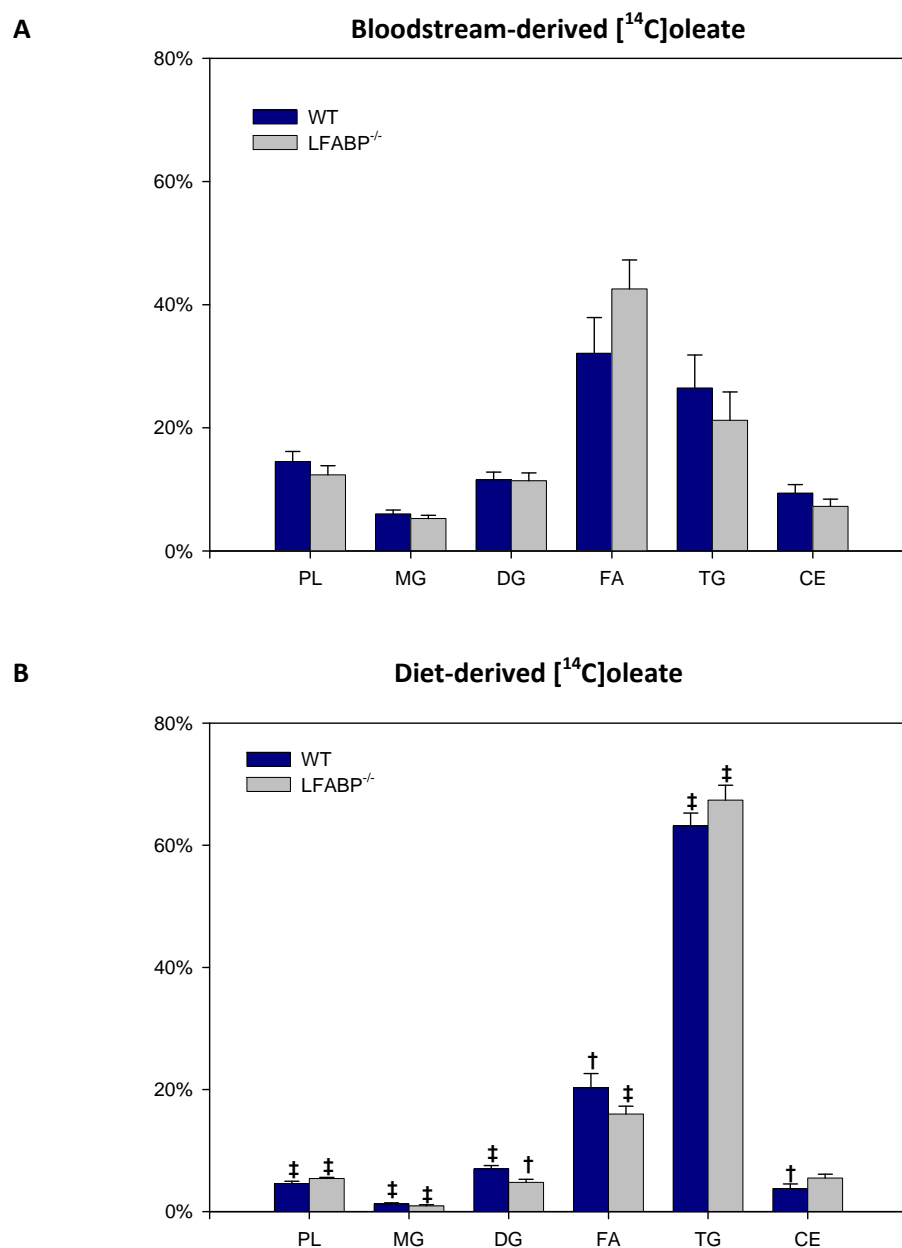
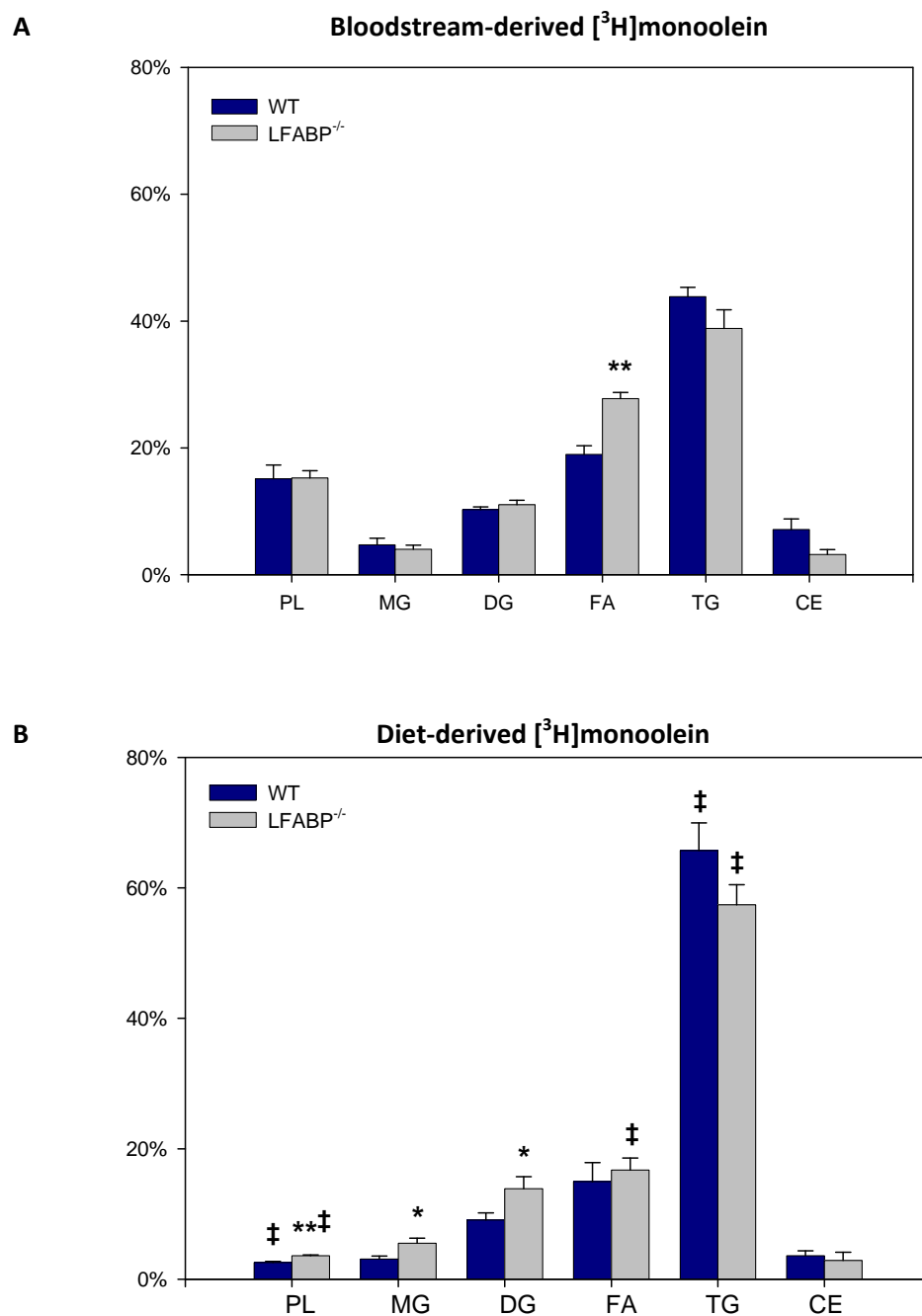


**Figure 3-4. Metabolism of bloodstream-derived and dietary-derived [ $^{14}\text{C}$ ]oleate in the small intestinal mucosa of 48h fasted mice.** Incorporation of [ $^{14}\text{C}$ ]oleate into fat-soluble metabolites in the small intestinal mucosa 2 minutes after bloodstream (A) or dietary (B) administration as described in Materials and Methods. Results are means  $\pm$  SE,  $n=10$  (WT) or 5 (LFABP<sup>-/-</sup>) for bloodstream delivery and  $n=7$  for dietary delivery in both WT and LFABP<sup>-/-</sup>, ‡ $p<0.01$ , † $p<0.05$  vs. bloodstream-derived FA.

# *EFFECT OF LFABP-ABLATION ON FA AND MG METABOLISM IN THE SMALL INTESTINE*

Incorporation of [ $^{14}\text{C}$ ]oleate, delivered either by dietary or bloodstream administration, into complex lipids was largely unaffected by LFABP-ablation. In contrast, compared to WT, recovery of mucosal [ $^3\text{H}$ ] from intraduodenally-administered [ $^3\text{H}$ ]monoolein was significantly increased in phospholipids ( $2.6\% \pm 0.2\%$  vs.  $3.6\% \pm 0.1\%$ , for WT and LFABP $^{-/-}$ , respectively,  $p < 0.01$ ), monoacylglycerols ( $3.1\% \pm 0.5\%$  vs.  $5.5\% \pm 0.8\%$ ,  $p < 0.05$ ), and diacylglycerols ( $9.1\% \pm 1.1\%$  vs.  $13.9\% \pm 1.8\%$ ,  $p < 0.05$ ). The recovery of [ $^3\text{H}$ ]monoolein in triacylglycerols was modestly reduced in LFABP $^{-/-}$  ( $65.7\% \pm 4.2\%$  vs.  $57.4\% \pm 3.1\%$ , for WT and LFABP $^{-/-}$ , respectively, NS) (**Figure 3-5b**). This resulted in a significant reduction in the TG/PL ratio ( $26.4 \pm 2.3$  vs.  $15.9 \pm 0.5$ , for WT and LFABP $^{-/-}$ , respectively;  $p < 0.01$ ) (**Figure 3-6b**). In contrast to dietary-derived lipids, the acute processing of bloodstream-derived [ $^{14}\text{C}$ ]oleate and [ $^3\text{H}$ ]monoolein was essentially unaffected in LFABP $^{-/-}$  intestinal mucosa. Only one difference was found, with recovery of bloodstream-derived [ $^3\text{H}$ ]monoolein in the free fatty acid fraction significantly increased in LFABP-null mice ( $19.0\% \pm 1.4\%$  vs.  $27.8\% \pm 0.9\%$ , for WT and LFABP $^{-/-}$ , respectively,  $p < 0.01$ ) (**Figure 3-5a**).

Figure 3-5

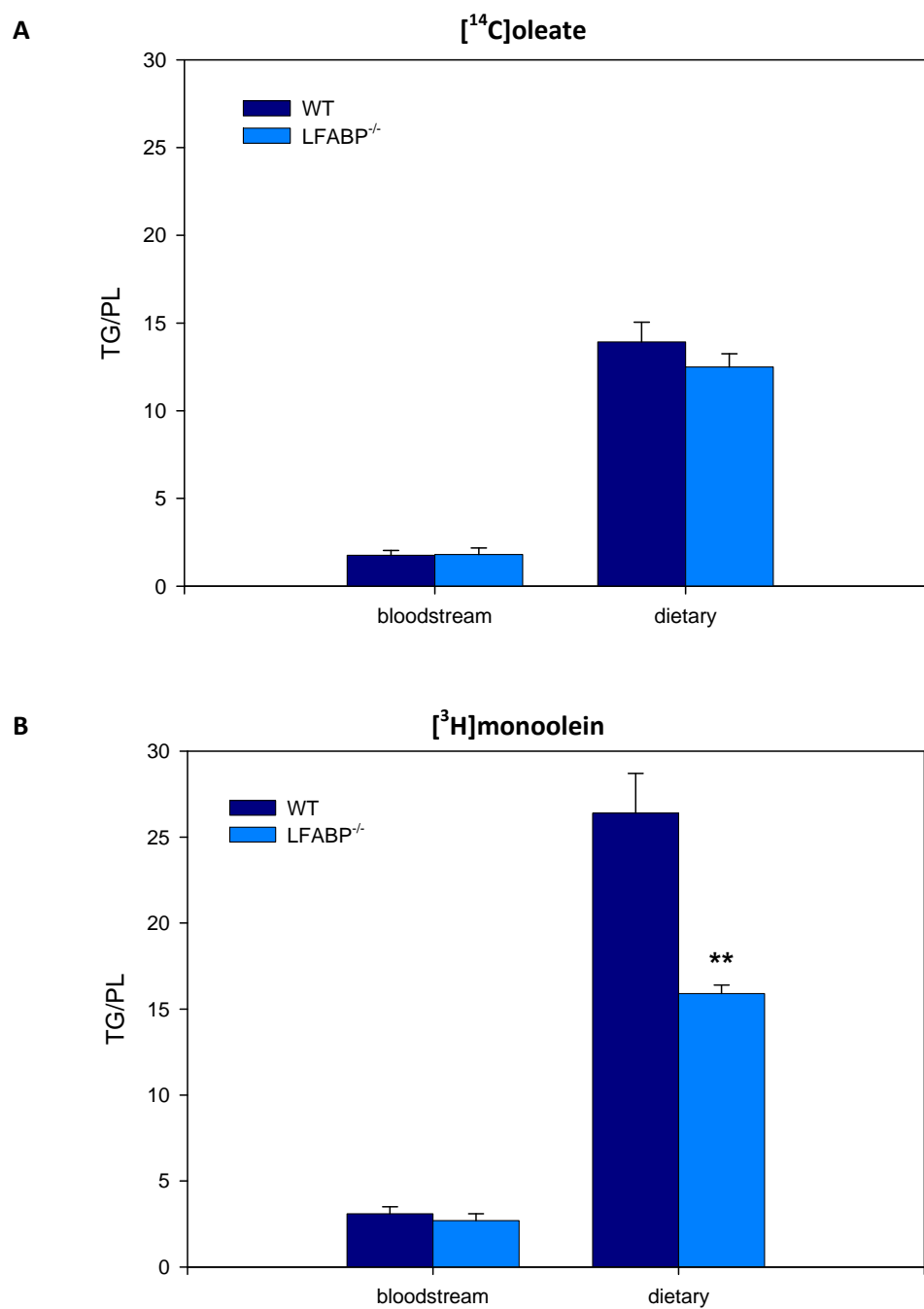


**Figure 3-5. Metabolism of bloodstream-derived and dietary-derived [ $^3\text{H}$ ]monoolein in the small intestinal mucosa of 48h fasted mice.** Incorporation of [ $^{14}\text{C}$ ]oleate into fat-soluble metabolites in the small intestinal mucosa 2 minutes after dietary (A) or bloodstream (B) administration as described in Materials and Methods. Results are means  $\pm$  SE,  $n=5-7$ , \*\* $p<0.01$ , \* $p<0.05$  vs. WT; ‡ $p<0.01$  vs. dietary-derived.

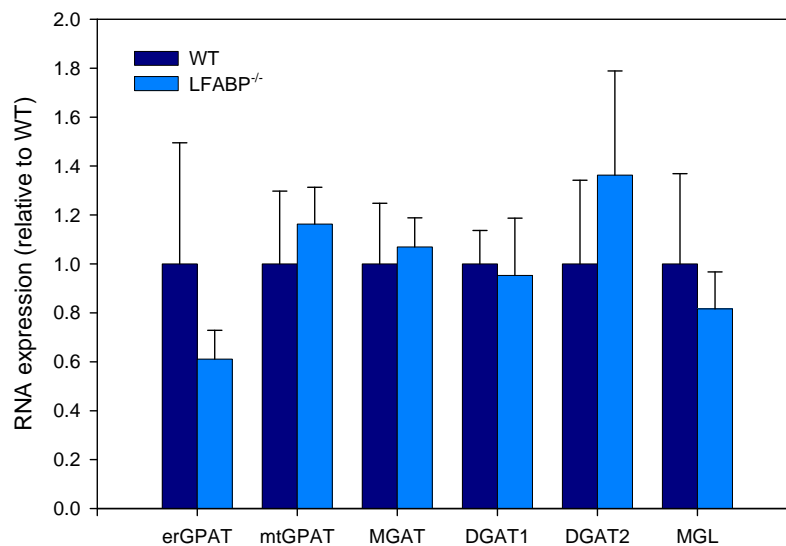
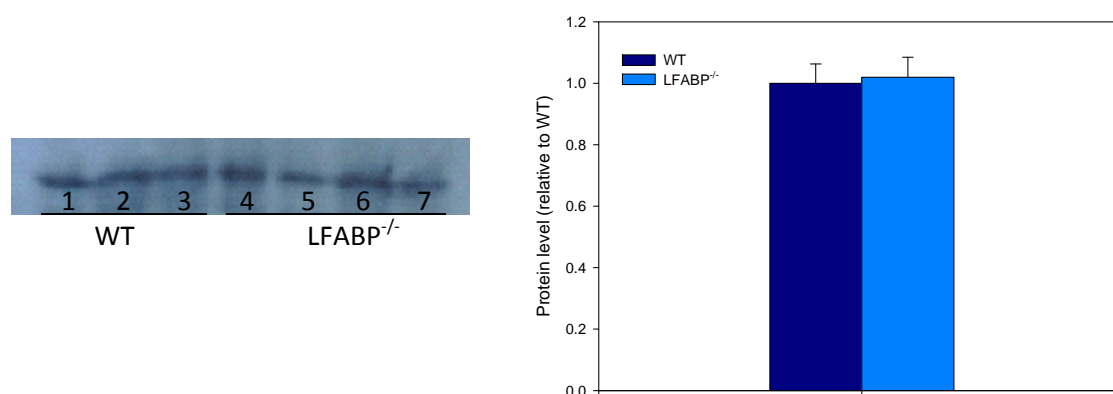
*NO EFFECT OF LFABP-ABLATION ON THE EXPRESSION OF LIPID SYNTHETIC GENES IN THE  
INTESTINAL MUCOSA*

To determine if any of the observed changes in the acute metabolism of fatty acids and monoacylglycerol were due to alterations in the expression of lipid synthetic genes in the LFABP-null animal, qPCR and immunoblotting were performed. The RNA levels of endoplasmic reticulum glycerol-3-phosphate acyltransferase (erGPAT), mitochondrial glycerol-3-phosphate acyltransferase (mtGPAT), monoacylglycerol acyltransferase-2 (MGAT2), diacylglycerol acyltransferase-1 (DGAT1), diacylglycerol acyltransferase-2 (DGAT2), and monoacylglycerol lipase (MGL) were analyzed by qPCR (**Figure 3-7a**). MGAT2 was also analyzed at the protein level by immunoblotting (**Figure 3-7b**). There were no significant differences found in any of the genes tested.



**Figure 3-6**

**Figure 3-6. Partitioning of oleate and monoolein in the intestinal mucosa.** Incorporation of  $[^{14}\text{C}]$ oleate (A) and  $[^3\text{H}]$ monoolein (B) into triacylglycerol relative to phospholipids 2 minutes after bloodstream or dietary administration as described in Materials and Methods. Results are means  $\pm$  SE,  $n=5-7$ , \*\* $p<0.01$  vs. WT.

**Figure 3-7****A****B**

**Figure 3-7. Expression of lipid metabolism genes in the small intestinal mucosa. (A)** Relative gene expression was determined by qPCR. Reaction conditions and primers are described in Materials and Methods and **Table 3-1**, n=3-4 per group. **(B)** Representative immunoblot of intestinal mucosa membrane fractions for MGAT2 as described in Materials and Methods, n=3-4 per group

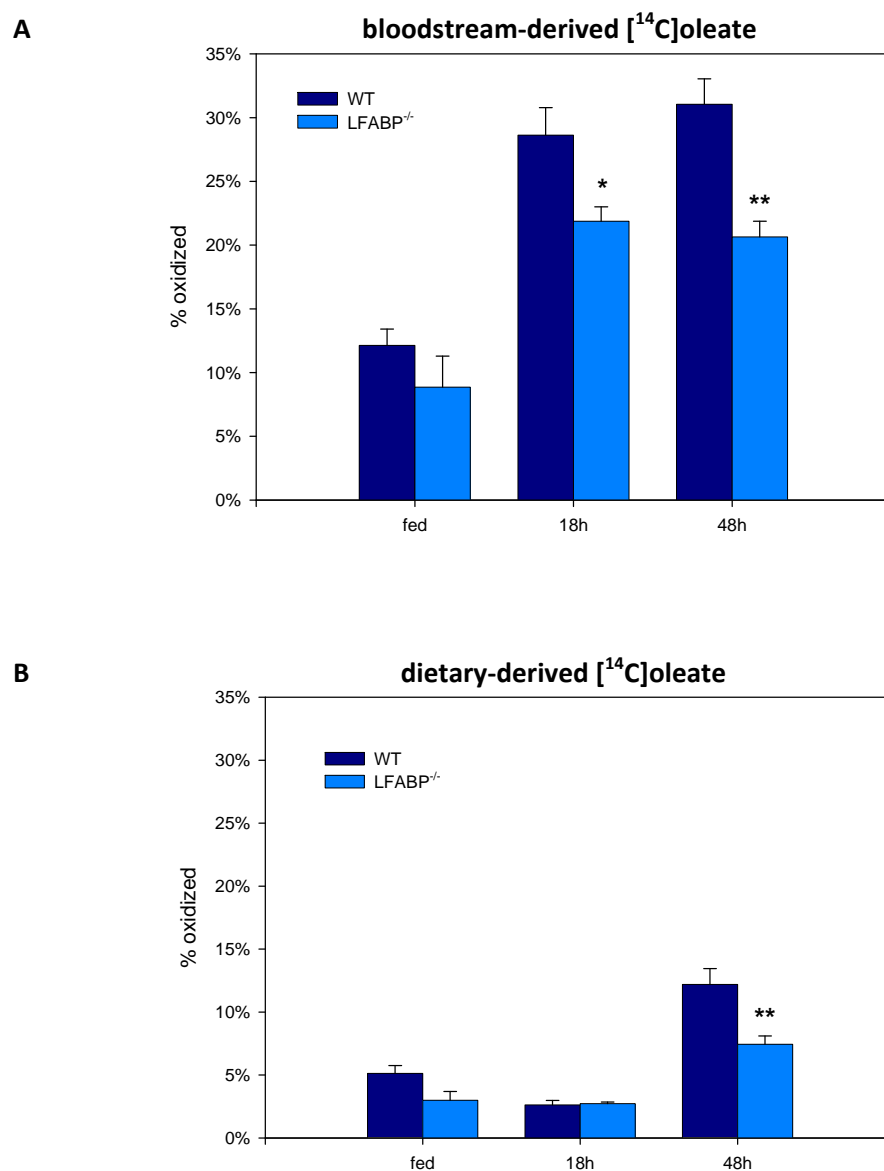
### *IMPAIRED OXIDATION OF BLOODSTREAM-DERIVED FATTY ACIDS IN LFABP<sup>-/-</sup> INTESTINAL MUCOSA*

The aforementioned studies focused on the anabolic fates of oleate in the intestinal mucosa; fatty acid oxidation was also measured by quantifying the appearance of  $^{14}\text{CO}_2$  and  $^{14}\text{C}$ -labeled acid-soluble metabolites of [ $^{14}\text{C}$ ]oleate in the same experiments. In the intestinal enterocytes of fed animals,  $12.1\% \pm 1.3\%$  of the [ $^{14}\text{C}$ ]oleate was oxidized within 2 minutes of bolus administration of the label into the jugular vein of fed mice (**Figure 3-8a**). Food deprivation significantly increased the oxidation of bloodstream-derived [ $^{14}\text{C}$ ]oleate to  $31.2\% \pm 1.6\%$  ( $p < 0.01$ ). Interestingly, this was significantly lower in LFABP<sup>-/-</sup> where only  $20.6\% \pm 1.2\%$  of the [ $^{14}\text{C}$ ]oleate was oxidized ( $p < 0.01$ ). Thus, the food deprivation significantly increased intestinal fatty acid oxidation in LFABP<sup>-/-</sup> mice, suggesting an intact fasting response, however the increase was blunted compared to WT mice.

### *IMPAIRED OXIDATION OF DIET-DERIVED FATTY ACIDS IN LFABP<sup>-/-</sup> INTESTINAL MUCOSA*

Intraduodenal administration of [ $^{14}\text{C}$ ]oleate resulted in a significantly lower recovery in  $^{14}\text{C}$ -labeled acid soluble products and  $^{14}\text{CO}_2$  compared to intravenous administration ( $12.1\% \pm 1.3\%$  vs.  $5.1\% \pm 0.6\%$ , for diet- and bloodstream-derived fatty acids, respectively,  $p < 0.01$ ) (**Figure 3-8**). Similar to oxidation of bloodstream-derived fatty acids in the fed state, oxidation of dietary fatty acids was not affected by ablation of LFABP. Food deprivation more than doubled oxidation of dietary fatty acids in WT mice, to  $12.2\% \pm 1.3\%$  ( $p < 0.01$ ). This increase was also impaired in LFABP<sup>-/-</sup> ( $7.5\% \pm 0.6\%$ ,  $p < 0.01$ ) intestinal mucosa.

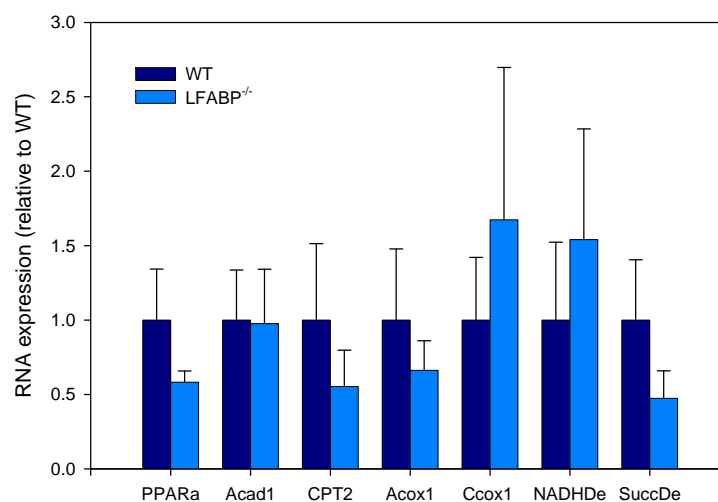
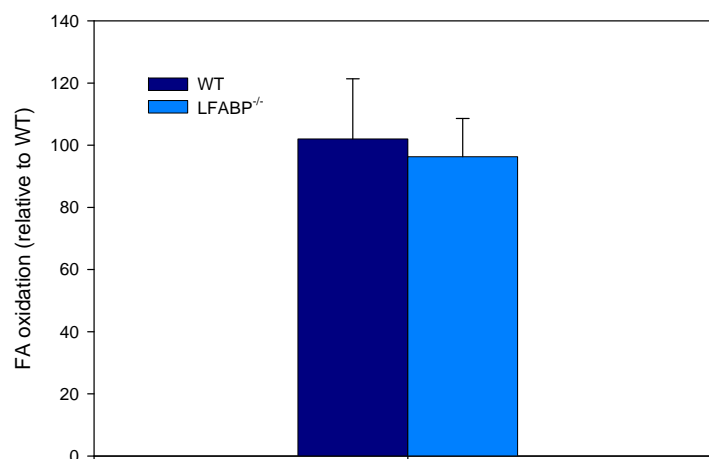
Figure 3-8



**Figure 3-8. Oxidation of [ $^{14}\text{C}$ ]oleate intestinal mucosa.** Oxidative metabolites of [ $^{14}\text{C}$ ]oleate 2 minutes after bloodstream (A) or dietary (B) administration as described in Materials and Methods. Results are means  $\pm$  SE,  $n=5-10$ , \*\* $p<0.01$ , \* $p<0.05$  vs. WT.

*FATTY ACID OXIDATION DEFECT IN LFABP<sup>-/-</sup> MICE IS NOT DUE TO ALTERED OXIDATIVE CAPACITY*

To distinguish a global reduction in oxidative capacity from a trafficking defect, fatty acid oxidative capacity was assessed by two methods. First, mRNA expression of key fatty acid oxidative enzymes were assessed by qPCR. None of the genes tested involved in mitochondrial  $\beta$ -oxidation (acyl-CoA dehydrogenase-1, carnitine palmitoyltransferase-2), peroxisomal fatty acid oxidation (acyl-CoA oxidase-1), electron transport (cytochrome C oxidase, NADH dehydrogenase, succinate dehydrogenase), or peroxisome proliferator-activated receptor- $\alpha$  were altered by LFABP ablation (**Figure 3-9a**). Next, fatty acid oxidation was analyzed in mucosa homogenates *in vitro* with [1-<sup>14</sup>C]oleic acid bound to albumin as the substrate. The use of a homogenate and albumin circumvent any trafficking defect that might be imposed by LFABP ablation and tests oxidative capacity directly. In accord with the hypothesized trafficking function of LFABP, oxidative capacity was unaffected in homogenates derived from LFABP<sup>-/-</sup> intestinal mucosa (**Figure 3-9b**).

**Figure 3-9****A****B**

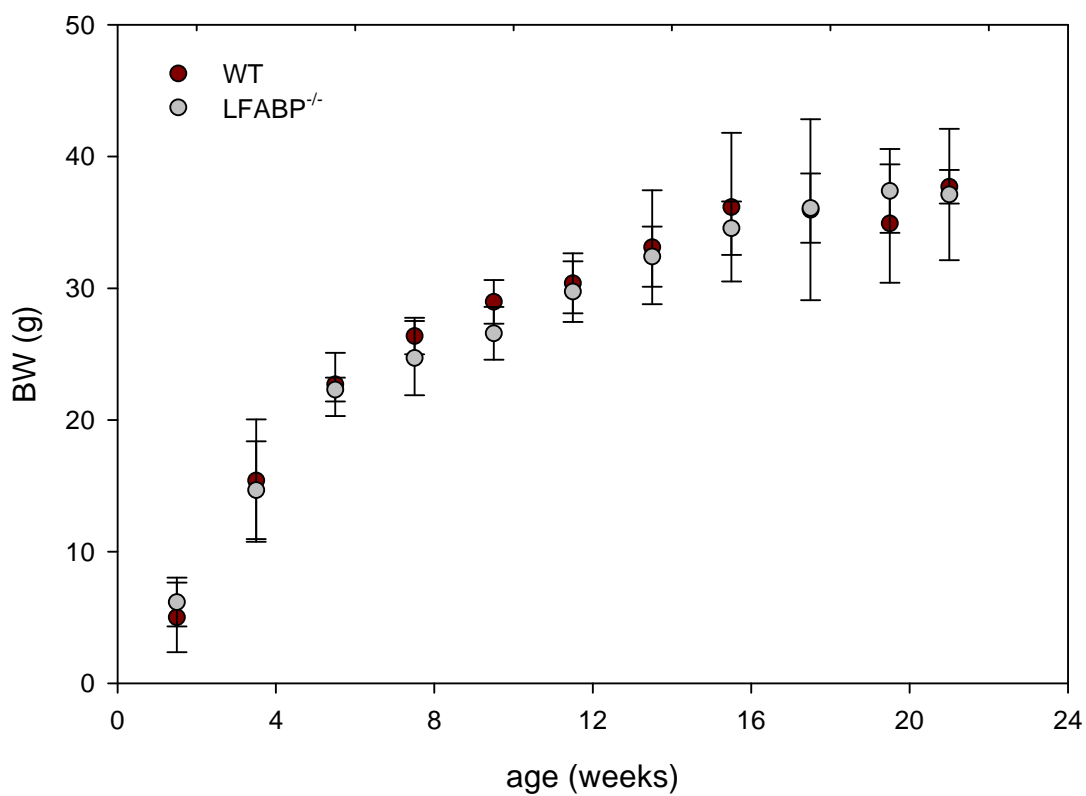
**Figure 3-9. Oxidative capacity is not affected by LFABP ablation.** (A) qPCR analysis of fatty acid oxidation enzymes in the small intestinal mucosa. Results are means  $\pm$  SE, n=3-4. (B) Fatty acid oxidation in homogenates from small intestinal mucosa of 48 hour fasted male mice as described in Materials and Methods. Results are means  $\pm$  SE, n=3-4.

### *BODY WEIGHT*

At no point between birth and at least 5 months of age did the body weight of LFABP<sup>-/-</sup> mice differ from WT (**Figure 3-10**).

### *BODY COMPOSITION*

In the fed state, WT mice weighing  $31.1 \pm 1\text{g}$  were comprised of  $24.2 \pm 0.5\text{g}$  fat-free mass ( $78.1\% \pm 1.8\%$  of total body weight) and  $6.9 \pm 0.7\text{g}$  fat mass ( $21.8\% \pm 1.8\%$  of total body weight) (**Table 3-3**). After 48 hours of food deprivation, bodyweight decreased by  $18.9\% \pm 1.9\%$  to  $25.3 \pm 1.0\text{g}$  ( $p < 0.01$ ). Fat-free mass was reduced by  $4.3 \pm 0.2\text{g}$  ( $17.8\% \pm 1.0\%$ ) to  $19.9 \pm 0.5\text{g}$  ( $p < 0.01$ ) and fat mass reduced by  $1.5 \pm 0.4\text{g}$  ( $21.9\% \pm 5.6\%$ ) to  $5.3 \pm 0.7\text{g}$  ( $p < 0.01$ ). Thus during starvation mice lose relatively similar fat and fat-free mass (~20% of the initial amount) but significantly more fat-free mass on an absolute basis. As seen in **Table 3-4**, LFABP<sup>-/-</sup> mice weighed  $29.9 \pm 1.2\text{g}$  and had modestly reduced fat-free mass in the fed state ( $22.7 \pm 0.5\text{g}$ ,  $p < 0.05$ ), although it was similar on a percentage basis ( $76.5\% \pm 2.5\%$ , NS). Upon food deprivation, LFABP<sup>-/-</sup> mice lost a similar amount of body weight ( $4.0 \pm 0.9\text{g}$ ), but less fat-free mass than their WT counterparts ( $2.7 \pm 0.5\text{g}$ ,  $p < 0.05$ ).

**Figure 3-10**

**Figure 3-10. Growth of LFABP<sup>-/-</sup> and WT mice.** Before weaning, the mean body weight includes both male and female pups. After weaning, only values for male mice are shown. Upon weaning, mice were housed 3-4 per cage and weighed weekly. Results are means  $\pm$  SE, n=12-15 per group.



**Table 3-2****WT**

	fed	fasted	$\Delta$
BW (g)	31.1 $\pm$ 0.9	25.3 $\pm$ 1.0	5.8 $\pm$ 0.6
FFM (g)	24.2 $\pm$ 0.5	19.9 $\pm$ 0.5	4.3 $\pm$ 0.2
fat (g)	6.9 $\pm$ 0.7	5.3 $\pm$ 0.7	1.5 $\pm$ 0.4
% fat	22.2%	20.9%	

**LFABP<sup>-/-</sup>**

	fed	fasted	$\Delta$
BW (g)	29.9 $\pm$ 1.2	25.9 $\pm$ 1.4	4.0 $\pm$ 0.9
FFM (g)	22.7 $\pm$ 0.5	20.0 $\pm$ 0.6	2.7 $\pm$ 0.5*
fat (g)	7.2 $\pm$ 1.0	5.9 $\pm$ 0.9	1.3 $\pm$ 0.7
% fat	23.4%	21.9%	

**Table 3-2. Effect of LFABP ablation on body composition in the fed and fasted state.** Body weight and composition as assessed by DEXA (Lunar PIXIMUS) in the fed state and after 48 hours of food deprivation, as described in Materials and Methods. Results are means  $\pm$  SE, n=7-8 per group, \* $p$ <0.05 vs. WT.

### FOOD INTAKE

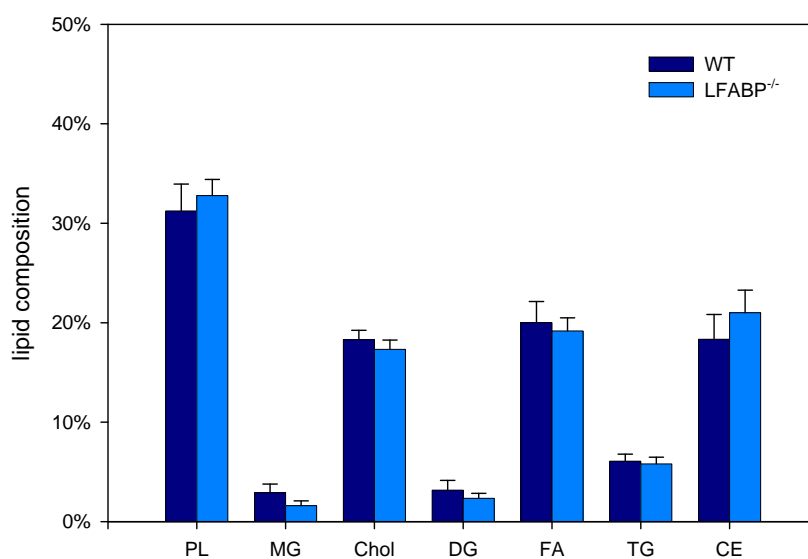
WT mice weighing  $30.6 \pm 0.7$ g fed a standard chow diet consumed  $2.3 \pm 0.1$ g/day ( $11.4 \pm 0.3$  kcal/day). LFABP<sup>-/-</sup> mice weighing  $28.7 \pm 1.1$ g consumed  $2.5 \pm 0.1$ g/day ( $12.3$ kcal/day) (NS).

### FECAL WEIGHT AND LIPID COMPOSITION

As a gross measurement of fat absorption, fecal lipid content and composition were measured. Total daily excrement amounted to  $0.77 \pm 0.06$  grams in WT mice and  $0.72 \pm 0.09$  grams in LFABP<sup>-/-</sup> mice (NS). The total lipid mass was  $8.7 \pm 1.6$ μg/mg feces in WT mice, and as seen in **Figure 3-11**, the lipid composition was mainly phospholipids ( $2.9 \pm 0.8$  μg/mg feces, or  $31.2\% \pm 2.7\%$  of the lipids), cholesterol ( $1.6 \pm 0.3$ μg/mg feces,  $18.3\% \pm 1.0\%$ ), fatty acids ( $1.7 \pm 0.2$ μg/mg feces,  $20.0\% \pm 2.1\%$ ), and cholesteryl esters ( $1.7 \pm 0.4$ μg/mg feces,  $18.3\% \pm 2.5\%$ ). Ablation of LFABP did not alter any of these parameters, suggesting that lipid absorption was largely unaffected.

### RESPIRATORY QUOTIENT

In WT mice,  $V_{O_2}$  was  $76.1 \pm 1.6$ mL/kg/min in the fed state and  $51.0 \pm 1.4$ mL/kg/min when fasting.  $V_{CO_2}$  was  $68.4 \pm 1.4$ mL/kg/min in the fed state and  $38.9 \pm 1.5$ mL/kg/min when fasting (**Table 3-4**). As expected, the respiratory quotient was reduced from  $0.90 \pm 0.02$  to  $0.76 \pm 0.01$  upon food deprivation, reflecting a greater reliance on fat oxidation to meet energy requirements (**Table 3-4, Figure 3-12**). In WT mice, total metabolic rate was  $22.5 \pm 0.5$ kcal/hr/kg ( $0.66 \pm 0.02$ kcal/hr) in the fed state and  $14.8 \pm 0.4$ kcal/hr/kg ( $0.42 \pm 0.01$ kcal/hr) when fasting (**Figure 3-13**). As seen in **Table 3-4**, fasting  $V_{O_2}$  and metabolic rate were significantly increased in LFABP-null mice ( $p < 0.05$ ).

**Figure 3-11**

**Figure 3-11. Fecal fat is unaffected by LFABP ablation.** Feces were collected every other day for 4-8 days, dried, weighed, and the dry weight was divided by 4-8 to determine daily fecal output. Lipids were extracted by the method of Folch and lipid subclasses were separated by TLC with standards of known mass, and stained with iodine for densitometric quantification as described in Materials and Methods. Data are expressed as % of total fecal lipid mass. Results are means  $\pm$  SE, n=7-8 per group.

**Table 3-3**

V <sub>O2</sub> , V <sub>CO2</sub> , and RQ under fed and fasting conditions			
		WT	LFABP <sup>-/-</sup>
Fed	V <sub>O2</sub> (mL/kg/min)	76.1 ± 1.6	72.5 ± 3.7
	V <sub>CO2</sub> (mL/kg/min)	68.4 ± 1.4	65.0 ± 3.5
	RQ	0.90 ± 0.02	0.90 ± 0.01
Fasted	V <sub>O2</sub> (mL/kg/min)	51.0 ± 1.4†	55.3 ± 1.3*
	V <sub>CO2</sub> (mL/kg/min)	38.9 ± 1.5‡	42.1 ± 0.8‡
	RQ	0.76 ± 0.01‡	0.76 ± 0.02‡
Δ	V <sub>O2</sub> (mL/kg/min)	25.1 ± 1.8	17.2 ± 2.5*
	V <sub>CO2</sub> (mL/kg/min)	29.6 ± 0.8	22.9 ± 3.2
	RQ	0.14 ± 0.01	0.13 ± 0.02

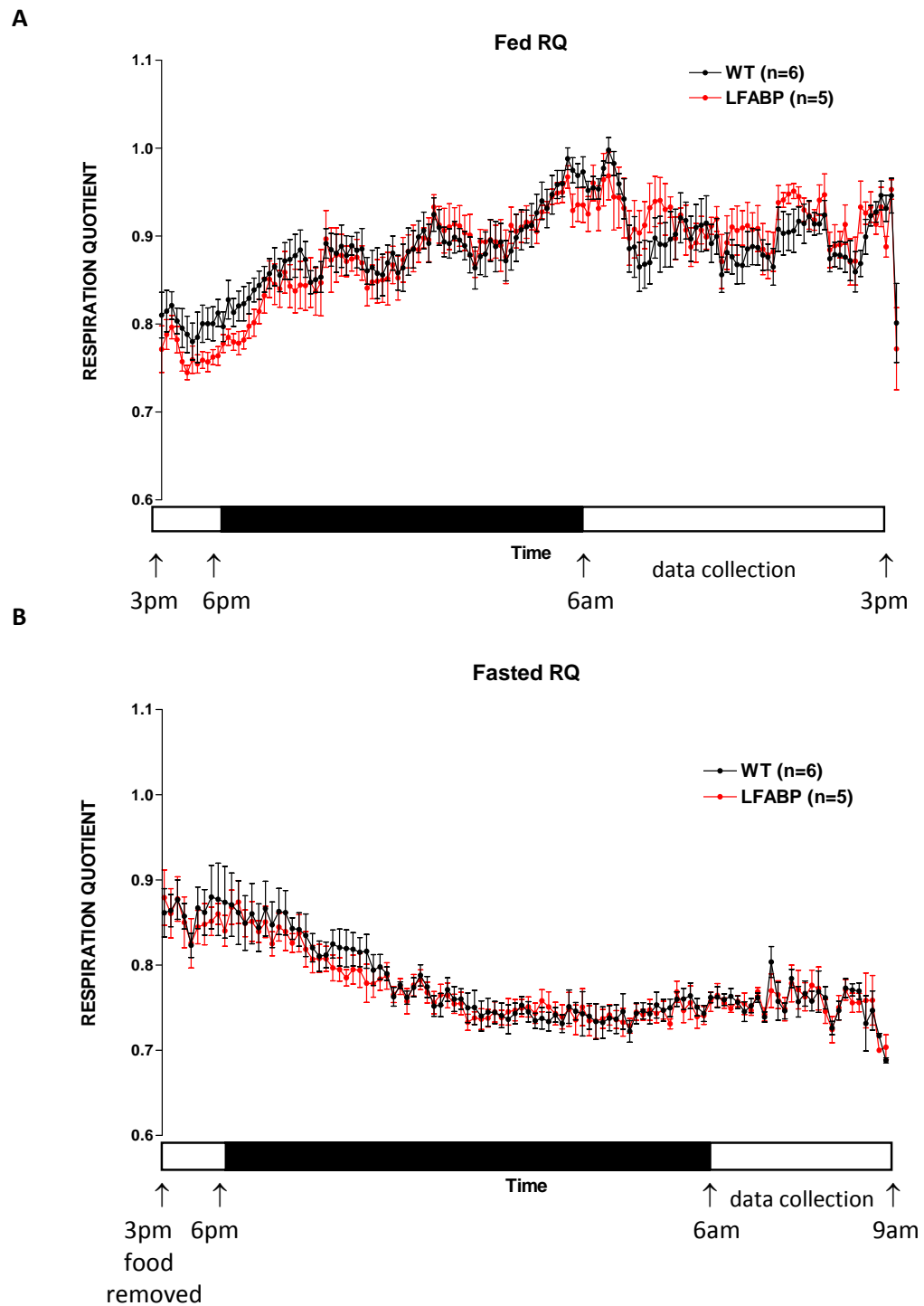
**Table 3-3. Respiratory quotient is normal in 3-4 month old male LFABP<sup>-/-</sup> mice.** Mice were placed in an indirect calorimeter and gas exchange was measured to calculate the respiratory quotient as described in Materials and Methods. Results are means ± SE, n=5-6 per group, \**p*<0.05 vs. WT, ‡ *p*<0.01, †*p*<0.05 vs. fed.

**Table 3-4**

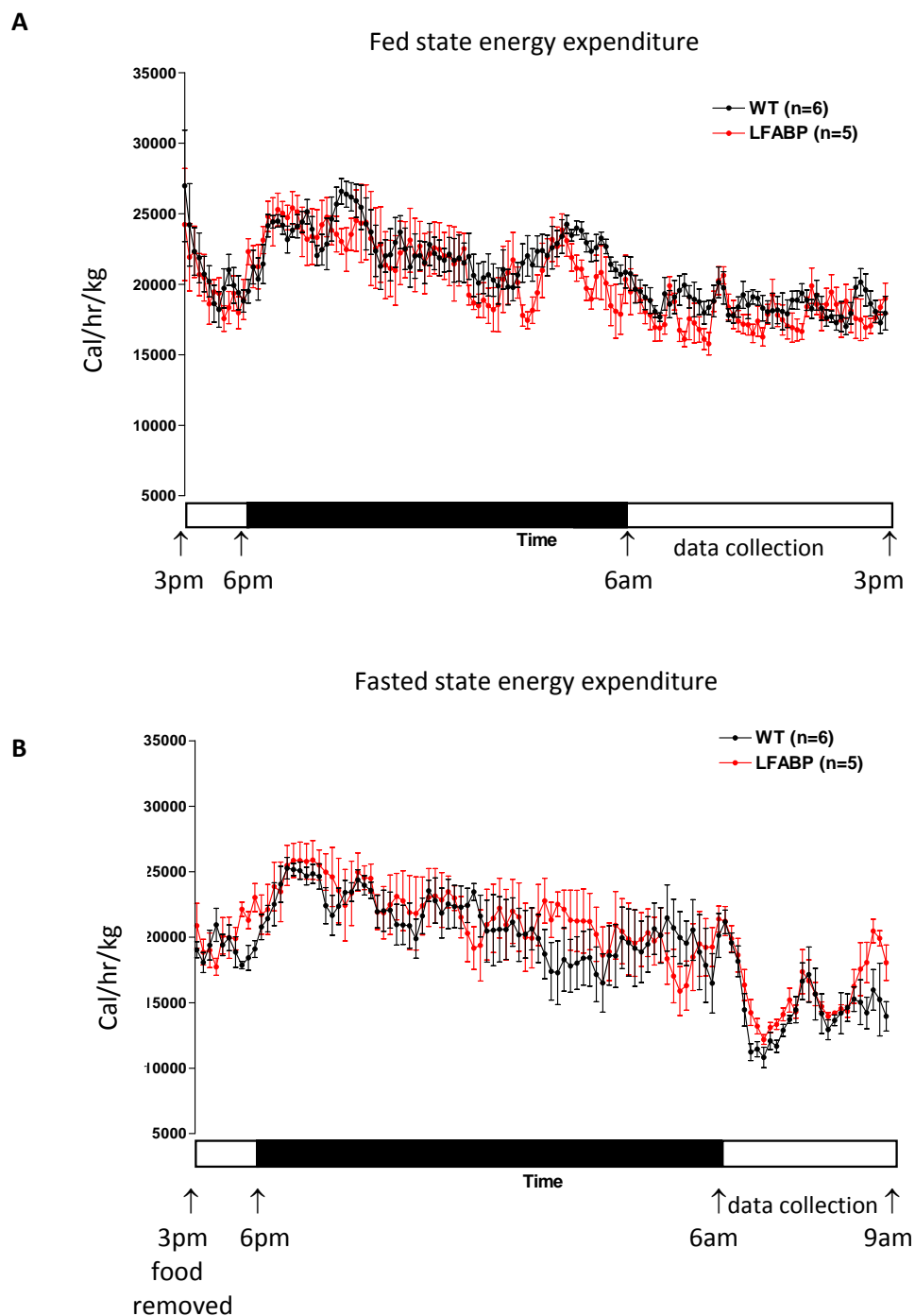
Metabolic rate under fed and fasting conditions			
		WT	LFABP <sup>-/-</sup>
Fed	kcal/hr/kg	22.5 ± 0.5	21.3 ± 1.1
	kcal/hr	0.66 ± 0.02	0.64 ± 0.02
Fasted	kcal/hr/kg	14.8 ± 0.4‡	16.0 ± 0.3‡
	kcal/hr	0.42 ± 0.01‡	0.47 ± 0.01‡*
Δ	kcal/hr/kg	7.7 ± 0.5	5.4 ± 0.7*
	kcal/hr	0.24 ± 0.02	0.18 ± 0.02*

**Table 3-4. Metabolic rate is normal in 3-4 month old male LFABP<sup>-/-</sup> mice.** Mice were placed in an indirect calorimeter and gas exchange was measured to calculate the metabolic rate as described in Materials and Methods. Results are means ± SE, n=5-6 per group, \**p*<0.05 vs. WT, ‡ *p*<0.01, †*p*<0.05 vs. fed.

Figure 3-12



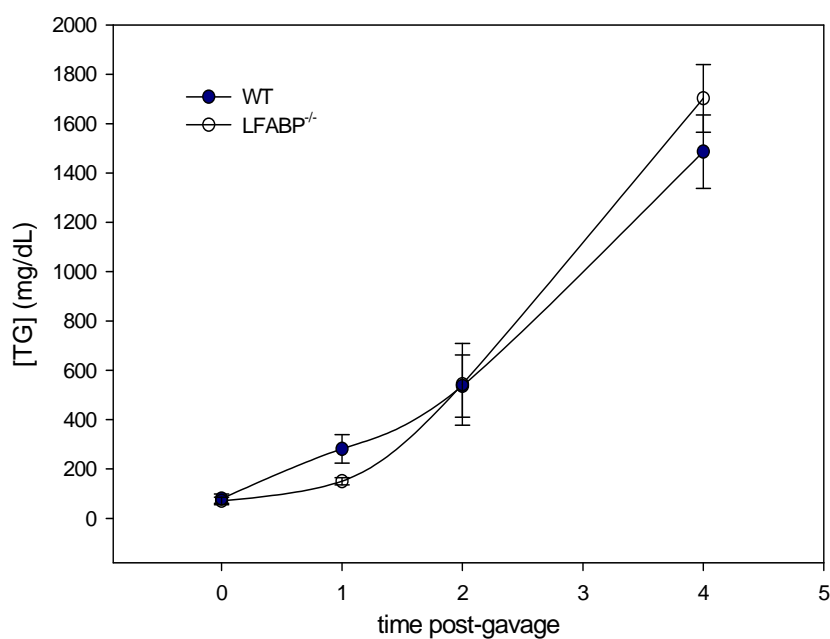
**Figure 3-12. 24h Respiratory quotient.** RQ was measured in 10 minute intervals over the course of 24 hours in fed (**A**) and fasting (**B**) mice as described in Materials and Methods. N=5-6 per group.

**Figure 3-13**

**Figure 3-13. Metabolic rate is normal in fed and fasting LFABP<sup>-/-</sup> mice.** Metabolic rate was measured as described in Materials and Methods. **(A)** 24 hour metabolic rate in mice with ad libitum access to Purina Rodent Chow. **(B)** 24 hour metabolic rate in fasting mice. N=5-6 per group.

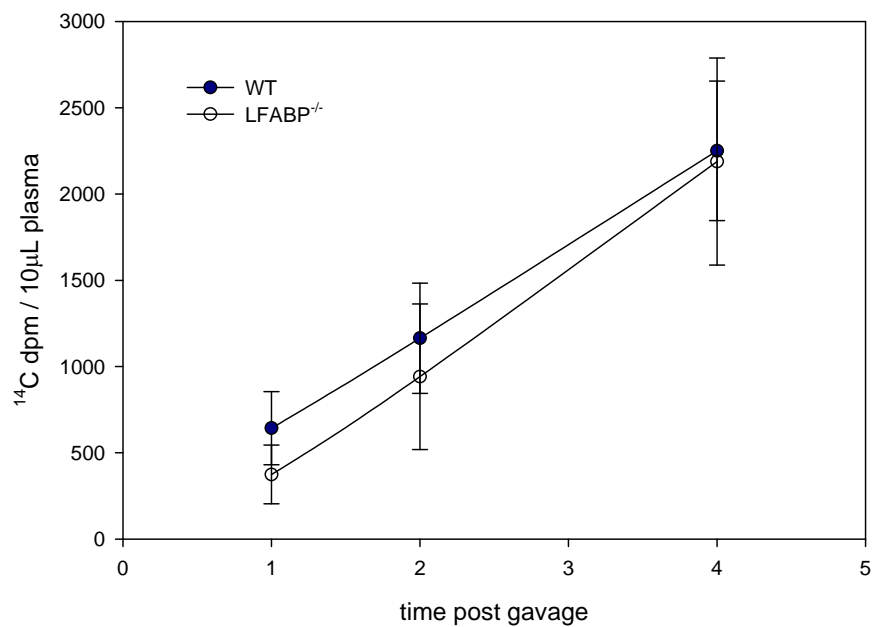
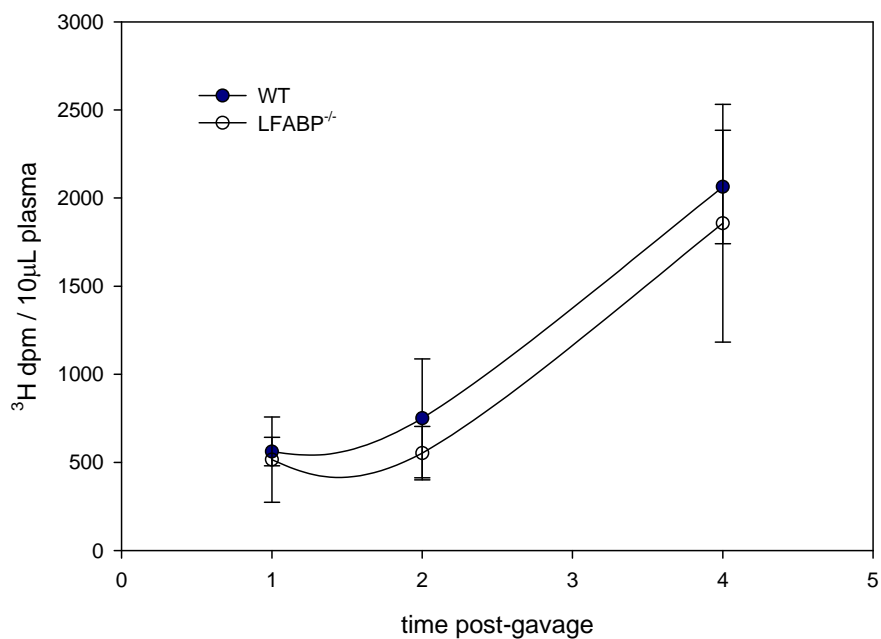
### ORAL FAT-TOLERANCE TEST

To assess the intestinal processing of a large lipid load, an oral fat tolerance test (OFTT) was performed. An intraperitoneal injection of tyloxal was employed to block peripheral triacylglycerol clearance, thus the increase in plasma triacylglycerols after an oral dose reflects specifically intestinal triacylglycerol secretion. Fasting plasma triacylglycerols were  $79.6 \pm 19.0$  mg/dL in WT mice and this was unchanged in LFABP<sup>-/-</sup> ( $70.6 \pm 15.2$  mg/dL, NS). After an orogastric gavage of 500  $\mu$ L olive oil containing [<sup>14</sup>C]oleate and [<sup>3</sup>H]monoolein (t=0), plasma triacylglycerols rose steadily in WT and LFABP-null mice (**Figure 3-14**). Plasma [<sup>14</sup>C] and [<sup>3</sup>H] radioactivity reflect the net absorption of intestinal lipid digestion end products, bulk triacylglycerol re-synthesis, and intestinal secretion. As seen in **Figure 3-15**, plasma radioactivities were slightly lower in LFABP-ablated mice, however differences were not statistically significant. This is in accord with the finding that two minutes after an intraduodenal injection of [<sup>14</sup>C]oleate or [<sup>3</sup>H]monoolein, intestinal triacylglycerol synthesis proceeds normally in LFABP<sup>-/-</sup> mice.

**Figure 3-14**

**Figure 3-14. No effect of LFABP ablation on intestinal triacylglycerol secretion.** Fasting, conscious mice were administered an intraperitoneal injection of tyloxapol and then given 500 $\mu$ L olive oil, [ $^{14}$ C]oleate, and [ $^3$ H]monoolein by oro-gastric gavage as described in Materials and Methods. Blood was drawn prior to the gavage and at various time points thereafter. Results are means  $\pm$  SEM, n=4-5 per group.



**Figure 3-15****A****B**

**Figure 3-15. No effect of LFABP ablation on intestinal triacylglycerol secretion.** Plasma radioactivity during the oral fat-tolerance test described in **Figure 3-13**. **(A)** Plasma  $^{14}\text{C}$  from the  $^{14}\text{C}$ oleate present in the oral lipid bolus. **(B)** Plasma  $^3\text{H}$  from the  $^3\text{H}$ monoolein present in the oral lipid bolus. Results are means  $\pm$  SEM,  $n=4-5$  per group.

## DISCUSSION

### *FABP EXPRESSION*

Expression of IFABP was not upregulated in the intestinal mucosa of LFABP<sup>-/-</sup> mice, in agreement with previous findings (Newberry et al., 2003). Reciprocal results were observed in IFABP<sup>-/-</sup> mice (Chapter 2). The fact that each of the enterocyte FABPs possesses independent regulatory mechanisms indirectly supports the hypothesis that the enterocyte FABPs possess divergent functions *in vivo*. This hypothesis is further suggested by the broader ligand specificity of LFABP, and the different *in vitro* transfer mechanisms of IFABP and LFABP. Further, the appearance of [<sup>3</sup>H]triacylglycerols in pre-chylomicron transport vesicles *in vitro* was much greater when [<sup>3</sup>H]triolein-loaded endoplasmic reticulum was incubated with LFABP than with IFABP (Neeli et al., 2007).

### *MUCOSAL LIPID COMPOSITION*

LFABP-ablation had no major affect on the proximal or distal intestine mucosal lipid composition, although small decreases in monoacylglycerols, fatty acids, and cholesterol were observed. LFABP is relatively enriched in the proximal intestine, so if LFABP influenced mucosal lipid composition, a greater genotype effect may have been expected in the proximal rather than distal intestinal. Indeed, this was the case. Given the relatively high affinity of LFABP for fatty acids and monoacylglycerols, and in accord with the findings presented in Chapter 4, these reductions may reflect reduced intracellular binding capacity.

LFABP is highly abundant in enterocyte cytosol and transfers fatty acids to and from membranes by a diffusional mechanism. These aspects have led to the suggestion that LFABP may function, in part, as a cellular buffer for free fatty acids, which can be toxic at high levels. The mucosal samples in these studies were obtained from animals deprived of food for 48

hours, clearly not a time associated with high intestinal lipid levels. Newberry et al. (2006) showed that 4 hours after an oral lipid bolus, the triacylglycerol content was in fact increased in the proximal quarter of the intestine in two separate groups of female LFABP-null mice relative to WT (12-14 week old mice on a standard chow diet; and 20 week old mice that were fed a high-fat Western diet for 8 weeks). Although the cellular free fatty acid buffer theory would have predicted elevated free fatty acids in LFABP<sup>-/-</sup> under these conditions, they were not reported. Moreover, elevated triacylglycerols in LFABP<sup>-/-</sup> intestine suggest an *enhanced* capacity to store fatty acids. It may also reflect a reduced capacity for secretion, in keeping with the role of LFABP in PCTV formation (Neeli et al., 2007).

#### *FA/MG METABOLISM IN VIVO*

We examined the metabolic fate of apical (diet-derived) and basolateral (bloodstream-derived) fatty acids and monoacylglycerol in the intestinal mucosa of WT and LFABP<sup>-/-</sup> mice. LFABP-ablation did not affect the partitioning of oleate into triacylglycerols or phospholipids regardless of its mode of presentation to the enterocyte (apical vs. basolateral).

The intestine has two major lipid synthetic pathways. Fatty acids and monoacylglycerol are substrates for the MGAT pathway, and the product is triacylglycerols. Fatty acids are also a substrate for the G3P pathway, and the products are triacylglycerols and phospholipids. The incorporation of a substrate into triacylglycerol relative to phospholipids ("TG/PL") reflects, in part, its partitioning into these pathways. Similar to what was seen in fed mice and rats (Gangl and Ockner, 1975; Storch et al., 2008), in intestinal mucosa from 48 hour starved mice: i) diet-derived (apical) lipid substrates favor incorporation into triacylglycerol relative to phospholipids, with monoolein showing a greater TG/PL than oleate (26.4 vs. 8.9,  $p < 0.01$ ); ii) bloodstream-derived (basolateral) lipid substrates also favor incorporation into triacylglycerol relative to

phospholipids, albeit to a 90% lesser extent than apical substrates ( $p < 0.01$ ), and monoacylglycerol still demonstrated a stronger propensity than fatty acid for incorporation into triacylglycerol relative to phospholipid (3.1 vs. 1.8,  $p < 0.05$ ). It is interesting to note that although the absolute TG/PL values for fatty acid and monoacylglycerol differ approximately 2-fold, the effect of compartmentation is maintained remarkably within 2% for both of these lipid substrates; the TG/PL ratio for basolateral compared to apical delivery is reduced 87% for fatty acids and 89% for monoacylglycerol relative to apical substrate.

#### *MONOACYLGLYCEROL METABOLISM IS ALTERED IN LFABP<sup>-/-</sup> SMALL INTESTINAL MUCOSA*

Although LFABP-ablation did not have a major effect on the steady state intestinal lipid composition, we did observe effects of LFABP ablation on the acute synthesis of several lipid products. Examination of lipid soluble metabolites showed that two minutes after an intraduodenal delivery of [<sup>14</sup>C]-oleate to LFABP-null mice, mucosal [<sup>14</sup>C] was recovered primarily in triacylglycerols, with no difference from WT. In contrast, after intraduodenal delivery of *sn*-2-[9,10-<sup>3</sup>H]monoolein, mucosal [<sup>3</sup>H] recovery in phospholipids and diacylglycerol were significantly increased, with a concomitant reduction in TG in the LFABP<sup>-/-</sup> mice. [<sup>3</sup>H] recovery was also increased in the MG fraction. The resulting TG/PL ratio was thus markedly reduced in LFABP<sup>-/-</sup> mice. Although a specific trafficking defect was our main hypothesis, it was also possible that expression of one or more lipid metabolic enzymes were altered. However, a qPCR analysis of genes involved in complex lipid synthesis (erGPAT, mtGPAT, MGAT2, DGAT1, and DGAT2) was performed and showed no significant genotype-induced alterations, supporting a trafficking function for LFABP. Similarly, increased [<sup>3</sup>H]monoolein recovery in the monoacylglycerol fraction was not due to decreased expression of monoacylglycerol lipase, suggesting slower

assimilation of newly arrived monoacylglycerol. Again, we hypothesize that this is due to defective monoacylglycerol trafficking in the LFABP<sup>-/-</sup> mouse intestinal cell.

These results suggest that LFABP is involved in the transport of MG away from phospholipid synthesis (as per the increased recovery of [<sup>3</sup>H]monoolein in diacylglycerols [an intermediate in the synthesis of phospholipids from monoacylglycerol] and phospholipids in LFABP<sup>-/-</sup>) and possibly toward triacylglycerol synthesis. The observation that no effects were found on the incorporation of fatty acids into complex lipids in LFABP<sup>-/-</sup> mice may be due to the high expression of IFABP in the intestine, which binds fatty acids but not monoacylglycerol.

#### *FATTY ACID OXIDATION IS IMPAIRED IN LFABP<sup>-/-</sup>*

Although fatty acid oxidation is neither an important source of energy for enterocytes (3.4% of mucosal CO<sub>2</sub> production, Windmueller and Spaeth, 1978), nor a quantitatively important component of total body energy expenditure (<0.1%), it is a regulated process. As expected, food deprivation significantly increased oxidation of [<sup>14</sup>C]oleate to CO<sub>2</sub> and water-soluble metabolites in WT intestine. In LFABP<sup>-/-</sup> intestine, however, this was markedly attenuated. Interestingly, genes involved in mitochondrial  $\beta$ -oxidation, peroxisomal fatty acid oxidation, electron transport, and PPAR $\alpha$  were unchanged relative to wild-type, suggesting a non-transcriptional effect of LFABP ablation. Moreover, LCFA oxidative capacity was unchanged in LFABP<sup>-/-</sup> intestinal mucosa homogenates *in vitro* in an experiment utilizing albumin to bypass the theoretical trafficking defect incurred by LFABP ablation. Erol and colleagues (2003) observed a similar phenotype in LFABP<sup>-/-</sup> livers, whereby palmitate oxidation was reduced in intact hepatocytes but not liver homogenates, and fatty acid oxidation genes were unchanged. Collectively, these results strongly imply that LFABP is involved in trafficking long-chain fatty acids toward oxidative pathways.

### WHOLE BODY PHENOTYPE

In accord with previous findings, LFABP<sup>-/-</sup> mice on a chow diet grow normally and maintain a body weight similar to wild-type mice (e.g., Newberry et al., 2003). Food intake and fecal lipids were also comparable to WT, suggesting LFABP is not necessary for gross lipid absorption.

LFABP ablation does not alter body composition when the mice are fed a variety of diets (e.g., Atshaves et al., 2005; Martin et al., 2005). Nevertheless, LFABP<sup>-/-</sup> mice experience a marked defect in hepatic and intestinal fat oxidation when fasted (Erol et al., 2003; **Figure 3-8**). Therefore, body composition was assessed before and after 48 hours of food deprivation. Although LFABP-null mice had comparable fat-free mass (FFM) in the fed state (78% vs. 77% of total body weight in WT and LFABP<sup>-/-</sup>, respectively), they lost significantly less FFM during 48h food deprivation (-4.3g vs. -2.7g,  $p < 0.05$ ) suggesting LFABP somehow hastens fasting-induced lean tissue degradation. Accordingly, the metabolic rate of LFABP<sup>-/-</sup> mice did not decrease as much as WT after 24 hours of fasting (-7.7 vs. -5.4 kcal/hr/kg, for WT and LFABP<sup>-/-</sup>, respectively,  $p < 0.05$ ). LFABP is involved in hepatic fatty acid oxidation during starvation, which provides energy for the liver to convert skeletal muscle-derived amino acids into glucose. Thus, it is possible that in LFABP-null mice, decreased hepatic fatty acid oxidation could result in less fuel for gluconeogenesis, thus reducing the use of skeletal muscle amino acids. It was found, however, that plasma glucose levels were maintained in 18 and 48 hour starved LFABP-null mice (Erol et al., 2004; Davidson et al., 2003). Moreover, enhanced lipolysis could have compensated for the reduced proteolysis, but we found that fat mass was not significantly reduced in LFABP<sup>-/-</sup> compared to WT. Thus, the mechanism of apparent FFM preservation in fasting LFABP<sup>-/-</sup> mice is uncertain.

Indirect calorimetry is a sensitive method to measure energy [heat] production and respiratory gas exchange ratio (RER). The latter is particularly relevant as it is determined by the relative contributions of fat and carbohydrate to total oxidation. LFABP ablation had no effect on RER in fed and overnight-fasted mice. Reduced intestinal fatty acid oxidation did not affect RER, as expected, because RER is a global measurement and therefore more affected by tissues that use the most energy (e.g., skeletal muscle). These results are also in accord with the presence of similar fat mass in fed and 48h fasted WT and LFABP-null mice.

#### *ORAL FAT TOLERANCE TEST*

The oral fat-tolerance test can be used to assess the net process of lipid digestion and absorption, and intestinal metabolism and secretion. A large lipid bolus spiked with [ $^3\text{H}$ ]monoolein and [ $^{14}\text{C}$ ]oleate is administered via oro-gastric gavage, and plasma samples are taken at various time points for analysis. Appearance of triacylglycerols in the plasma reflects: intestinal triacylglycerol hydrolysis; absorption of the resultant monoacylglycerol and fatty acids, their resynthesis into triacylglycerol within the enterocyte; and the packaging and secretion of chylomicrons. [ $^3\text{H}$ ]monoolein was included because it is assimilated primarily by the MGAT pathway (Lehner and Kuksis, 1996; Oxley et al., 2006), and also to determine if the lack of LFABP's monoacylglycerol-binding capacity had a physiologically relevant impact on the assimilation of monoacylglycerol after an oral lipid bolus.

We found that LFABP-null mice exhibited a tendency toward reduced lipemic response during the oral fat-tolerance test, although the difference was not statistically significant. Diet-derived triacylglycerols and endogenous, or pre-formed, phospholipids are incorporated into chylomicrons (Scow et al., 1967; Mansbach, 1977). LFABP ablation had no effect on the acute synthesis of triacylglycerols in intestinal cells but increased the recovery of [ $^3\text{H}$ ]monoolein in

phospholipids. Thus, LFABP ablation would not be expected to affect plasma [ $^{14}\text{C}$ ] (from [ $^{14}\text{C}$ ]oleate), [ $^3\text{H}$ ] (from [ $^3\text{H}$ ]monoolein), or triacylglycerols. Newberry et al. (2006) found that LFABP-null mice exhibited significantly reduced intestinal triacylglycerol secretion in a similar experiment to the present. However, the mice used in that study were female, and LFABP-null mice exhibit gender dimorphism in lipid metabolism (e.g., Erol et al., 2003; Atshaves et al., 2005), possibly accounting for the varying extent of the effect.

Neeli et al. (2007) demonstrated that budding of pre-chylomicron transport vesicles was markedly impaired (-40%) in a cell-free preparation derived from the intestinal cells of LFABP-null mice. This was found to be due specifically to an absence of LFABP. Pre-chylomicron transport vesicles are thought to be the precursor of chylomicrons, so defective PCTV synthesis should result in reduced chylomicronemia following an oral fat bolus. The preparation utilized by Neeli includes a 30-minute incubation of enterocytes with [ $^3\text{H}$ ]oleate, isolation of the ER, and a 30-minute budding assay whereby ~12-15% of ER-derived [ $^3\text{H}$ ]triolein is incorporated into PCTVs. The PCTV generated in the absence of LFABP contained less triacylglycerol, were slightly larger, and were unable to fuse with the Golgi (Neeli et al., 2007). In the present studies, we found that intestinal triacylglycerol synthesis two minutes after administration of a tracer dose of [ $^{14}\text{C}$ ]oleate or [ $^3\text{H}$ ]monoolein to fasted mice was unaffected in LFABP<sup>-/-</sup> mice, and that the plasma appearance of triacylglycerol, [ $^{14}\text{C}$ ], and [ $^3\text{H}$ ] one, two and four hours after an oral fat load, was little changed, although we noticed a trend toward decreased appearance of radiolabeled lipids in LFABP-null mice. The reduced chylomicronemia observed by Newberry et al. (2006) was not quantitatively recapitulated in our studies, however such an effect is in accord with the postulated role of LFABP in PCTV generation. Neeli et al. used male mouse cytosol, thus a gender dimorphism may not explain our observed normal OFTT in LFABP-null mice. It is likely that the TG synthesis results and the PCTV generation results are reflecting differing



aspects in the complex process of intestinal lipid assimilation. Although the budding of PCTVs is believed to precede the appearance of plasma chylomicrons, it is only one component of the process. Virtually none of the [ $^3\text{H}$ ]triolein from LFABP<sup>-/-</sup> PCTVs was recovered in the Golgi (Neeli et al., 2007), which is the step that theoretically occurs between PCTV budding and chylomicron secretion, thus the LFABP-null mice could have been expected to have no chylomicrons in their bloodstream, however, TG definitely made it to the plasma compartment, as seen in our results and in those of Newberry. It is likely that the entirety of intestinal lipid assimilation is not adequately assessed by measuring TG synthesis, PCTV budding activity, or any single step. Redundancy is seen at numerous steps in dietary fat absorption. For example, multiple enzymes contribute to the hydrolysis of dietary triacylglycerols within the gut (e.g., gastric lipase, bile-salt activated lipase, pancreatic lipase), there are two pathways responsible for incorporating the end products of fat digestion (fatty acids and monoacylglycerol) back into triacylglycerols within the enterocytes (MGAT and G3P pathways), two distinct fatty acid-binding proteins are expressed at very high levels in the intestinal absorptive epithelium (i.e. IFABP and LFABP), etc. Thus, the modest effect of LFABP ablation in the overall process in intestinal lipid absorption, metabolism, and secretion, is in keeping with the remarkably multifaceted capability of the intestine to assimilate dietary fat.

## CONCLUSIONS

In conclusion, this report presents two novel functions for LFABP in intestinal lipid metabolism. 1) The fasting-induced increase in intestinal fatty acid oxidation was blunted in LFABP<sup>-/-</sup>, and neither the expression of oxidative enzymes nor the oxidative capacity of mucosal homogenates were altered suggesting that LFABP physically transports fatty acids toward catabolic pathways. 2) The incorporation of monoacylglycerol into triacylglycerols relative to

phospholipids was markedly reduced in LFABP<sup>-/-</sup>, with no changes in the expression of lipid synthetic genes. Along with the demonstration that LFABP binds monoacylglycerol (Chapter 4), the results collectively suggest that LFABP binds and transports monoacylglycerol toward lipid synthetic pathways. These findings support the hypothesis that LFABP's function *in vivo* is trafficking lipid substrates toward specific metabolic fates. The enzymes in the MGAT or G3P pathways that accept monoacylglycerol from, or provide a monoacylglycerol-derived precursor (e.g., a fatty acid, lysophospholipid, etc.) to LFABP still need to be elucidated, to further clarify the precise function of LFABP in intestinal monoacylglycerol metabolism, at the molecular level.

## **Chapter 4.**

**LFABP is a cytosolic monoacylglycerol-binding protein**

**ABSTRACT**

Liver fatty acid-binding protein (LFABP) is expressed in the liver and intestine and has high affinity for a variety of hydrophobic ligands *in vitro*. Monoacylglycerol (MG) metabolism is perturbed in mice null for LFABP, and this does not appear to be due to changes in gene expression. While these results suggest a trafficking defect, the binding of MG by LFABP is not certain, with variable reports in the literature. Therefore, we examined the MG-binding capability of liver cytosol from wild-type (WT) and LFABP-null (LFABP<sup>-/-</sup>) mice. Liver cytosol was incubated with [<sup>14</sup>C]oleate and [<sup>3</sup>H]monoolein and fractionated by gel filtration chromatography. The ~66kDa fractions retained a large amount of [<sup>14</sup>C]oleate and [<sup>3</sup>H]monoolein, most likely due to the presence of albumin which was confirmed by immunoblotting. As expected, the [<sup>14</sup>C]oleate associated with the ~14kDa fractions was absent in LFABP<sup>-/-</sup> liver cytosol. Interestingly, [<sup>3</sup>H]monoolein was present in the ~14kDa fractions from WT but not LFABP<sup>-/-</sup> cytosol. Immunoblotting confirmed the presence of LFABP in the ~14kDa fractions from WT, but not LFABP<sup>-/-</sup>. These results suggest that LFABP is an MG-binding protein in a physiological setting. Along with other results from the laboratory using purified LFABP, these studies demonstrate that LFABP is an MG-binding protein and is likely to function as such in intestinal and liver cytosol.

## INTRODUCTION

### *MONOACYLGLYCEROL*

Due to the hydrophobic nature of monoacylglycerol (MG), insolubility should markedly hinder its movement through the aqueous cytosol. However, we know that MG must traverse the cytosol because: 1) MG penetrates the plasma membrane into cells intact; 2) MG is acylated to diacylglycerol by monoacylglycerol acyltransferase in the endoplasmic reticulum; and 3) the plasma membrane and the endoplasmic reticulum are spatially separated. It is currently unclear how intracellular MG solubility and transport are achieved.

### *ALBUMIN BINDS MG*

In 1969, Arvidsson first reported a binding interaction between albumin and MG (Arvidsson and Belfrage, 1969). [ $^3\text{H}$ ]MG/hexane was mixed with albumin/water or water alone and allowed to equilibrate, then the radioactivity present in the two aqueous phases was compared. Considerably more [ $^3\text{H}$ ]MG was retained in the albumin/water solution than with water alone and it was estimated that albumin had 7 binding sites for MG. Later, Thumser and coworkers (1998) confirmed the MG-binding capacity of albumin using a fluorescence-quenching assay, although they estimated only 2-3 binding sites. These studies also estimated the dissociation constant of MG to be  $\sim 2.5\mu\text{M}$ . Lastly, Duff et al. (2000) utilized [ $^{13}\text{C}$ ]nuclear magnetic resonance to show that albumin has 3-5 MG-binding sites and preferred the *sn*-2 isomer. Although these studies clearly demonstrate albumin binding to MG, this is more physiologically relevant in blood plasma where MG arises via hydrolysis of circulating lipoprotein TG. Moreover, albumin is a secreted protein and not present in all cell types where MG binding and transport is suspected to occur. Therefore, albumin is not a likely candidate for an intracellular MG-binding protein.

### *LFABP AND MG*

In 1996, Thumser and coworkers reported no appreciable binding affinity of MG for LFABP using a DAUDA-displacement assay. DAUDA is a short chain fatty acid analogue which fluoresces upon exposure to a hydrophobic environment (e.g., inside the binding cavity of LFABP). Oleate, a high-affinity ligand of LFABP, caused a great reduction in DAUDA fluorescence of when added to an LFABP/DAUDA complex reflecting the displacement of DAUDA by oleate in the binding cavity of LFABP. MG caused little reduction in fluorescence intensity leading the authors to conclude that LFABP had no appreciable binding affinity for MG. However, that may have been due to a methodological issue rather than a property of LFABP. The critical micellar concentration (CMC) of a molecule is the concentration above which micelles form and the monomer concentration no longer increases. Monomers, not micelles, are candidates to displace DAUDA from LFABP. The concentrations of MG used by Thumser may have exceeded its CMC (Ho and Storch, 2001). Oleate's higher solubility (and thus higher CMC) and greater displacement of DAUDA from LFABP is in accord with this line of reasoning, although it could also simply reflect a higher affinity of LFABP for oleate than MG.

In 1993, Storch reported LFABP, but not IFABP, bound monoolein using an entirely different experimental paradigm. Anthracene is a fluorophore whose fluorescence intensity increases in a hydrophobic environment, and anthroyloxy fatty acids have been used as long chain fluorescent fatty acid analogs. The fluorescence intensity of solutions containing anthroyloxy-oleate (AOFA) with LFABP or IFABP increased with increasing concentrations of AOFA. Addition of unlabeled oleate quenched the fluorescence, suggesting competitive binding and similar binding properties of oleate and AOFA. Fluorescence intensity of a solution containing anthroyloxy-monoolein (AOMG) with LFABP, but not IFABP, increased with increasing concentrations of AOMG and was quenched by unlabeled monoolein. Moreover, both

enterocyte FABPs possess intrinsic fluorescent amino acid residues (tryptophan in IFABP and tyrosine in LFABP) whose fluorescence is quenched by anthracene. Increasing concentrations of AOMG caused dose-dependent quenching of the intrinsic fluorescence of LFABP but not IFABP. Addition of unlabeled monoolein de-quenched the intrinsic fluorescence of solutions containing LFABP with AOMG, further indicating the ability of LFABP to bind monoolein.

Although the possibility of micellar monoolein is still present, these studies (Storch, 1993) are fundamentally less sensitive to the problem it presents. In other words, micellar monoolein would be unavailable to displace DAUDA from LFABP, but could not falsely displace AOMG from LFABP (i.e., something must have been bound as a monomer *because* AOMG was displaced). On the other hand, other work in the lab has indicated that the affinity of LFABP for monoolein is about one tenth that of oleate (unpublished findings), so it is also possible that monoolein was unable to effectively compete with DAUDA in Thumser's studies.

The solution structures of apo- and oleate-bound holo-LFABP were determined by NMR spectroscopy (He et al., 2007). The results identified the conformational fluctuations LFABP undergoes upon ligand binding, including adjustments in the  $\alpha$ -helices of the portal region that are thought to facilitate ligand entry/exit by diffusion. The amino acid residues shifted upon ligand binding were also identified. Importantly, in recent studies the structure of monoolein-bound holo-LFABP was determined by NMR spectroscopy and the amino acid residues shifted in holo MG-bound LFABP relative to apo-LFABP are similar to those shifted by oleate (unpublished findings), further suggesting a specific binding interaction between LFABP and MG.

The focus of this portion of my research is to determine the MG-binding capability of LFABP in a physiological context. Liver cytosol was used because hepatocytes lack other FABP types, and this study was designed to investigate LFABP specifically. Moreover, the cytosol

preparations from liver homogenates contain albumin which functions as an intrinsic positive control for MG- and oleate-binding.



## MATERIALS AND METHODS

### *a. Materials*

[<sup>14</sup>C]oleic acid ([1-<sup>14</sup>C]oleic acid, 54 mCi/mmol) was obtained from Perkin Elmer-New England Nuclear (Stelton, CT). [<sup>3</sup>H]monoolein (*sn*-2-[9,10-<sup>3</sup>H]monoolein, 40–60 Ci/mmol) was from American Radiochemical (St. Louis, MO). Antibodies to human albumin were obtained from Sigma-Aldrich (St. Louis, MO). Rabbit antibodies to purified rat LFABP and IFABP were generated by Affinity Bioreagents (Golden, CO). All other materials were reagent grade or better.

### *b. Animals and tissue harvest*

Liver tissue was harvested from 48 hour fasted male mice and homogenized with a Potter-Elvehjem homogenizer in PBS pH 7.4 with 0.5% protease inhibitor cocktail (Sigma 8340) on ice. The homogenate was centrifuged at 600g for 10 minutes at 4°C and the supernatant was further centrifuged at 105,000g for 90 minutes at 4°C to acquire a cytosol fraction. Protein concentration was determined by the Bradford method (Bradford, 1976).

### *c. Cytosolic FA and MG binding*

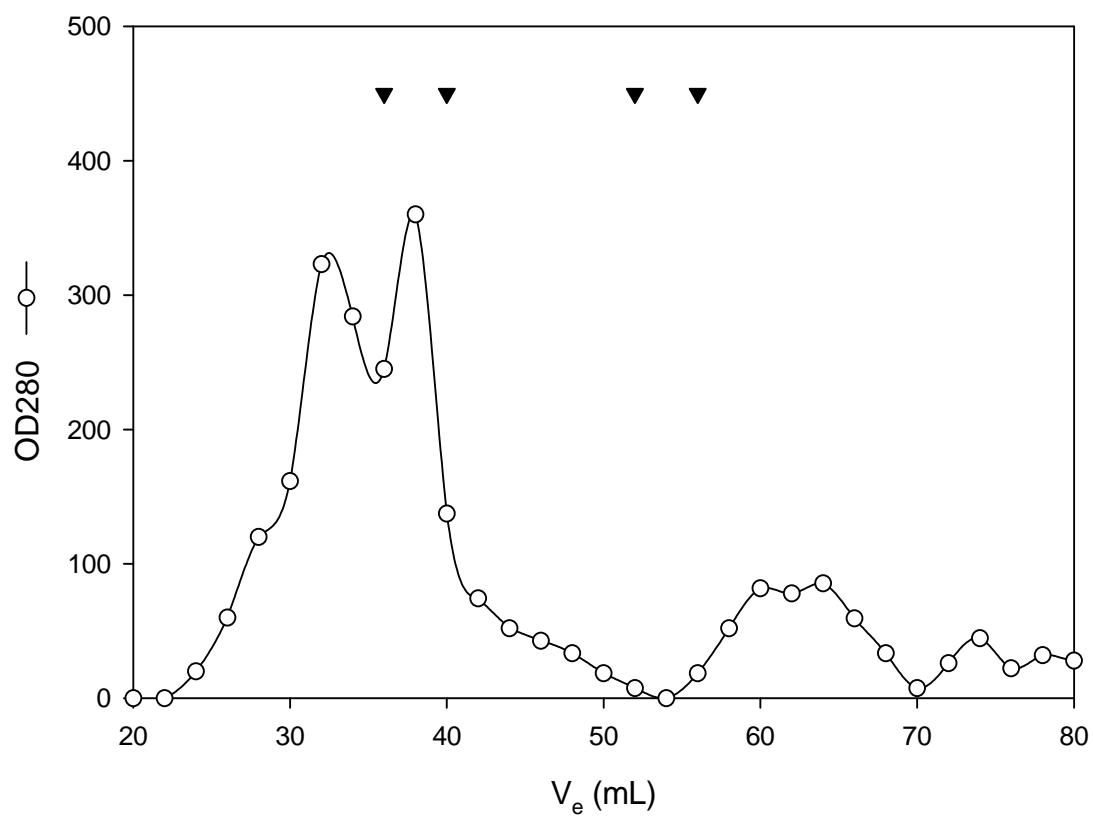
Cytosolic lipid binding capability was assessed as described by Martin et al. (2003). In brief, a 1.5 x 30cm Superdex G75 column was equilibrated with PBS and calibrated with a molecular mass kit (Sigma, St. Louis, MO) including aprotinin (6.5kDa), cytochrome c (12.4kDa), carbonic anhydrase (29kDa), and albumin (66kDa). 10mg of cytosol protein in 250μL PBS was incubated with 5μCi [<sup>14</sup>C]oleate and 5μCi [<sup>3</sup>H]monoolein for 10 minutes at 25°C and loaded onto the column. Fractions were eluted with PBS at 1mL/min and protein concentration of the eluent was monitored continuously by spectrophotometry ( $\lambda_{\text{abs}}$  280nm). 2mL fractions were collected and frozen at -4°C for analysis. 10μL aliquots were used for scintillation counting and 50μL for immunoblotting.

*d. Immunoblotting*

50 $\mu$ L of a fraction or 50 $\mu$ g of cytosol protein was loaded onto 12% polyacrylamide gels and separated by SDS-PAGE. The proteins were transferred onto polyvinylidene difluoride membranes using a semi-dry transfer system (BioRad) for 1 hour at 20V. The membranes were incubated in a 5% nonfat dry milk blocking solution (for LFABP immunoblots) or 2% gelatin (for albumin immunoblots) overnight at 4 °C and then probed with the appropriate primary antibody for 1 hour. After 3 five-minute rinses with wash buffer (0.05M Tris-HCl, 0.15M NaCl, 0.1% Tween-20, pH 7.6), membranes were incubated with secondary antibody for 1 hour and then visualized by chemiluminescence (ECL reagent, GE Healthcare, Piscataway, NJ).

## RESULTS

Protein standards of known molecular weight were loaded onto the column and chromatographed in order to determine the range of elution volumes that encompassed the relevant range of molecular weights. As seen in **Figure 4-1**, albumin (66kDa), carbonic anhydrase (29kDa), cytochrome c (12.4kDa), and aprotinin (6.5kDa) eluted at 36mL, 40mL, 52mL, and 56mL respectively. A standard curve was generated by plotting the log of the standard proteins' molecular weights against their respective elution volumes. Proteins were monitored by recording the optical density at 280nm. A representative chromatogram of WT liver cytosol is shown in **Figure 4-1**. The bulk of cytosolic proteins eluted in the peak centered 36mL, reflecting a high concentration of one or more ~66kDa proteins. Since our protein of interest (LFABP, 14.2kDa) eluted at ~50mL, and this column does not effectively resolve proteins smaller than 3kDa (~55mL), only fractions obtained between 25mL (void volume) and 55mL were included in subsequent analyses.

**Figure 4-1**

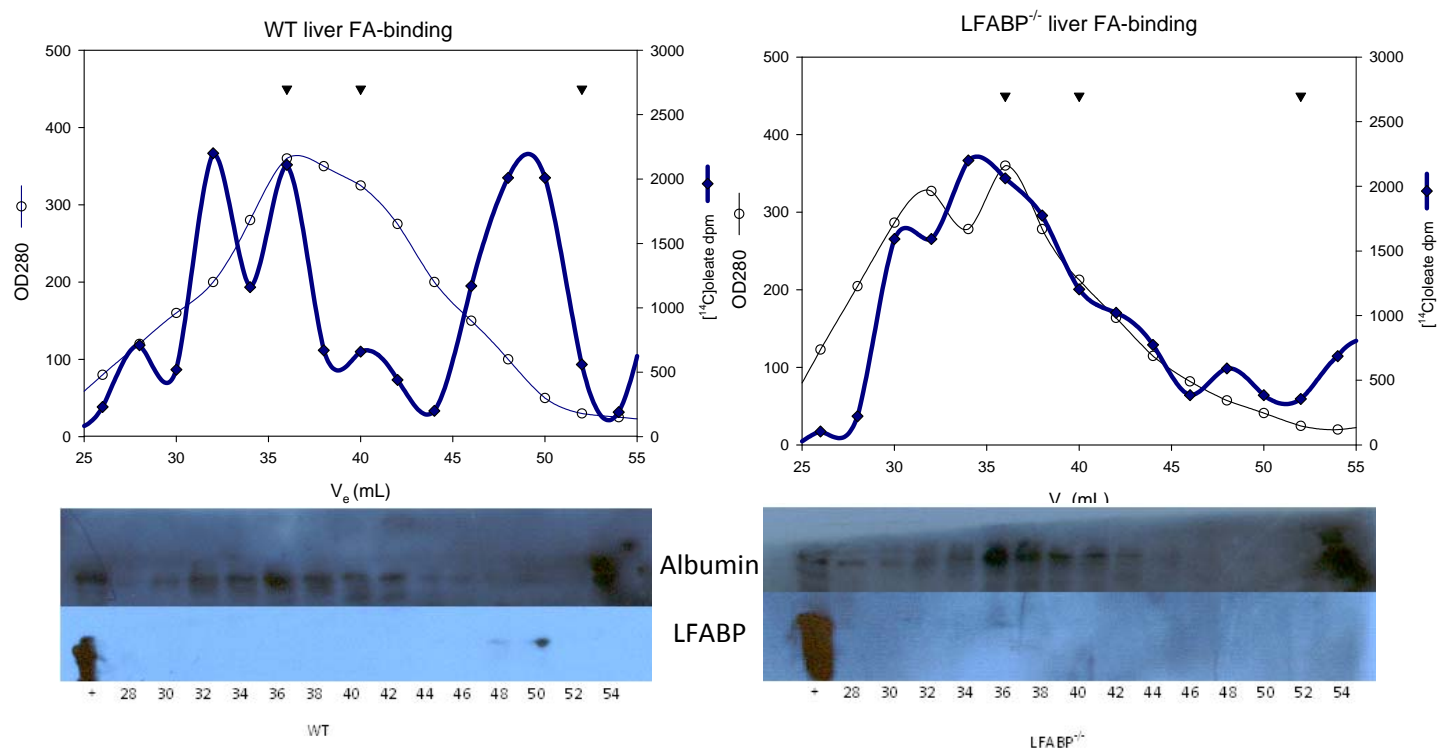
**Figure 4-1.** Representative chromatogram of WT liver cytosol (hollow symbols, OD280) plotted against elution volume (mL). The molecular weight markers are shown as solid triangles (from left to right: 66kDa, 29kDa, 12.4kDa, and 6.5kDa).

*REDUCED FA BINDING IN LFABP<sup>-/-</sup> LIVER CYTOSOL*

The elution profile of [<sup>14</sup>C]oleate is shown in **Figure 4-2**. A large quantity of [<sup>14</sup>C]oleate eluted around 32-36mL, roughly corresponding to the region with the greatest optical density at 280nm (i.e., highest protein concentration). Although there was considerable variability in the shape of the [<sup>14</sup>C]oleate peak, it was clearly distinguishable in each experiment. Immunoblotting demonstrated the presence of albumin in fractions 32-36, in agreement with the 66kDa molecular weight standard (**Figure 4-2b**).

[<sup>14</sup>C]oleate also eluted in another distinct set of fractions at approximately 50mL (~14kDa) (**Figure 4-2a**). This peak was absent in the corresponding fractions from LFABP<sup>-/-</sup> cytosol (**Figure 4-2**). Immunoblotting confirmed the presence of LFABP in these fractions from WT but not LFABP<sup>-/-</sup> (**Figure 4-2**). These results are in agreement with the work of Martin et al. (2003), and indicate that LFABP is the major binding protein for oleate in liver cytosol. It is worth noting that fatty acid binding to albumin is very high in the liver cytosolic fraction as well, but in the intact hepatocyte albumin is present in the secretory vesicle system, not as a cytosolic protein.

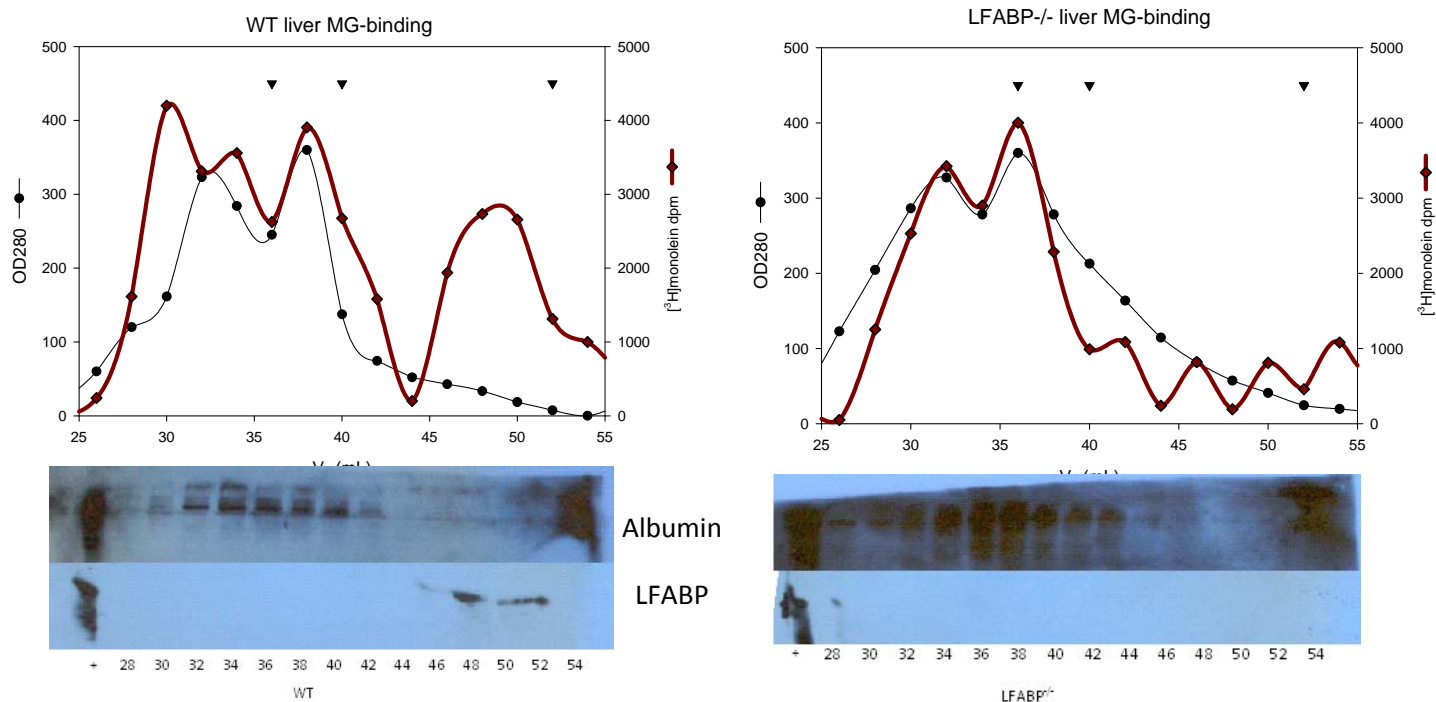
Figure 4-2



**Figure 4-2. [<sup>14</sup>C]Oleate retention by WT and LFABP<sup>-/-</sup> liver cytosol.** Representative chromatogram of 10mg WT and LFABP<sup>-/-</sup> cytosol (OD280, hollow symbols) and [<sup>14</sup>C]oleate radioactivity (dpm, solid symbols) plotted against elution volume (mL). The molecular weight markers are shown as solid triangles (from left to right: 66kDa, 29kDa, and 12.4kDa). 50μL of fraction volume was probed for albumin and LFABP; representative immunoblots are shown below each chromatogram. The fractions are labeled by their elution volumes and the last lane in each immunoblot is the appropriate positive control (+, 4μg albumin or 80μg WT liver cytosol). MW, molecular weight marker.

#### MG BINDING IN WT AND LFABP<sup>-/-</sup> LIVER CYTOSOL

After the column was calibrated with molecular weight standards and validated by measuring [<sup>14</sup>C]oleate-binding capacity of WT and LFABP<sup>-/-</sup> liver cytosol, the ability of LFABP to bind [<sup>3</sup>H]monoolein was tested. As shown in **Figure 4-3**, a large amount of [<sup>3</sup>H]monoolein eluted in the fractions containing albumin (32-36mL), in accord with albumin's high affinity for monoolein. Similar to what was seen for [<sup>14</sup>C]oleate, a second distinct [<sup>3</sup>H]monoolein peak was observed in the 14kDa region in liver cytosol from WT but not LFABP<sup>-/-</sup> (**Figures 4-3**). These results indicate that LFABP is the major intracellular binding protein for monoacylglycerol. Although these data show monoacylglycerol binding to albumin, this is probably irrelevant *in vivo* because, as mentioned above, albumin is not a cytosolic protein.

**Figure 4-3**

**Figure 4-3. [<sup>3</sup>H]Monoolein retention by WT and LFABP<sup>-/-</sup> liver cytosol.** Representative chromatogram of 10mg WT and LFABP<sup>-/-</sup> cytosol (OD280, black circles) and [<sup>3</sup>H]monoolein radioactivity (dpm, red squares) plotted against elution volume (mL). The molecular weight markers are shown as solid triangles (from left to right: 66kDa, 29kDa, and 12.4kDa). 50μL of fraction volume was probed for albumin and LFABP; representative immunoblots are shown below each chromatogram. The fractions are labeled by their elution volumes and, where indicated, the last lane in each immunoblot is the appropriate positive control (+, 4μg albumin or 80μg WT liver cytosol). MW, molecular weight marker.



## DISCUSSION AND CONCLUSIONS

In light of recent evidence implicating LFABP in monoacylglycerol-metabolism (Chapter 3) and the conflicting reports of monoacylglycerol -binding by LFABP, we set out to determine if LFABP would bind monoacylglycerol in a physiological context. As demonstrated by Martin and coworkers (2003), fatty acid binding in liver cytosol is comprised of two distinct compartments: a high molecular weight region around 66kDa and a low molecular weight region around 14kDa. Due to their presence in each respective compartment and their high affinity for fatty acids, albumin is most likely responsible for sequestering fatty acids in the former and LFABP in the latter. This is supported by the abolished fatty acid-binding capacity by 14kDa proteins in LFABP<sup>-/-</sup> liver cytosol. The present report demonstrates a similar phenomenon with monoacylglycerol, whereby 14kDa protein-containing fractions retain [<sup>3</sup>H]monoolein in fractions from WT but not LFABP<sup>-/-</sup> liver cytosol.

This study clarifies two important points regarding LFABP and monoacylglycerol. First, reports on the ability of LFABP to bind monoacylglycerol are conflicting. Second, there are no major candidates for an intracellular monoacylglycerol -binding protein. The current findings strongly suggest that LFABP does, in fact, bind monoacylglycerol, supporting the earlier findings of Storch (1993). Even though LFABP and albumin were found to bind monoacylglycerol in these experiments, they probably do not compete for monoacylglycerol *in vivo* because albumin is a secreted protein found primarily in the vasculature; intracellularly, it is present inside protein secretory vesicles. Thus, these findings suggest that LFABP may be the major intracellular monoacylglycerol -binding protein in the liver, intestine, and kidney.

If LFABP is the monoacylglycerol-binding protein in its native tissues, then what binds monoacylglycerol in other tissues where monoacylglycerol metabolism occurs?

Monoacylglycerol acyltransferase and monoacylglycerol lipase are expressed in a variety of

tissues including adipose, brain, and testis (Kupiecki, 1966; Jamdar and Cao, 1992; Karlsson et al., 1997) and LFABP is not expressed in any these tissues. Determining the necessity and identity of the monoacylglycerol-binding protein(s) in these tissues would provide interesting and important information regarding monoacylglycerol metabolism.

In conclusion, we have identified LFABP as the major intracellular monoacylglycerol-binding protein in liver cytosol. Since there are no other candidates for a cytosolic monoacylglycerol-binding protein, it is likely that LFABP performs this function in the intestine also.

## **Chapter 5.**

### **General conclusions and future directions**

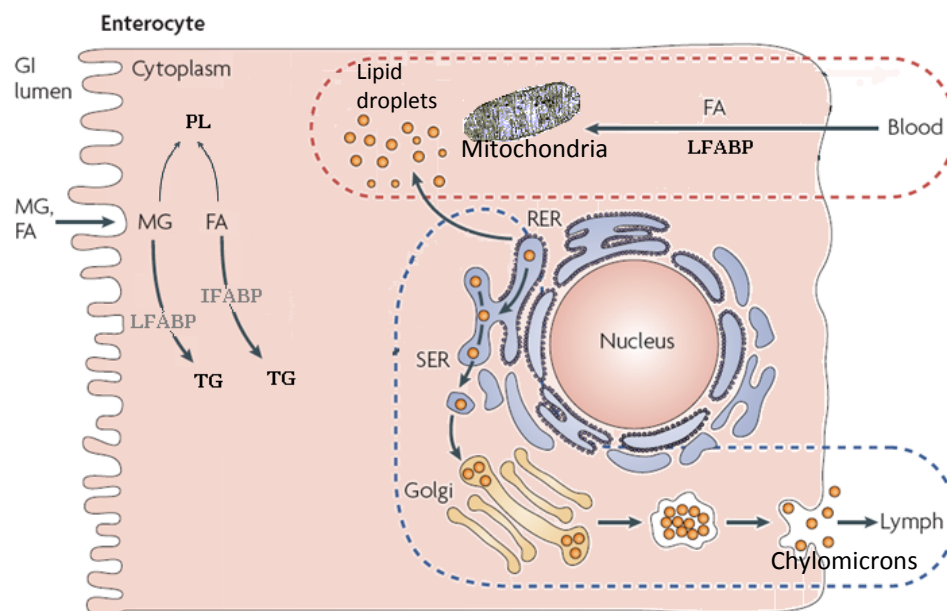
What is the significance of a single cell type having high expression of two related proteins? Evolution rarely displays complete functional redundancies, suggesting that these two proteins have divergent roles in intestinal lipid metabolism. The findings presented herein suggest that, indeed, the enterocyte FABPs are not complete functional redundancies. Along with the cellular effects on lipid metabolism, deletion of either enterocyte FABP manifested unique downstream systemic effects.

IFABP interacts with dietary-derived fatty acids and appears to target them toward triacylglycerol synthesis. LFABP directs fatty acids, independent of their site of cellular entry, toward catabolic fates, and targets dietary-derived monoacylglycerol toward triacylglycerol synthesis (**Figure 1**). These findings clearly point to a physiologic role for enterocyte FABPs, however the precise metabolic pathways involved are still unclear. Given that both MGAT and G3P triacylglycerol synthetic pathways function in the intestine and both can produce triacylglycerol and phospholipids, at present it is not clear if the enterocyte FABPs facilitate the G3P or MGAT pathway-derived triacylglycerol synthesis.

To prove that an enterocyte FABP favors one mode of triacylglycerol synthesis over another requires evidence supporting one mechanism and evidence against the other. In the case of enterocyte FABPs, this is particularly difficult because the two pathways are not exclusive and redundancy occurs at many levels of intestinal lipid metabolism. If LFABP performs the same functions in the intestine and liver, as the oxidation data in particular would imply, then it is possible that LFABP might favor the G3P pathway. Consider: 1) LFABP targets fatty acids toward oxidation, and both fatty acid oxidation and the G3P pathway occur at the mitochondria (mitochondrial glycerol-3-phosphate acyltransferase, an enzyme in the G3P pathway); 2) hepatic VLDL secretion is reduced in LFABP<sup>-/-</sup> mice-- this may occur at the level of pre-VLDL transport vesicles; and 3) the G3P pathway of triacylglycerol synthesis is characteristic

of the liver, not intestine. Collectively, this line of logic would support an LFABP-G3P pathway link. However, non-mitochondrial fatty acid oxidation and glycerol-3-phosphate acyltransferase activity are possible, and there are plausible arguments supporting an LFABP-MGAT pathway link: 1) LFABP binds monoacylglycerol; 2) LFABP is expressed at high levels in the intestine; 3) the liver is unlikely to encounter nearly as much monoacylglycerol as the postprandial intestine; and 4) monoacylglycerol is not a substrate for the G3P pathway. The phospholipid content of the intestinal mucosa was modestly increased in LFABP<sup>-/-</sup>. If these phospholipids, along with dietary/biliary phospholipids, are utilized for chylomicron biogenesis, then it is possible that LFABP provides pre-formed, or endogenous phospholipids for chylomicrons, and directs diet-derived monoacylglycerols toward chylomicron triacylglycerols, in support of the PCTV-LFABP findings of Neeli et al., 2007. It is certainly possible that LFABP could play a role in both the G3P and MGAT pathways. At present, however, the precise mechanism of LFABP in intestinal lipid synthesis remains unclear.

Similar difficulties are encountered when trying to determine the precise role for IFABP. IFABP may divert fatty acids from phospholipid synthetic pathways and target them toward triacylglycerol synthesis. The coincidence of IFABP, the MGAT pathway, and chylomicrons in the intestine suggest IFABP may utilize the MGAT pathway to facilitate the synthesis of triacylglycerols destined for chylomicrons. The ileum expresses IFABP at lower levels than the duodenum and jejunum, which corresponds with the reduced chylomicron secretory capacity of the distal intestine. However, this would imply that incorporation into phospholipids is a “default” pathway for fatty acids; membrane phospholipids perform an essential function therefore their synthesis is not likely a “default” pathway. Thus, the precise mechanism by which IFABP acts to alter intestinal lipid metabolism is also unclear.

**Figure 5-1**

**Figure 5-1. Potential trafficking routes for enterocyte FABP-bound lipids.** This scheme is suggested based on the results of the present studies. One enterocyte is pictured, with IFABP targeting dietary fatty acids toward triacylglycerols and LFABP targeting dietary monoacylglycerol toward triacylglycerols and bloodstream-derived fatty acids toward oxidation. Not shown is the targeting of dietary fatty acids toward oxidation by LFABP. (Modified from Porter et al., 2007)

Questions still remain regarding intestinal triacylglycerol synthesis. For example, do the fatty acids that acylate each position of the triacylglycerol molecule come from the same precursor pool, as pictured in **Figure 2**? Or, conversely, does each fatty acid molecule have a distinct source as pictured in **Figure 3**? Of course, these figures are oversimplified; neither depicts a scenario with multiple pools of fatty acids, diacylglycerols, and triacylglycerols, or single pools of all three.

Figure 5-2

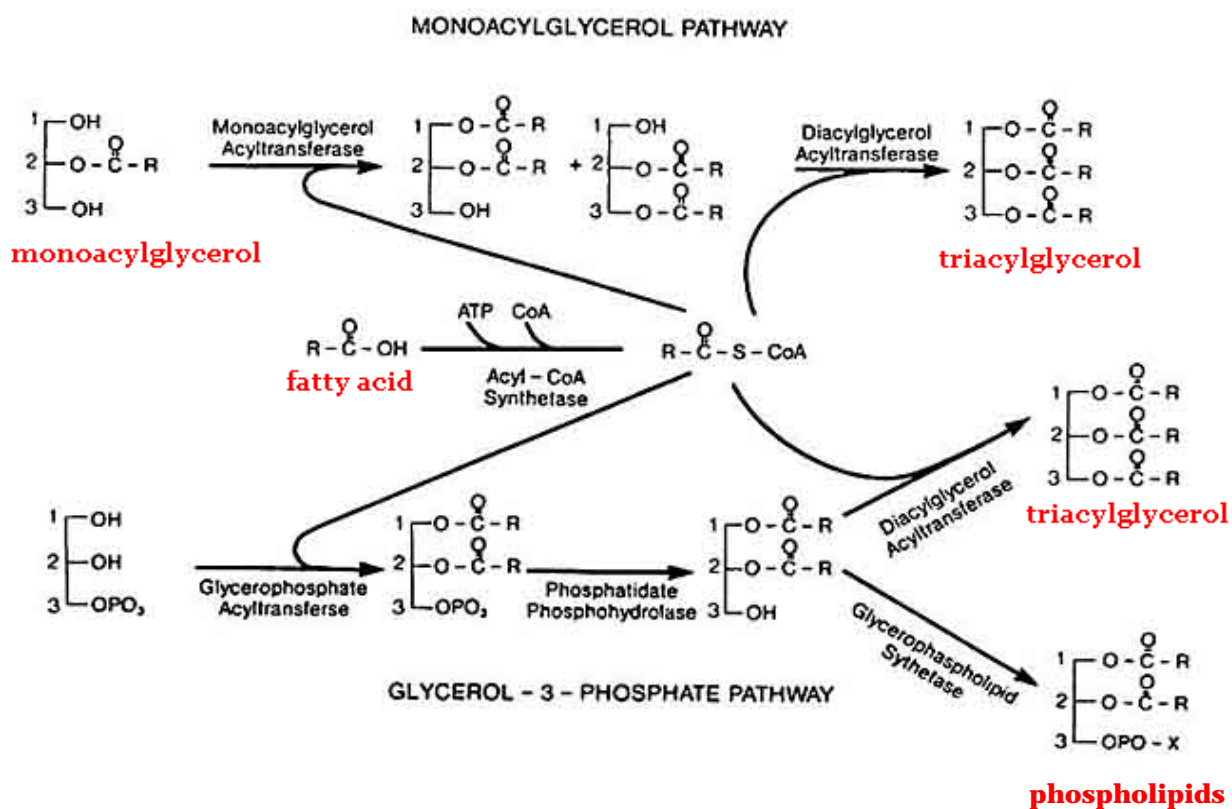


**Figure 5-2. One precursor pool of fatty acids to acylate each position of the triacylglycerol.** This image depicts one pool of fatty acids to supply both the MGAT pathway and the G3P pathway. Note separate pools of diacylglycerols and triacylglycerols synthesized from each pathway (Adapted from Phan and Tso, 2001).



Figure 3

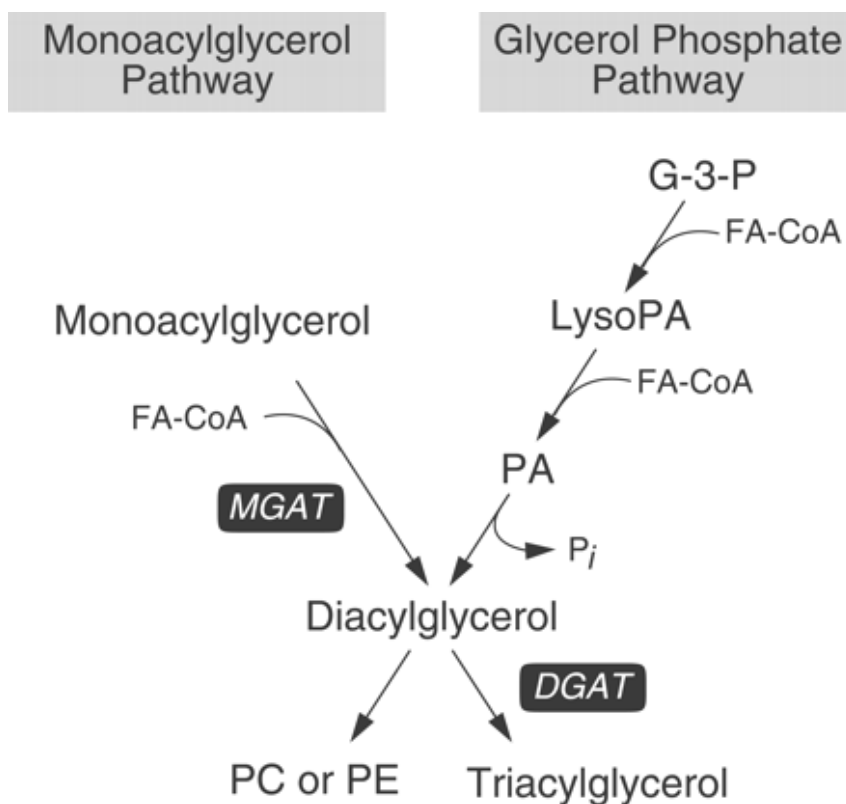


**Figure 5-3. Multiple precursor pools of fatty acids supplying each position of the triacylglycerol molecule.** Note multiple pools of fatty acids but one pool of diacylglycerols and triacylglycerols (from Yen et al., 2002). G-3-P, glycerol-3-phosphate; LysoPA, *sn*-1-lysophosphatidic acid; FA-CoA, fatty acyl-CoA; MGAT, monoacylglycerol acyltransferase; DGAT, diacylglycerol acyltransferase; PC, phosphatidylcholine; PE, phosphatidylethanolamine.

Much progress has been made toward understanding the functions of fatty acid-binding proteins (FABP) by studying genetically modified mice. Interestingly, given their high level of expression and the critical role lipids play in almost all aspects of human biology, all of the FABP knockouts created to date are viable. In general, FABP-ablation presents two distinct phenotypes: 1) specific cellular impairments in the native tissue of the deleted FABP; 2) modest changes in metabolite flux through the affected organ which causes downstream systemic effects.

#### *SYSTEMIC IMPACT OF FABP DELETION: EXAMPLES FROM OTHER FABP TYPES*

Adipocyte fatty acid-binding protein (AFABP) is expressed in adipose tissue and macrophages, and mice null for AFABP were found to be modestly resistant to high-fat diet-induced hyperglycemia (Shaughnessy et al., 2000). Interestingly, unlike the co-expressed enterocyte FABPs, deletion of AFABP caused a dramatic upregulation in keratinocyte FABP (KFABP) in adipocytes, but not macrophages, suggesting that, in accord with their similar ligand transfer mechanisms (Shaughnessy et al., 2000), these two FABPs may have similar functions. Indeed,  $KFABP^{-/-}/AFABP^{-/-}$  mice, which express no adipocyte FABPs, were found to be resistant to obesity and insulin resistance (Maeda et al., 2005), suggesting that KFABP upregulation in  $AFABP^{-/-}$  adipocytes may have been functionally compensating to maintain the total cellular FABP concentration. These remarkable effects have prompted interest in AFABP inhibition as a therapeutic intervention.

Other FABP knockout models have, thus far, been shown to have cell-specific rather than downstream/systemic effects. For example, heart FABP is expressed in cardiac myocytes and its genetic deletion relatively clearly demonstrated its cellular role. Fatty acids are the primary fuel for heart muscle contractions, and HFABP ablation switched the heart from fat to

glucose utilization, causing exercise intolerance and cardiac hypertrophy (Binas et al., 1999).

Similar to what was observed in LFABP<sup>-/-</sup> hepatocytes (Newberry et al., 2003), and our own findings in LFABP<sup>-/-</sup> intestine, this was found to be a trafficking defect, affecting both cardiomyocyte fatty acid uptake and oxidation (Murphy et al., 2004; Schaap et al., 1999). Given the detrimental role of cardiac hypertrophy in hypertensive disorders, these findings should be further explored to determine if modulating HFABP could dissociate cardiac hypertrophy from hypertension in susceptible individuals.

Brain FABP is expressed in the developing and mature brain and has a high affinity for docosahexanoic acid (DHA), a fatty acid important in brain development and function (Xu et al., 1996). Interestingly, polymorphisms in BFABP were found to be correlated with certain schizophrenic behaviors (Watanabe et al., 2007). Although mice null for BFABP appear phenotypically normal, they exhibit enhanced anxiety and fear memory, and have reduced brain DHA content (Owada et al., 2006). Thus, BFABP may function as a biological link between the mind and body.

#### *SYSTEMIC EFFECTS OF LFABP DELETION*

Although LFABP null mice appear normal they exhibit some very interesting phenotypic responses to food deprivation relative to WT: 1) reduced ketosis despite euglycemia; 2) attenuated metabolic rate depression; and 3) reduced loss of fat-free mass. The blunted decrease in metabolic rate in fasting LFABP<sup>-/-</sup> mice is likely related to their reduced loss of fat-free mass. However, skeletal muscle proteolysis provides a major substrate for gluconeogenesis during fasting, and ketogenesis provides the ATP, yet LFABP<sup>-/-</sup> maintained normal blood glucose relative to WT. How these three responses occur is unclear. The differences from WT were too small to impact overall body weight. Nevertheless, the results were obtained using two entirely

different paradigms suggesting this is probably a physiologically meaningful observation- in other words, metabolic rate was measured in fed and 24 hour fasted mice by indirect calorimetry, and body composition was measured in fed and 48 hour fasted mice by dual X-ray absorptiometry. Given that the LFABP<sup>-/-</sup> mice defended their fat-free mass and otherwise appear healthy, future studies could be designed to address the possibility of targeting LFABP activity as a treatment for sarcopenia and skeletal muscle wasting disorders.

#### *NON-INTESTINAL EFFECTS OF IFABP DELETION*

Similar to LFABP<sup>-/-</sup> mice, IFABP<sup>-/-</sup> mice appear phenotypically normal but exhibit an interesting response to fasting. IFABP<sup>-/-</sup> mice lost more fat mass than WT during food deprivation and, accordingly, had a larger reduction in their respiratory quotient (i.e., greater oxidation of fat relative to glucose). Although increased intestinal fatty acid oxidation would not likely be able to account for this difference due to its minimal contribution to total O<sub>2</sub> consumption, it was, in any case, not increased in IFABP<sup>-/-</sup> relative to WT. This suggests a non-intestinal (systemic/downstream) effect of IFABP gene deletion. Exhaustion of fat mass is incompatible with survival, although accelerating fat loss is the primary goal of obesity treatments. Future research is warranted regarding how deletion of IFABP, an intestine-specific protein, from an organ that does not rely on fat oxidation to meet its energetic demands and is greatly compromised during food deprivation, accentuates fat loss.

As seen in Chapter 2, IFABP seems to target dietary fatty acids away from phospholipid synthesis. Liver and intestine are the two major sources of plasma HDL, and accumulating phospholipids is an important step in HDL formation (Brunham et al., 2006; Singaraja et al., 2006). IFABP<sup>-/-</sup> mice may be a good model to determine if IFABP is involved with intestinal HDL

genesis. A detailed analysis of total and intestine-derived lipoproteins in IFABP<sup>-/-</sup> mice would help to clarify this.

In conclusion, we provided evidence to support the previously hypothesized divergent functions of the two enterocyte FABPs in intestinal lipid metabolism, and systemic consequences of their deletion. IFABP targets dietary-derived fatty acids away from phospholipid synthesis and possibly toward incorporation into triacylglycerols, and IFABP-null mice retain less fat mass during food deprivation relative to WT. LFABP binds dietary-derived monoacylglycerol and traffics it toward triacylglycerol synthesis, transports fatty acids to oxidative endpoints, and LFABP-null mice retain more fat-free mass during food deprivation relative to WT. Plans for future studies that will further elucidate the functions of the enterocyte FABPs include: exploring FABP-protein interactions, which could provide insight into which pathways enterocyte FABPs are active in, or it could provide completely novel information. Further, because of the differential binding affinities of enterocyte FABPs for saturated vs. unsaturated fatty acids, the impact of high fat diets enriched in fats of varying degrees of saturation (e.g., high tristearin vs. high trilinolenin) should be assessed in WT, IFABP<sup>-/-</sup> and LFABP<sup>-/-</sup> mice.

## Literature cited

Agellon LB, Drozdowski L, Li L, Iordache C, Luong L, Clandinin MT, Uwiera RR, Toth MJ, Thomson AB. (2007) Loss of intestinal fatty acid binding protein increases the susceptibility of male mice to high fat diet-induced fatty liver. *Biochimica et Biophysica Acta* 1771(10):1283-8.

Agellon LB, Li L, Luong L, Uwiera RR. 2006 Adaptations to the loss of intestinal fatty acid binding protein in mice. *Molecular and Cellular Biochemistry* 284(1-2):159-66.

Agren JJ, Valve R, Vidgren H, Laakso M, Uusitupa M. (1998) Postprandial lipemic response is modified by the polymorphism at codon 54 of the fatty acid-binding protein 2 gene. *Arteriosclerosis, Thrombosis, and Vascular Biology* 18(10):1606-10.

Alpers DH, Bass NM, Engle MJ, DeSchryver-Kecsckemeti K. (2000) Intestinal fatty acid binding protein may favor differential apical fatty acid binding in the intestine. *Biochimica et Biophysica Acta – Molecular and Cell Biology of Lipids* 1438(3):352-362.

Arvidsson EO, Belfrage P. (1969) Monoglyceride-protein interaction. The binding of monoolein to native human serum albumin. *Acta Chemica Scandinavica* 1969;23(1):232-6.

Atshaves BP, McIntosh AL, Payne HR, Mackie J, Kier AB, Schroeder F. (2005) Effect of branched-chain fatty acid on lipid dynamics in mice lacking liver fatty acid binding protein gene. *American Journal of Physiology* 288(3):C543-558.

Baier LJ, Bogardus C, Sacchettini JC. (1996) A polymorphism in the human fatty acid binding protein alters fatty acid transport across Caco-2 cells. *Journal of Biological Chemistry* 271(18):10892-10896.

Baier LJ, Sacchettini JC, Knowler WC, Eads J, Paolisso G, Tataranni PA, Mochizuki H, Bennett PH, Bogardus C, Prochazka M. (1995) An amino acid substitution in the human intestinal fatty acid binding protein is associated with increased fatty acid binding, increased fat oxidation, and insulin resistance. *Journal of Clinical Investigation* 95(3):1281-7.

Binas B, Danneberg H, McWhir J, Mullins L, Clark AJ. (1999) Requirement for HFABP in cardiac fatty acid utilization. *Federation of American Societies for Experimental Biology* 13(8):805-12.

Bradford MM. (1976) A rapid and sensitive method for the quantitation of microgram quantities of protein utilizing the principle of protein-dye binding. *Annals of Biochemistry* 72:248-254.

- Braissant O, Foufelle F, Scotto C, Dauça M, Wahli W. (1996) Differential expression of peroxisome proliferator-activated receptors (PPARs): tissue distribution of PPAR-alpha, -beta, and -gamma in the adult rat. *Endocrinology* 137(1):354-66.
- Brunham LR, Kruit JK, Iqbal J, Fievet C, Timmins JM, Pape TD, Coburn BA, Bissada N, Staels B, Groen AK, Hussain MM, Parks JS, Kuipers F, Hayden MR. (2006) Intestinal ABCA1 directly contributes to HDL biogenesis in vivo. *Journal of Clinical Investigation* 116(4):1052-62
- Brunham LR, Singaraja RR, Duong M, Timmins JM, Fievet C, Bissada N, Kang MH, Samra A, Fruchart JC, McManus B, Staels B, Parks JS, Hayden MR. (2009) Tissue-specific roles of ABCA1 influence susceptibility to atherosclerosis. *Arteriosclerosis, Thrombosis, and Vascular Biology* 29(4):548-54.
- Bugaut M, Myher JJ, Kuksis A, Hoffman AG. (1984) An examination of the stereochemical course of acylation of 2-monoacylglycerols by rat intestinal villus cells using [2H3]palmitic acid. *Biochimica Biophysica et Acta* 792(3):254-69.
- Cao H, Gerhold K, Mayers JR, Wiest MM, Watkins SM, Hotamisligil GS. (2008) Identification of a lipokine, a lipid hormone linking adipose tissue to systemic metabolism. *Cell* 134(6):933-44.
- Cao J, Lockwood J, Burn P, Shi Y. (2003) Cloning and functional characterization of a mouse intestinal acyl-CoA:monoacylglycerol acyltransferase, MGAT2. *Journal of Biological Chemistry* 278(16):13860-6.
- Chon SH, Zhou YX, Dixon JL, Storch J. (2007) Intestinal monoacylglycerol metabolism: developmental and nutritional regulation of monoacylglycerol lipase and monoacylglycerol acyltransferase. *Journal of Biological Chemistry* 282(46):33346-57.
- Córsico B, Cistola DP, Frieden C, Storch J. (1998) The helical domain of intestinal fatty acid binding protein is critical for collisional transfer of fatty acids to phospholipid membranes. *Proceedings of the National Academy of Sciences* 95(21):12174-8.
- Córsico B, Franchini GR, Hsu KT, Storch J. (2005) Fatty acid transfer from intestinal fatty acid binding protein to membranes: electrostatic and hydrophobic interactions. *Journal of Lipid Research* 46(8):1765-72.
- Darimont C, Gradoux N, Persohn E, Cumin F, De Pover A. (2000) Effects of intestinal fatty acid-binding protein overexpression on fatty acid metabolism in Caco-2 cells. *Journal of Lipid Research* 41(1):84-92.



Drover VA, Ajmal M, Nassir F, Davidson NO, Nauli AM, Sahoo D, Tso P, Abumrad NA. CD36 deficiency impairs intestinal lipid secretion and clearance of chylomicrons from the blood. *Journal of Clinical Investigation* 115(5):1290-1297.

Drozdowski L, Clement M, Keelan M, Niot I, Clandinin MT, Agellon L, Wild G, Besnard P, Thompson ABR. (2004) Dietary lipids modify intestinal lipid-binding protein RNA abundance in diabetic and control rats. *Digestion* 70:192-198.

Dworatzek PD, Hegele RA, Wolever TM. (2004) Postprandial lipemia in subjects with the threonine 54 variant of the fatty acid-binding protein 2 gene is dependent on the type of fat ingested. *American Journal of Clinical Nutrition* 79(6):1110-7.

Erol E, Kumar LS, Cline GW, Shulman GI, Kelly DP, Binas B. Liver fatty acid binding protein is required for high rates of hepatic fatty acid oxidation but not for the action of PPARalpha in fasting mice. (2004) *Federation of American Societies for Experimental Biology* 18(2):347-349.

Folch J, Lees M, Sloane Stanley GH. (1957) A simple method for the isolation and purification of total lipids from animal tissues. *Journal of Biological Chemistry* 226(1):497-509.

Furuhashi M, Hotamisligil GS. (2008) Fatty acid-binding proteins: role in metabolic diseases and potential as drug targets. *Nature Reviews Drug Discovery* 7:489-503.

Gangl A, Ockner RK. (1975) Intestinal metabolism of plasma free fatty acids. Intracellular compartmentation and mechanisms of control. *Journal of Clinical Investigation* 55(4):803-813.

Gangl A, Renner F. (1978) In vivo metabolism of plasma free fatty acids by intestinal mucosa of man. *Gastroenterology* 74(5 Pt 1):847-850.

Georgopoulos A, Aras O, Tsai MY. Codon-54 polymorphism of the fatty acid-binding protein 2 gene is associated with elevation of fasting and postprandial triglyceride in type 2 diabetes. (2000) *Journal of Clinical Endocrinology and Metabolism* 85(9):3155-60.

Glatz JFC, Baerwaldt CCF, Veerkamp JH. (1984) Diurnal variation of cytosolic fatty acid-binding protein content and palmitate oxidation in rat liver and heart. *Journal of Biological Chemistry* 259(7):4296-4300.

Gomez LC, Real SM, Ojeda MS, Gimenez S, Mayorga LS, Roqué M. (2007) Polymorphism of the FABP2 gene: a population frequency analysis and an association study with cardiovascular risk markers in Argentina. *BioMed Central Medical Genetics* 8:39.

Gordon JL, Elshourbagy N, Lowe JB, Liao WS, Alpers DH, Taylor JM. (1985) Tissue specific expression and developmental regulation of two genes coding for rat fatty acid binding proteins. *Journal of Biological Chemistry* 260(4):1995-8.

Goudriaan JR, Dahlmans VE, Febbraio M, Teusink B, Romijn JA, Havekes LM, Voshol PJ. (2002) Intestinal lipid absorption is not affected in CD36 deficient mice. *Molecular and Cellular Biochemistry* 239(1-2):199-202.

Goudriaan JR, den Boer MA, Rensen PC, Febbraio M, Kuipers F, Romijn JA, Havekes LM, Voshol PJ. (2005) CD36 deficiency in mice impairs lipoprotein lipase-mediated triglyceride clearance. *Journal of Lipid Research* 46(10):2175-2181.

Hanada K, Kumagai K, Yasuda S, Miura Y, Kawano M, Fukasawa M, Nishijima Masahiro. (2003) Molecular machinery for non-vesicular trafficking of ceramide. *Nature* 426(18/25): 803-809.

He Y, Yang X, Wang H, Estephan R, Francis F, Kodukula S, Storch J, Stark RE. (2007) Solution-state molecular structure of apo and oleate-liganded liver fatty acid-binding protein. *Biochemistry* 46(44):12543-56.

Ho SY, Storch J. (1994) Monoacylglycerol transfer from rat-liver fatty acid-binding protein to phospholipid vesicles. *Federation of American Societies for Experimental Biology* 8(5):A731.

Ho SY, Storch J. (2001) Common mechanisms of monoacylglycerol and fatty acid uptake by human intestinal Caco-2 cells. *American Journal of Physiology Cell Physiology* 281(4):C1106-17.

Hoffman AF, Borgstroem B. (1964) The intraluminal phase of fat digestion in man: the lipid content of the micellar and oil phases of intestinal content obtained during fat digestion and absorption. *Journal of Clinical Investigation* 43:247-257.

Holehouse EL, Liu ML, Aponte GW. (1998) Oleic acid distribution in small intestinal epithelial cells expressing intestinal-fatty acid binding protein. *Biochimica Biophysica et Acta* 1390(1):52-64.

Hostetler HA, McIntosh AL, Atshaves BP, Storey SM, Payne HR, Kier AB, Schroeder F. (2009) Liver type fatty acid binding protein (L-FABP) directly interacts with peroxisome proliferator-activated receptor- $\alpha$  in cultured primary hepatocytes. *Journal of Lipid Research* In press.

Hotamisligil GS, Johnson RS, Distel RJ, Ellis R, Papaioannou VE, Spiegelman BM. (1996) Uncoupling of obesity from insulin resistance through a targeted mutation in aP2, the adipocyte fatty acid binding protein. *Science* 274(5291):1377-9.

Hsu KT, Storch J. (1996) Fatty acid transfer from liver and intestinal fatty acid-binding proteins to membranes occurs by different mechanisms. *Journal of Biological Chemistry* 271(23):13317-13323.

Huang H, Starodum O, McIntosh A, Atshaves BP, Woldegiorgis G, Kier AB, Schroeder F. (2004) Liver fatty acid-binding protein colocalizes with peroxisome proliferators activated receptor alpha and enhances ligand distribution to nuclei of living cells. *Biochemistry* 43(9):2484-2500.

Huggins KW, Camarota LM, Howles PN, Hui DY. (2003) Pancreatic triglyceride lipase deficiency minimally affects dietary fat absorption but dramatically decreases dietary cholesterol absorption in mice. *Journal of Biological Chemistry* 278(44):42899-42905.

Hyun SA, Vahouny V, Treadwell CR (1967) Portal absorption of fatty acids in lymph- and portal vein-cannulated rats. *Biochimica Biophysica et Acta* 137(2):296-305.

Jamdar SC, Cao WF. (1992) Properties of monoglycerol acyltransferase in rat adipocytes. *Archives of Biochemistry and Biophysics* 296(2):419-25.

Karlsson M, Contreras JA, Hellman U, Tornqvist H, Holm C. (1997) cDNA cloning, tissue distribution, and identification of the catalytic triad of monoglyceride lipase. Evolutionary relationship to esterases, lysophospholipases, and haloperoxidases. *Journal of Biological Chemistry* 272(43):27218-23.

Khan SH, Sorof S. (1994) Liver fatty acid-binding protein: specific mediator of the mitogenesis induced by two classes of carcinogenic peroxisome proliferators. *Proceedings of the National Academy of Sciences* 91(3):848-852.

Knudsen J, Jensen MV, Hansen JK, Faergeman NJ, Neergaard TBF, Gaigg B. (1999) Role of acylCoA binding protein in acylCoA transport, metabolism and cell signaling. *Molecular and Cellular Biochemistry* 193:95-103.

Kumar NS, Mansbach CM. (1996) Prechylomicron transport vesicle: isolation and partial characterization. *American Journal of Physiology* 276(2):G378-386.

Kupiecki FP. (1966) Partial purification of monoglyceride lipase from adipose tissue. *Journal of Lipid Research* 7(2):230-5.

Lehner R, Kuksis A. (1996) Biosynthesis of triacylglycerols. *Progress in Lipid Research* 35:169-201.

Levy E, Menard D, Delvin E, Stan S, Mitchell G, Lambert M, Ziv E, Feoli-Fonseca JC, Seidman E. (2001) The polymorphism at codon 54 of the FABP2 gene increases fat

absorption in human intestinal explants. *Journal of Biological Chemistry* 276(43): 39679-39684.

Lomize MA, Lomize AL, Pogozheva ID, Mosberg HI (2006) OPM: Orientations of Proteins in Membranes database. *Bioinformatics* 22, 623-625.

Lowe JB, Strauss AW, Gordon JL (1984) Expression of a mammalian fatty acid-binding protein in *Escherichia coli*. *Journal of Biological Chemistry* 259(20):12696-704.

Luxon BA. (1996) Inhibition of binding to fatty acid binding protein reduces the intracellular transport of fatty acids. *American Journal of Physiology* 271(1 Pt 1):G113-20.

Luxon BA, Milliano MT. (1999) Cytoplasmic transport of fatty acids in rat enterocytes: role of binding to fatty acid-binding protein. *American Journal of Physiology* 277(2 Pt 1):G361-6.

Maeda K, Cao H, Kono K, Gorgun CZ, Furuhashi M, Uysal KT, Cao Q, Atsumi G, Malone H, Krishnan B, Minokoshi Y, Kahn BB, Parker RA, Hotamisligil GS. (2005) Adipocyte/macrophage fatty acid binding proteins control integrated metabolic responses in obesity and diabetes. *Cell Metabolism* 1(2):107-19.

Makowski L, Boord JB, Maeda K, Babaev VR, Uysal KT, Morgan MA, Parker RA, Suttles J, Fazio S, Hotamisligil GS, Linton MF. (2001) Lack of macrophage fatty-acid-binding protein aP2 protects mice deficient in apolipoprotein E against atherosclerosis. *Nature Medicine* 7(6):699-705.

Mansbach CM. (1977) The origin of chylomicron phosphatidylcholine in the rat. *Journal of Clinical Investigation* 60(2):411-20.

Mansbach CM, Dowell RF. (1992) Uptake and metabolism of circulating fatty acids by rat intestine. *American Journal of Physiology* 263(6 Pt1):G927-933.

Mansbach CM, Dowell RF. (1993) Portal transport of long acyl chain lipids: effect of phosphatidylcholine and low infusion rates. *American Journal of Physiology* 264(6 Pt1):G1082-1089.

Mansbach CM, Dowell RF, Pritchett D. (1991) Portal transport of absorbed lipids in rats. *American Journal of Physiology* 261(3 Pt1):G530-538.

Mansbach CM, Nevin P. (1998) Intracellular movement of triacylglycerols in the intestine. *Journal of Lipid Research* 39(5):963-968.

McIntosh AL, Atshaves BP, Hostetler HA, Huang H, Davis J, Lyuksyutova OI, Landrock D, Kier AB, Schroeder F. (2009) Liver type fatty acid binding protein (L-FABP) gene ablation reduces nuclear ligand distribution and peroxisome proliferator-activated receptor- $\alpha$  activity in cultured primary hepatocytes. *Archives of Biochemistry and Biophysics* 485(2):160-73.

Martin GG, Atshaves BP, McIntosh AL, Mackie JT, Kier AB, Schroeder F. (2005) Liver fatty-acid-binding protein (L-FABP) gene ablation alters liver bile acid metabolism in male mice. *Biochemical Journal* 391(Pt 3):549-560.

Martin GG, Atshaves BP, McIntosh AL, Mackie JT, Kier AB, Schroeder F. (2006) Liver fatty acid binding protein gene ablation potentiates hepatic cholesterol accumulation in cholesterol-fed female mice. *American Journal of Physiology Gastrointestinal and Liver Physiology* 290(1):G36-48.

Martin GG, Atshaves BP, McIntosh AL, Payne HR, Mackie JT, Kier AB, Schroeder F. (2009) Liver fatty acid binding protein gene ablation enhances age-dependent weight gain in male mice. *Molecular and Cellular Biochemistry* 324(1-2):101-15.

Martin GG, Danneberg H, Kumar LS, Atshaves BP, Erol E, Bader M, Schroeder F, Binas B. (2003) Decreased liver fatty acid binding capacity and altered liver lipid distribution in mice lacking the liver fatty acid-binding protein gene. *Journal of Biological Chemistry* 278(24):21429-21438.

Martin GG, Huang H, Atshaves BP, Binas B, Schroeder F. (2004) Ablation of the liver fatty acid binding protein gene decreases fatty acyl CoA binding capacity and alters fatty acyl CoA pool distribution in mouse liver. *Biochemistry* 42(39):11520-11532.

Montoudis A, Delvin E, Menard D, Beaulieu JF, Jean D, Tremblay E, Bendayan M, Levy E. (2006) Intestinal-fatty acid binding protein and lipid transport in human intestinal epithelial cells. *Biochemical and Biophysical Research Communications* 339(1):248-254.

Montoudis A, Seidman E, Boudreau F, Beaulieu JF, Menard D, Elchebly M, Mailhot G, Sane AT, Delvin E, Levy E. (2008) Intestinal fatty acid binding protein regulates mitochondrion beta-oxidation and cholesterol uptake. *Journal of Lipid Research* 49(5):961-972.

Murota K, Storch J. (2005) Uptake of micellar long-chain fatty acid and sn-2-monoacylglycerol into human intestinal Caco-2 cells exhibits characteristics of protein-mediated transport. *Journal of Nutrition* 135(7):1626-1630.

Murphy EJ, Barcelo-Coblijn G, Binas B, Glatz JF. (2004) Heart fatty acid uptake is decreased in heart fatty acid-binding protein gene-ablated mice. *Journal of Biological Chemistry* 279(33):34481-8.

Neeli I, Siddiqi SA, Siddiqi S, Mahan J, Lagakos WS, Binas B, Gheyi T, Storch J, Mansbach CM 2nd. (2007) Liver fatty acid-binding protein initiates budding of pre-chylomicron transport vesicles from intestinal endoplasmic reticulum. *Journal of Biological Chemistry* 282(25):17974-84.

Newberry EP, Kennedy SM, Xie Y, Luo J, Davidson NO. (2009) Diet-induced alterations in intestinal and extrahepatic lipid metabolism in liver fatty acid binding protein knockout mice. *Molecular and Cellular Biochemistry* 326(1-2):79-86.

Newberry EP, Kennedy SM, Xie Y, Sternard BT, Luo J, Davidson NO. (2008) Diet-induced obesity and hepatic steatosis in L-Fabp / mice is abrogated with SF, but not PUFA, feeding and attenuated after cholesterol supplementation. *American Journal of Physiology Gastrointestinal and Liver Physiology* 294(1):G307-14.

Newberry EP, Xie Y, Kennedy S, Han X, Buhman KK, Luo J, Gross RW, Davidson NO. (2003) Decreased hepatic triglyceride accumulation and altered fatty acid uptake in mice with deletion of the liver fatty acid-binding protein gene. *Journal of Biological Chemistry* 278(51):51664-51672.

Newberry EP, Xie Y, Kennedy SM, Luo J, Davidson NO. (2006) Protection against Western diet-induced obesity and hepatic steatosis in liver fatty acid-binding protein knockout mice. *Hepatology* 44(5):1191-205.

Nevin P, Koelsch D, Mansbach CM. (1995) Intestinal triacylglycerol storage pool size changes under differing physiological conditions. *Journal of Lipid Research* 36(11):2405-2412.

Ockner RK, Hughes FB, Isselbacher KJ. (1969) Very low density lipoproteins in intestinal lymph: origin, composition, and role in lipid transport in the fasting state. *Journal of Clinical Investigation* 48(11):2079-2088.

Ockner RK, Manning JA. (1974) Fatty acid-binding protein in small intestine. Identification, isolation, and evidence for its role in cellular fatty acid transport. *Journal of Clinical Investigation* 54(2):326-338.

Ockner RD, Manning JA. (1976) Fatty acid binding protein. Role in esterification of absorbed long chain fatty acid in rat intestine. *Journal of Clinical Investigation* 58(3):632-641.

Ontko JA, Jackson D. (1964) Factors affecting the rate of oxidation of fatty acids in animal tissues. Effect of substrate concentration, pH, and coenzyme A in rat liver preparations. *Journal of Biological Chemistry* 239:3674-3682.

Owada Y, Abdelwahab SA, Kitanaka N, Sakagami H, Takano H, Sugitani Y, Sugawara M, Kawashima H, Kiso Y, Mobarakeh JI, Yanai K, Kaneko K, Sasaki H, Kato H, Saino-Saito S, Matsumoto N, Akaike N, Noda T, Kondo H. (2006) Altered emotional behavioral responses in mice lacking brain-type fatty acid-binding protein gene. *European Journal of Neuroscience* 24(1):175-87.

Oxley A, Jutfelt F, Sundell K, Olsen RE. (2007) Sn-2-monoacylglycerol, not glycerol, is preferentially utilised for triacylglycerol and phosphatidylcholine biosynthesis in Atlantic salmon (*Salmo salar* L.) intestine. *Comparative Biochemistry and Physiology B Biochemistry and Molecular Biology* 146(1):115-23.

Petit V, Arnould L, Martin P, Monnot M, Pineau T, Besnard P, Niot I. (2007) Chronic high-fat diet affects intestinal fat absorption and postprandial triglyceride levels in the mouse. *Journal of Lipid Research* 48:278-287.

Phan CT, Tso P. (2001) Intestinal lipid absorption and transport. *Frontiers in Bioscience* 6:299-319.

Prows DR, Murphy EJ, Moncecchi D, Schroeder F. (1996) Intestinal fatty acid-binding protein expression stimulates fibroblast fatty acid esterification. *Chemistry and Physics of Lipids* 84(1):47-56.

Porter CJ, Trevaskis NL, Charman WN. (2007) Lipids and lipid-based formulations: optimizing the oral delivery of lipophilic drugs. *Nature Reviews Drug Discovery* 6(3):231-48.

Richieri GV, Ogata RT, Zimmerman AW, Veerkamp JH, Kleinfeld AM. (2000) Fatty acid binding proteins from different tissues show distinct patterns of fatty acid interactions. *Biochemistry* 39(24):7197-204.

Richieri GV, Ronald TO, Kleinfeld AM. (1994) Equilibrium constants for the binding of fatty acids with fatty acid-binding proteins from adipocyte, intestine, heart, and liver measured with the fluorescent probe ADIFAB. *Journal of Biological Chemistry* 269(39):24918-23930.

Robertson MD, Parkes M, Warren BF, Ferguson DJ, Jackson KG, Jewell DP, Frayn KN. (2003) Mobilisation of enterocyte fat stores by oral glucose in humans. *Gut* 52(6):834-9.

Sabesin SM, Holt PR. (1975) Intestinal lipid absorption: evidence for an intrinsic defect of chylomicron secretion by normal rat distal intestine. *Lipids* 10(12):840-6.

Salguero ML, Leon RE, Santos A, Roman S, Segura-Ortega JE, Panduro A. (2005) The role of FABP2 gene polymorphism in alcoholic cirrhosis. *Hepatology Research* 33(4):306-312.

Schaap FG, Binas B, Danneberg H, van der Vusse GJ, Glatz JF. (1999) Impaired LCFA utilization by HFABPko cardiac myocytes. *Circulation Research* 20;85(4):329-37.

Scow RO, Stein Y, Stein O. (1967) Incorporation of dietary lecithin and lysolecithin into lymph chylomicrons in the rat. *Journal of Biological Chemistry* 10;242(21):4919-24.

Shields HM, Bates ML, Bass NM, Best CJ, Alpers DH, Ockner RK. (1986) Light microscopic immunocytochemical localization of hepatic and intestinal types of fatty acid-binding proteins in rat small intestine. *Journal of Lipid Research* 27(5):549-557.

Singaraja RR, Van Eck M, Bissada N, Zimetti F, Collins HL, Hildebrand RB, Hayden A, Brunham LR, Kang MH, Fruchart JC, Van Berkel TJ, Parks JS, Staels B, Rothblat GH, Fiévet C, Hayden MR. (2006) Both hepatic and extrahepatic ABCA1 have discrete and essential functions in the maintenance of plasma high-density lipoprotein cholesterol levels in vivo. *Circulation* 114(12):1301-9.

Storch J, Bass NM, Kleinfeld AM. (1989) Studies of the fatty acid-binding site of rat liver fatty acid-binding protein using fluorescent fatty acids. *Journal of Biological Chemistry* 264(15):8708-13.

Storch J, Thumser AEA. (2000) The fatty acid transport function of fatty acid-binding proteins. *Biochimica et Biophysica Acta* 1486:28-44.

Storch J, Veerkamp JH, Hsu KT. (2002) Similar mechanisms of fatty acid transfer from human and rodent fatty acid-binding proteins to membranes: liver, intestine, heart muscle, and adipose tissue FABPs. *Molecular and Cellular Biochemistry* 239(1-2):25-33.

Storch J, Zhou YX, Lagakos WS. (2008) Metabolism of apical versus basolateral sn-2-monoacylglycerol and fatty acids in rodent small intestine. *Journal of Lipid Research* 49(8):1762-9.

Takikawa H, Kaplowitz N. (1986) Binding of bile acids, oleic acid, and organic anions by rat and human hepatic Z protein. *Archives of Biochemistry and Biophysics* 251(1):385-92.

Thumser AE, Buckland AG, Wilton DC. (1998) Monoacylglycerol binding to human serum albumin: evidence that monooleoylglycerol binds at the dansylsarcosine site. *Journal of Lipid Research* May;39(5):1033-8.

Thumser AE, Storch J. (2000) Liver and intestinal fatty acid-binding proteins obtain fatty acids from phospholipid membranes by different mechanisms. *Journal of Lipid Research* 41(4):647-56.



Thumser AE, Wilton DC. (1996) The binding of cholesterol and bile salts to recombinant rat liver fatty acid-binding protein. *Biochemical Journal* 320(Pt 3):729-33.

Trotter PJ, Storch J. (1991) Fatty acid uptake and metabolism in a human intestinal cell line (Caco-2): comparison of apical and basolateral incubation. *Journal of Lipid Research* 32(2):293-304.

Trotter PJ, Storch J. (1993) Fatty acid esterification during differentiation of the human intestinal cell line Caco-2. *Journal of Biological Chemistry* 268(14):10017-23.

Tso P, Drake DS, Black DD, Sabesin SM. (1984) Evidence for separate pathways of chylomicron and very low-density lipoprotein assembly and transport by rat small intestine. *American Journal of Physiology* 247(6 Pt 1):G599-610.

Uysal KT, Scheja L, Wiesbrock SM, Bonner-Weir S, Hotamisligil GS. (2000) Improved glucose and lipid metabolism in genetically obese mice lacking aP2. *Endocrinology* 141(9):3388-96.

Vassileva G, Huwyler L, Poirier K, Agellon LB, Toth MJ. (2000) The intestinal fatty acid binding protein is not essential for dietary fat absorption in mice. *Federation of American Societies for Experimental Biology* 14:2040-2046.

Veerkamp JH, van Moerkerk HTB. (1986) Peroxisomal fatty acid oxidation in rat and human tissues. Effect of nutritional state, clofibrate treatment and postnatal development in the rat. *Biochimica et Biophysica Acta* 875: 301-310.

Veerkamp JH, van Moerkerk HTB, Glatz JFC, Van Hinsbergh VWM. (1983) Incomplete palmitate oxidation in cell-free systems of rat and human muscles. *Biochimica et Biophysica Acta* 753: 399-410.

Verkade HJ, Tso P. "Biophysics of intestinal luminal lipids." Intestinal lipid metabolism. New York, NY: Kluwer Academic / Plenum Publishers, 2001. 1-14.

Wang CS, Kuksis A, Manganaro F, Myher JJ, Downs D, Bass HB. (1983) Studies on the substrate specificity of purified human milk bile salt-activated lipase. *Journal of Biological Chemistry* 258(15):9197-202.

Watanabe A, Toyota T, Owada Y, Hayashi T, Iwayama Y, Matsumata M, Ishitsuka Y, Nakaya A, Maekawa M, Ohnishi T, Arai R, Sakurai K, Yamada K, Kondo H, Hashimoto K, Osumi N, Yoshikawa T. (2007) Fabp7 maps to a QTL for a schizophrenia endophenotype. *Public Library of Science Biology* 5(11):e297.

Watford M, Lund P, Krebs HA. (1979) Isolation and metabolic characteristics of rat and chicken enterocytes. *Biochemical Journal* 178(3):589-596.

Weiss WP, Brown MD, Shildiner AR, Hagberg JM. (2002) Fatty acid binding-2 gene variants and insulin resistance: gene and gene-environment interaction effects. *Physiological Genomics* 10:145-157.

Wilkinson TCI, Wilton DC. (1987) Studies on fatty acid-binding proteins. The binding properties of rat liver fatty acid-binding protein. *Biochemical Journal* 247:485-488.

Windmueller HG, Spaeth AE. (1978) Identification of ketone bodies and glutamine as the major respiratory fuels in vivo for postabsorptive rat small intestine. *Journal of Biological Chemistry* 253(1):69-76.

Wolfrum C, Borrmann CM, Borchers T, Spener F. (2001) Fatty acids and hypolipidemic drugs regulate peroxisome proliferator-activated receptors alpha - and gamma-mediated gene expression via liver fatty acid binding protein: a signaling path to the nucleus. *Proceedings of the National Academy of Sciences* 98(5):2323-8.

Xie Y, Newberry EP, Kennedy SM, Luo J, Davidson NO. (2009) Increased susceptibility to diet-induced gallstones in liver fatty acid binding protein knockout mice. *Journal of Lipid Research* 50(5):977-87.

Xu LZ, Sánchez R, Sali A, Heintz N. (1996) Ligand specificity of brain lipid-binding protein. *Journal of Biological Chemistry* 271(40):24711-9.

Yamada K, Yuan X, Ishiyama S, Koyama K, Ichikawa F, Koyanagi A, Koyama W, Nonaka K. (1997) Association between Ala54Thr substitution of the fatty acid-binding protein 2 gene with insulin resistance and intra-abdominal fat thickness in Japanese men. *Diabetologia* 40(6):706-10.

## Curriculum Vitae

**William Stacy Lagakos**

<b>October 2009</b>	<b>Doctor of Philosophy in Nutritional Sciences</b> Rutgers, The State University of New Jersey, NJ
<b>May 2003</b>	<b>Bachelor of Science in Nutritional Sciences</b> Rutgers, The State University of New Jersey, NJ
<b>September 2003 to May 2004</b>	<b>Teaching Assistant</b> Department of Life Sciences Rutgers, The State University of New Jersey, NJ
<b>September 2004 to May 2006</b>	<b>Teaching Assistant</b> Department Nutritional Sciences Rutgers, The State University of New Jersey, NJ
<b>September 2006 to June 2009</b>	<b>Graduate Assistant</b> Department Nutritional Sciences Rutgers, The State University of New Jersey, NJ

### **Publications:**

Manso Filho HC, McKeever KH, Gordon ME, Manso HE, Lagakos WS, Wu, G, Watford M. (2009) Developmental changes in the concentrations of glutamine and other amino acids in plasma and skeletal muscle of the Standardbred foal. *Journal of Animal Science* (in press).

Manso Filho HC, McKeever KH, Gordon ME, Costa HE, Lagakos WS, Watford M. (2008) Changes in glutamine metabolism indicate a mild catabolic state in the transition mare. *Journal of Animal Science* 86(12):3424-31.

Storch J, Zhou YX, Lagakos WS. Metabolism of apical versus basolateral sn-2-monoacylglycerol and fatty acids in rodent small intestine. (2008) *Journal of Lipid Research* 49(8):1762-9.

Neeli I, Siddiqi SA, Siddiqi S, Mahan J, Lagakos WS, Binas B, Gheyi T, Storch J, Mansbach CM 2nd. (2007) Liver fatty acid-binding protein initiates budding of pre-chylomicron transport vesicles from intestinal endoplasmic reticulum. *Journal of Biological Chemistry* 282(25):17974-84.